## Title

Ellagic Acid and Urolithin A Improve Insulin Sensitivity in Diet-Induced Insulin Resistant Mice and Reduce Detrimental Effects of Palmitate Administration in Differentiated C2C12 Myotubes.



## Author

Chan, Brenda

## Publication Date

2018

Peer reviewed|Thesis/dissertation

UNIVERSITY OF CALIFORNIA

Los Angeles

# Ellagic Acid and Urolithin A Improve Insulin Sensitivity in Diet-Induced Insulin Resistant Mice and Reduce Detrimental Effects of Palmitate Administration in Differentiated C2C12 Myotubes.

A thesis submitted in partial satisfaction

of the requirements for the degree Master of Science

in Biochemistry, Molecular and Structural Biology

by

Brenda Chan

2018

ABSTRACT OF THE THESIS

Ellagic Acid and Urolithin A Improve Insulin Sensitivity in Diet-Induced Insulin Resistant Mice and Reduce Detrimental Effects of Palmitate Administration in Differentiated C2C12 Myotubes.

by

Brenda Chan

Master of Science in Biochemistry, Molecular and Structural Biology

University of California, Los Angeles, 2018

Professor Catherine F. Clarke, Chair

Insulin resistance has been spreading as food and sedentary lifestyles are becoming more common. Major bodily complications often result, necessitating a search for affordable solutions. Phytochemicals are commonly used in alternative medicine but less so in areas where obesity and T2D prevail. This thesis studies ellagic acid (EA) and its metabolite urolithin A (UA) as potential treatments for insulin resistance, focusing on the main site of glucose uptake, skeletal muscle. In diet-induced insulin-resistant mice, long-term dietary EA&UA administration reduced glucose levels in IPITTs, while UA alone also reduced serum FFA and fasting glucose levels. Mitochondrial turnover and ROS detoxification markers increased with treatment, indicating improved mitochondrial quality control. Differentiated C2C12 mouse myotubes were utilized to study cellular effects of EA and UA. In insulin resistant myotubes, treatment enhanced ATP

production and reduced ROS, cytotoxicity, and apoptosis. With insulin, UA increased uncoupled respiration while decreasing ROS, implying increased fuel oxidation without adding oxidative stress. UA tended to decrease glucose uptake as it increased cellular respiration, suggesting a stronger utilization of fatty acids. The results of this thesis support EA and UA as promising treatments for insulin resistance and the metabolic syndrome.

The thesis of Brenda Chan is approved.

Zhaoping Li

Steven G. Clarke

Catherine F. Clarke, Committee Chair

University of California, Los Angeles

2018

# DEDICATION

This thesis is dedicated to my family, other loved ones, and all my mentors along the way. I couldn't have asked for a more supportive crew.

## Table of Contents

## List of Figures and Tables

**Acknowledgements**

I would like to thank a number of individuals for their support and guidance throughout my education. I am greatly indebted to my mentor, Jieping Yang, who has opened my eyes to the field of research in countless ways. She has been incredibly understanding and patient, teaching me not only the necessary techniques required to work in a lab, but also how to think more critically. Thank you for always encouraging me to further my education and believing in me. I am also grateful for all the others in my lab who think I have yet to reach my full potential.

Next, I want to thank my committee members for taking the time to provide me with feedback on my thesis. They have been the kindest guides, using their decades of experience to discuss possible future paths in this field.

Third, my past mentors, Luo Mi and Joe Schinaman, deserve much appreciation for their patience in introducing me to research.

Fourth, I want to thank my friends who have supported me through my endeavors and pushed me to work as hard as they do. My roommates have provided me with both an intellectually stimulating and relaxing environment, helping me through this arduous journey.

Lastly, I would not have been able to complete, or even begin my education without my family. I must thank my grandparents for helping put my brother and me through college and stressing the importance of a good education. My parents have been the most instrumental in getting me to where I am today; they have been so supportive and caring in helping me prepare for my future. Also, my brother Kenny is a pretty cool guy.

## Introduction

*Insulin Resistance and Diabetes Overview*

Insulin resistance and diabetes have become epidemics in more parts of the world, affecting developed and now developing countries. Out of the three main types, Type I, Type II, and gestational, Type II Diabetes (T2D) is the major form responsible for the widespread prevalence of this disease (1,2). From 2015 to 2030, the International Diabetes Federation Diabetes Model predicted that the number of people with diabetes in the Unites States will increase by 54%, to 54,913,000 (3) and Shaw et al. estimated the number to reach 439 million worldwide in 2030 (4). Additionally, the cost will increase 53% from $407.6 billion to $622.3 billion in this time. Complications with accessing treatment in low and middle-income patients only augment the issue of diabetes and its comorbidities.

Magliano et al. (2012) found that those with diabetes had a two to three times higher risk of all-cause mortality compared to non-diabetic individuals in Mauritius over a 15 year follow up study. Since the population of Mauritius is representative of about two-thirds of the world, this has serious implications for the global population with regards to diabetes and death (5).

Diabetes is characterized by a group of metabolic disorders that result from defective insulin secretion, action, or both, causing chronic hyperglycemia. Impaired insulin regulation amounts to improper metabolism of nutrient fuels. The major sites that develop insulin resistance are skeletal muscle, adipose tissue, and liver tissue. Type I diabetes, an autoimmune disease where the body destroys its own pancreatic β cells, contributes about 5-10% of all diabetes cases. T2D constitutes 90-95% of diabetic subjects and is largely due to the growing obesity epidemic. In

2009, T2D was the cause of 20% of diabetes in children and has been on the rise due to the growing prevalence of an increasingly sedentary lifestyle and unhealthy diet (6).

*Insulin Signaling*

Insulin resistance, implicated in many metabolic diseases, is one of the strongest predictors for the development of T2D (7). Insulin is an essential hormone produced by pancreatic β cells which regulates nutrient utilization and storage. When nutrients are abundant, such as after a meal, insulin is secreted and promotes uptake and storage of energy metabolites in key tissues. In skeletal muscle, insulin stimulates glucose uptake and glycogen synthesis while it suppresses glycogenolysis. In the liver, insulin stimulates glycogen synthesis and lipogenesis and suppresses gluconeogenesis and lipolysis. In adipose tissue, insulin stimulates lipogenesis and suppresses lipolysis. However, when an individual has insulin resistance, insulin-mediated regulation in hepatic gluconeogenesis, adipotissue lipogenesis, and skeletal muscle glucose uptake and storage are impaired, leading to hyperglycemia (8).

Insulin signaling has been extensively studied, and new technologies are bringing even more clarity to its complexity. Insulin first binds the α-subunit of the heterotetrameric insulin receptor (IR) protein in the plasma membrane, triggering the tyrosine kinase autophosphorylation of its two transmembrane β subunits. Once phosphorylated, these β subunits serve as docking sites for tyrosine phosphorylated adaptor proteins like Insulin Receptor Substrates-1 and -2 (IRS-1 and -2). When IRS proteins bind IR, phosphatidylinositol-3-kinase (PI3K) and mitogen-activated protein kinase (MAPK) pathways are activated. The PI3K cascade is responsible for many of the metabolic effects of insulin through 3-phosphoinositide-dependent protein kinase 1 (PDK1)-dependent phosphorylation and activation of protein kinase B (PKB, also known as Akt) (2).

PKB then phosphorylates many downstream targets, such as glycogen synthase kinase (GSK-3) and mechanistic target of rapamycin (mTOR). The MAPK cascade involves Raf, MEK, and ERK1/2 and regulates cell differentiation, proliferation, and survival. Insulin signaling is negatively associated with serine phosphorylation of IRS1, as well as the dephosphorylation of IR and IRS1/2. In the liver, activation of Akt stimulates glycogen synthesis and fatty acid synthesis enzymes while it inhibits gluconeogenesis (9).

*The Role of Lipids in the Development of Insulin Resistance and Diabetes*

The original theory of free-fatty acid (FFA)-induced diabetes was proposed by Randle et al. which proposed that the rate of glyceride breakdown in muscle occurred faster than fatty acid re-esterification (10). This led to insulin insensitivity and inhibited glucose transport. They also suggested that in muscle glucose is shunted into glycogen rather than pyruvate which augments insulin resistance. However, other studies have demonstrated lower levels of glucose-6-phosphate and reduced glycogen synthesis in healthy subjects after lipid infusion, contradicting the initial model (11,12). Thus, other mechanisms of insulin resistance were likely the cause of reduced glucose uptake.

The current prevailing theory of obesity-related T2D proposes that excessive nutrient consumption saturates adipose tissue which is already at full capacity, forcing other tissues to take in the excess lipids. Subsequently, these tissues develop metabolic dysregulation and insulin resistance. A possible mechanism of how this dysregulation occurs is by the increased concentrations of lipid metabolites that reduce insulin signaling. Intramyocellular lipid accumulation has been strongly implicated in the development of insulin resistance. Studies have shown that muscle triglyceride (TG) content does not indicate insulin resistance, but levels of

diacylglycerides (DAGs) do (11,13). DAGs are lipid metabolites that also act as signaling molecules, activating the novel PKCθ. When these novel PKCs are activated, they inhibit insulin signaling by preventing IR from phosphorylating target enzymes. Possibly due to impaired β-oxidation or excess FFAs, ceramides and fatty acyl-CoAs have also been found to be elevated in T2D and correlate with the severity of insulin resistance (14). These lipid metabolites trigger a serine/threonine kinase cascade that lead to the phosphorylation of specific serine residues on IRS-1 and IRS-2. Proposed serine/threonine kinases responsible include c-Jun NH2-terminal kinase (JNK) which targets $Ser^{307}$ on IRS-1 in hamsters (15), and tumor necrosis factor α (TNF-α) which targets inhibitor kappa B kinase (IKK) and several serine residues on IRS-1 including $Ser^{312}$ in humans (16). TNF-α is a pro-inflammatory cytokine produced by lymphocytes and macrophages during stress that has been found to be elevated in obese individuals, likely due to the chronic inflammation associated with obesity. One study found evidence to support activation of JNK by TNF-α to phosphorylate IRS-1 at $Ser^{307}$, inhibiting insulin signaling. Additionally, TNF-α receptor knockout mice had significantly less insulin resistance in diet-induced obesity, suggesting a strong role for TNF-α in diet-induced insulin resistance (15,17). Phosphorylation of $Ser^{307}$ on IRS-1 impairs its ability to interact with insulin receptor and thus to phosphorylate the downstream PI3K (15). Additionally, when genes that regulate the uptake and oxidation of fatty acids were upregulated in skeletal muscle of mice, a diabetic phenotype was observed (18). Thus diet-induced insulin resistance may not be due to the accumulation of triacylglycerides per se, but likely the increased use of fatty acids as a fuel, as this may lead to a buildup of unfavorable lipid intermediates that dysregulate insulin signaling (19).

In a study where transgenic mice were engineered to carry the A-ZIP/F-1 protein, which heterodimerizes and inactivates certain transcription factors associated with fat cell formation,

insulin resistance was developed by 4 weeks of age (20). Insulin-stimulated glycogen synthesis, whole body glucose uptake, and glucose transport in skeletal muscle were all impaired in fatless mice. Basal IRS-1-stimulated PI3K activity in skeletal muscle was decreased, and insulin-stimulated IRS-1 and IRS-2 PI3K activity in skeletal muscle and liver, respectively, were largely decreased in fatless mice. Transplanting fat from wildtype mice into the fatless mice prevented the diabetic phenotype and increased glucose uptake to wildtype values. In addition, fat transplantation increased PI3K activation by IRS-1 and IRS-2 to wild type values in muscle and liver, respectively. Also interesting was the finding that TG levels in muscle and liver decreased by 67% and 55%, respectively, in mice receiving fat transplants, resulting in values resembling wild type mice. The authors suggested that fat transplantation caused a redistribution of lipids into these fat stores and away from ectopic tissues (21). Another study that inhibited carnitine palmitoyltransferase-1, which is involved in fatty acid oxidation, in diet-induced insulin resistant mice found an improvement in insulin sensitivity, along with reduced levels of lipid metabolites like ceramides, diacylglycerides, and long chain fatty acyl-CoAs (22). These findings support the hypothesis that an accumulation of lipids in non-adipose tissues like skeletal muscle and liver reduces insulin signaling, perhaps by causing a buildup of lipid metabolites such as DAGs, ceramides, and fatty-acyl-CoAs.

*Skeletal Muscle and Mitochondria in Metabolic Diseases*

Since skeletal muscle accounts for about 85% of total body glucose metabolism, this tissue has been emphasized as an important factor in the development and progression of insulin resistance (23). In lean, insulin resistant subjects, post-prandial glycogen synthesis was 60% less than matched lean, insulin sensitive subjects, while hepatic lipogenesis and hepatic TG synthesis both increased by more than two times in insulin resistant subjects. As a result, levels of plasma TGs

were increased and HDL were decreased. The reduced formation of glycogen likely shunts nutrient storage to lipid formation, promoting insulin resistance and atherosclerotic disease (24). Although the main determinant of diabetes is pancreatic β cell failure, the importance of skeletal muscle also demands great attention and this thesis will focus on this tissue in insulin resistance.

Within the cell, mitochondria play a major factor in metabolic diseases, as they regulate the production of energy metabolites and participate in apoptosis, among other roles. Their dysfunction has been implicated in aging and chronic diseases, including neurodegenerative diseases like Alzheimer's and Parkinson's, diabetes and other metabolic diseases, autoimmune diseases, cardiovascular diseases, psychiatric diseases, gastrointestinal and musculoskeletal diseases, cancer, and chronic inflammatory diseases (25). In mice fed high-fat, high-sucrose (HF/HS) diets, mitochondria were less abundant, transcription factors that promote mitochondrial biogenesis down regulated, and surface areas of mitochondria reduced. Further support for mitochondrial dysfunction in diabetes is reduced electron transport chain (ETC) function and lower succinate dehydrogenase levels in HF/HS diet-induced diabetic mice (26).

Mitochondria are in charge of producing the great majority of cellular ATP through aerobic respiration; energy is transferred from nutrient metabolites to electron carriers (NADH and $FADH_2$) which then send electrons to the ETC in the inner mitochondrial membrane. This process is coupled with the movement of hydrogen ions into the intermembrane space, creating both a charge and a chemical gradient. Thus, the inner membrane has a proton motive force (pmf) consisting of the electric potential ($\Delta\Psi_m$) due to a difference in charge across the membrane and a chemical potential ($\Delta$pH) from a difference in hydrogen ion concentration across the membrane. The pmf drives ATP production by driving hydrogen ions into the matrix through ATP synthase, which phosphorylates ADP as the energy potential is reduced. However,

there are other modes of reducing the pmf like proton-leak and uncoupler proteins (UCPs), which allow protons into the matrix without translocating through ATP synthase. When the pmf is too great and the capacity of electron transport is not sufficient to keep up, an increase in reactive oxygen species (ROS) results (27). One study using uncouplers to manipulate the electrochemical gradient in rat heart mitochondria showed that above a certain threshold pmf, hydrogen peroxide ($H_2O_2$) production was greatly enhanced. This supported the notion that electron leakage to molecular oxygen is increased when the pmf surpasses the ETC capacity, creating reactive oxygen species that then get converted to $H_2O_2$ (28).

Mitochondrial oxidative stress has been found in many models of insulin resistance, including chronic treatment of insulin, corticosteroids, proinflammatory cytokines, and lipids on muscle and adipose cells (29). Normally, four electrons are accepted by an oxygen molecule to produce two neutral $H_2O$ molecules, but occasionally only one electron will be transferred to the surrounding $O_2$ and produce the superoxide ion, $O_2^{\bullet -}$, which may in turn oxidize other cellular components and disrupt cellular function. The superoxide ion is usually converted to the less harmful $H_2O_2$ by manganese superoxide dismutase (MnSOD). $H_2O_2$ can then be converted to $H_2O$ by catalase, glutathione (GSH), or thioredoxin/peroxiredoxin systems (30). However, when antioxidant systems are inadequate or impaired, increased levels of ROS result which have been linked to the development of insulin resistance. In 3T3-L1 adipocytes with either TNF-α or dexamethasone-induced insulin resistance, higher levels of ROS were detected and preceded the development of insulin resistance. In addition, the anti-oxidants N-acetylcysteine (NAC) and manganese (III) tetrakis (4-benzoic acid) porphyrin (MnTBAP) were able to reduce the inhibition of glucose uptake associated with insulin resistance, reduce levels of protein carbonylation (a product of ROS oxidation), and restore mitochondrial density (19).

Furthermore, the overexpression of ROS scavenging enzymes CuZnSOD and MnSOD also reduced the inhibition of glucose uptake from insulin resistance (31). One hypothesis is that increased ROS signals to the cell that there is an overabundance of nutrients so glucose transport must be reduced in order to reach homeostasis. Elevated levels of $H_2O_2$ were found in mice with HF/HS diet-induced diabetes (19), but when catalase, an enzyme that converts $H_2O_2$ to $H_2O$ in peroxisomes, was targeted to the mitochondrial matrix, mice fed a high-fat diet maintained full-body insulin sensitivity comparative to wild-type mice on a control diet (32). Mitochondrially-targeted catalase also resulted in mitochondrial $H_2O_2$ reduction by 45%, which was associated with reductions in mtDNA damage and mitochondrial efficiency. This also prevented the increase in DAG content and PKCθ activity associated with aging (33). Yet another important study involved peroxiredoxins, one of the largest families of antioxidant proteins. When peroxiredoxin III (PrdxIII), which functions in the mitochondria, was knocked-out of mice, an increase in white adipotissue and whole body insulin resistance resulted, while PrdxIII transgenic mice remained insulin sensitive even on a high fat diet. These studies indicate a connection between mitochondria-derived ROS and insulin sensitivity (34).

To prevent an overproduction of ROS the cell removes dysfunctional mitochondria, a process known as mitochondrial autophagy (mitophagy). In support of this, mitophagy-deficient mice (from parkin-knockout) had an accumulation of dysfunctional mitochondrial and reduced survival (35). PINK1 is a kinase that increases the E3 ubiquitin ligase activity of parkin when it phosphorylates parkin at $Ser^{65}$ and ubiquitin at its equivalent of $Ser^{65}$ (forming pUb). When parkin allosterically binds pUb, it is less restricted and has a higher affinity for PINK1 (36). PINK1 resides on the outer membrane of mitochondria but is quickly degraded under normal circumstances, while parkin typically remains in the cytosol but is targeted to depolarized

mitochondria. PINK1 detects and accumulates on dysfunctional mitochondria where its kinase activity is required for parkin recruitment and ubiquination. This triggers the start of mitophagy (37). Mitochondria of obese and T2D patients are generally fewer, smaller and less efficient, so it would seem that the mitophagic system is improperly functioning in these individuals (38).

*Natural Compounds as Treatment*

The use of natural foods to assist in preventing and treating chronic diseases requires more attention, as many of the major current treatments are expensive and inaccessible to the most at-risk populations. Fruits, nuts, vegetables, and other botanicals contain an abundance of compounds found to improve the condition of many illnesses, especially those associated with inflammation like diabetes (39-41). Elevated levels of acute-phase proteins that indicate chronic inflammation have been linked to increased risk of developing insulin resistance (42). The mechanism by which inflammation participates in insulin resistance and diabetes may be by the pro-inflammatory cytokine TNF-α, and/or the IκB kinase-β (IKKβ)/NFkB pathway which regulates inflammatory responses (43), as mentioned earlier. Infusion of TNF-α in healthy humans induced insulin resistance in skeletal muscle by altering insulin signaling and reducing glucose uptake and metabolism (44). Despite the fact that TNF-α was initially considered a cytokine produced only by fat cells, it was found to be synthesized in the skeletal muscles of both rats and humans and was inversely correlated with glucose disposal rates (45). In support of the inflammatory marker IKKβ being involved in insulin resistance, mice on a high fat diet with hepatic IKKβ knockout retained better insulin sensitivity in the liver compared to control mice, although they still developed insulin resistance in peripheral tissues (46). Several phytochemicals, including berberine (47), corosolic acid (48), and galegine (49) have been previously reported to possess hypoglycemic properties (49). Li et al. reviewed berberine as an

anti-diabetic compound and reported its ability to inhibit mitochondrial activity, stimulate AMPK, regulate islet function, alter the microbiome, and upregulate IR expression (47). All compounds were reported to reduce oxidative stress in diabetic rat models and cells (50,51). Additionally, while studying the antidiabetic capabilities of banaba, the plant corosolic acid was extracted from, Hayashi et al. identified three ellagitannins responsible for improved glucose uptake in rat fat cells. Ellagitannins are polyphenols found in the plant cell walls and membranes of various fruits and nuts, including pomegranates, raspberries, strawberries, cranberries, grapes, pecans, and walnuts, which have antioxidant and anticancer activities (52-54). Plants hydrolyze ellagitannins to hexahydroxydiphenic acid, which then spontaneously lactonizes to ellagic acid (EA) (55). In the gut, EA is further processed by microflora into urolithins such as urolithin A (UA) as shown in Figure 1.

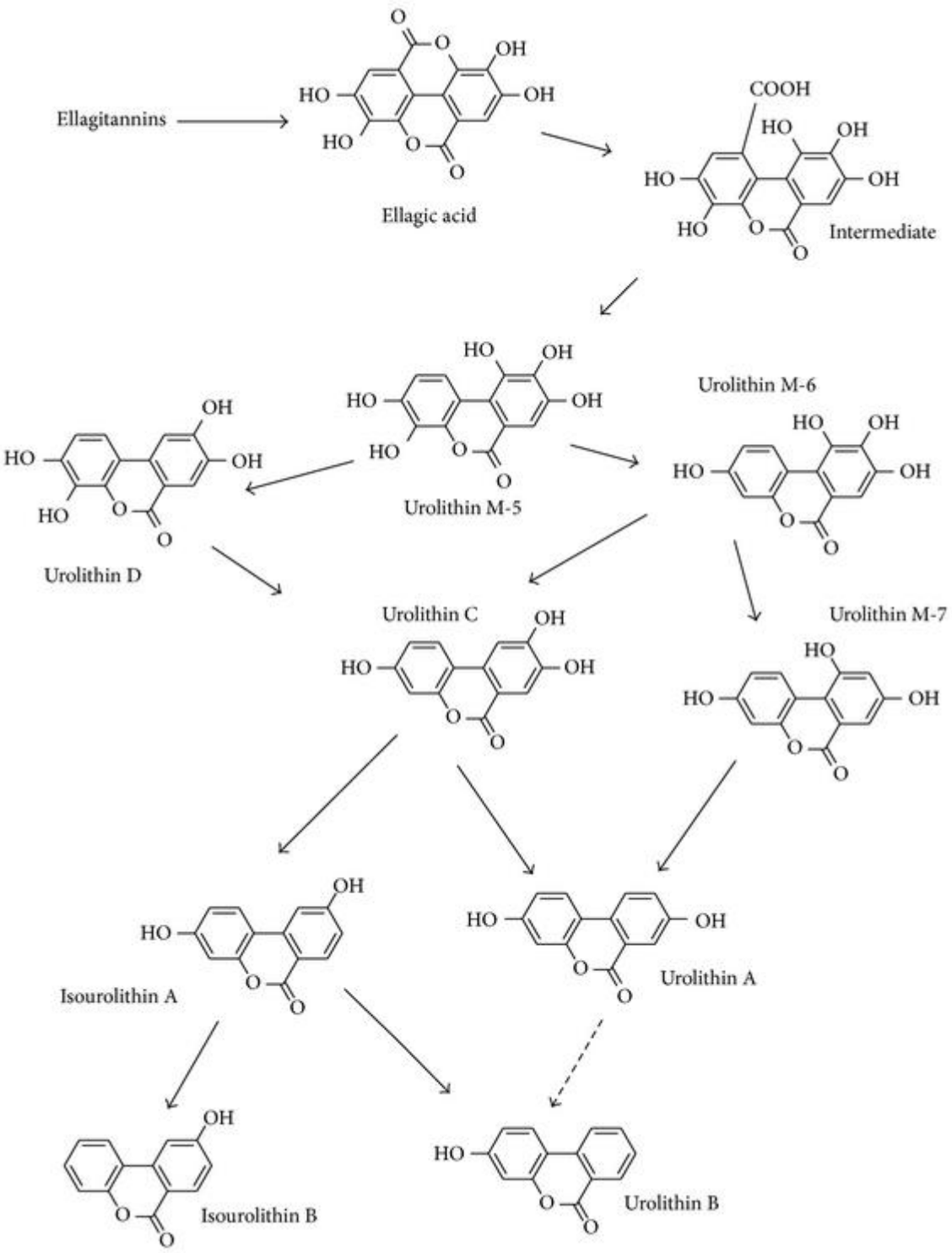


**Figure 1.** Gut microbiota metabolism of ellagitannins and ellagic acid. Image from (56).

*Ellagitannins and Their Metabolites as Potential Treatments*

One study discovered that β-d-pentagalloylglucose, a secondary plant metabolite from a member of the tannin family was capable of decreasing TNF-α levels in human peripheral blood mononuclear cells (PBMCs) and live rats after stimulation by the bacterial lipotoxin lipopolysaccharide (LPS) (57). LPS is a molecule on the cell walls of gram-negative bacteria which triggers the immune response by interacting with toll-like receptors (TLRs) on the host cells (58). As TNF-α is a marker of inflammation, this indicates potential for secondary plant metabolites of tannins to treat inflammatory diseases. Ellagic acid was found to inhibit lipid peroxidation induced by ADP and NADPH by 47% and inhibit cancer cell proliferation in oral, colon, and prostate cancer cell lines (59,60). At concentrations of 1-100 μM EA, cell proliferation was inhibited by inducing apoptosis in colon, breast, and prostatic cancer cell lines (61). One study found that EA reduced Akt phosphorylation in the colons of rats treated with DMH, an inducer of colon cancer. As activation of Akt by phosphorylation is associated with proliferation of cancer cells, the reduced phosphorylation suggests EA may promote anti-proliferation/pro-apopotosis pathways of cancer cells in rats (62). In addition, EA was found to prevent pancreatitis in Wistar Bonn/Kobori rats (an experimental model of spontaneous chronic pancreatitis), reducing pancreatic inflammation, neutrophil infiltration, collagen content, number of activated pancreatic stellate cells, and ROS production (63). EA was found to increase glucose uptake in 3T3-L1 adipocytes and C2C12 skeletal muscle cells in a dose dependent manner (1-100 nM EA for 3T3-L1 and 1-500 nM EA for C2C12 cells), which correlated with an increase in GLUT4 translocation to the plasma membrane. Additionally, EA inhibited adipogenesis and reduced lipid accumulation in 3T3-L1 cells and primary human adipocyte cell cultures by reducing fatty acid biosynthesis gene expression (64), while it increased β-oxidation in

hepatocytes (65). However, EA had no effect on Akt phosphorylation as it activated AMPK in these two cell lines, indicating the mechanism behind its metabolic effect was through AMPK, not Akt. This does seem to contradict the previous study where pAkt levels were decreased with EA treatment, but this may be accounted for by the different subject models. The authors then studied downstream targets of AMPK and found that the ERK-atypical PKC pathway was stimulated with EA treatment, indicating this was the path through which EA stimulated GLUT4 translocation (66).

All this evidence suggests that EA and its metabolites may be potential treatments for insulin resistance. This thesis will focus on EA and UA treatment in skeletal muscles of HF/HS diet-induced insulin resistant mice and palmitate-induced insulin resistant cultured mouse myotubes.

## Materials and Methods

### *Chemical Reagents*

All reagents and supplies were purchased from Thermo Fisher Scientific or Sigma-Aldrich unless otherwise stated. Ellagic acid for C2C12 treatment was purchased from Sigma-Aldrich, urolithin A was purchased from Jinan Feiteng Pharmaceutical Technology Corp Ltd.

### *Experimental Animal and Body Composition Analysis*

All mouse procedures were approved by the UCLA Animal Research Committee in compliance with the Association for Assessment and Accreditation of Laboratory Care (AAA-LAC) International. 5-week old male DBA/2J mice were purchased from Jackson Laboratory and were allowed to acclimate to the new environment for one week. Their metabolic types were assessed and determined to be all non-UA producers. Starting week 0, 12 mice were put on a Low Fat/Low Sucrose diet (LF/LS) while the rest of the 60 mice were given a High Fat/High Sucrose diet (HF/HS). The mice on the HF/HS diet were then randomly split into five groups of 10 to 12 mice with a similar distribution of weights. The resulting six groups were LF/LS (negative control), HF/HS, HF/HS + 0.1% EA, HF/HS + 0.1% UA, HF/HS + 0.1% EA & 0.1% UA, and HF/HS + 0.15% Metformin. Metformin is the positive treatment control, as it is the main drug being prescribed for Type 2 diabetes; it lowers blood glucose without causing hypoglycemia and increases insulin sensitivity. It may do this by increasing insulin receptor expression, tyrosine kinase activity, and reducing gluconeogenesis in the liver (67). Mouse diets were purchased from Envigo and the full composition of the LF/LS and HF/HS diets are given in Supplementary Table S1. Every week, food consumption and body weights were measured for each cage (four mice per cage) and every four weeks, intraperitoneal insulin and glucose tolerance tests were

administered. After eight weeks on their LF/LS or HF/HS diets, the experimental groups were given new diets supplemented with 0.1% EA, 0.1% UA, 0.1% EA& 1%UA, or 0.15% Metformin as described above. After another eight weeks, mice were fasted for six hours then sacrificed by isoflurane inhalation. Blood samples were harvested by cardiac puncture and stored at -80°C for later analysis. Liver, intestine, adipose tissue, pancreas, caecum, heart, kidney, and muscle tissue were then removed and stored at -80°C. All animal experiments were approved by the local ethics committee and housing conditions were as specified by the Belgian Law of 6 April 2010 on the protection of laboratory animals (agreement no. LA 1230314).

*Measurement of Intramyocellular Lipids*

Previously frozen skeletal muscle tissue from the hind limb was homogenized (~10 mg tissue/sample) in 200 μL of a 1% Triton X-100 in chloroform solution using Precellys ceramic beads (Item #10011152) and Fisherbrand Bead Mill 24 Homogenizer (45 seconds). Samples were then centrifuged for 10 minutes at 13,000xg to remove particle debris. The supernatant was allowed to evaporate overnight in a fume hood. Dried lipids were resuspended in 200 μL Fatty Acid Assay Buffer from the Free Fatty Acid Quantitation Kit (Sigma-Aldrich Cat#MAK044) by vortexing for 5 minutes. Free fatty acid, triglyceride, and cholesterol levels were then assayed following the manufacturers' protocols (Sigma-Aldrich Cat#MAK044, Pointe Scientific Cat#T7532 and #C7510, respectively).

*Skeletal Muscle mRNA and RT-qPCR*

Previously frozen skeletal muscle tissue from the hind limb (~15-20 mg) was homogenized in 350 μL RLT Buffer Plus using Precellys ceramic beads (Item #10011152) and a Fisherbrand Bead Mill 24 Homogenizer (45 seconds). RNA extraction was then completed with Qiagen

RNeasy Plus Mini Kit (Qiagen Cat#74134) according to the Manufacturer's protocol. cDNA was synthesized using SuperScript™ III First-Strand Synthesis System (Thermo Fisher Cat#1808005) in a 10 μL volume system without RNaseOUT. Real-time quantitative PCR was performed with the StepOnePlus™ real-time PCR system and software (Applied Biosystems) using SYBR Green for detection according to the manufacturer's instructions. GAPDH was used as the housekeeping gene. Primer sequences are given in Supplementary Table S2.

*C2C12 Cell Maintenance*

C2C12 mouse myoblasts were purchased from American Type Culture Collection (ATCC, Rockville, MD). Growth media consisted of 15% heat-inactivated FBS (Omega Cat#FB-12), 1% Strep-Pen (Gibco #15140122), in high glucose (5 mg/L) DMEM (Gibco #11995-065). Differentiation media consisted of 0.5% FBS and 1% Strep-Pen in high glucose DMEM. Frozen cells in liquid nitrogen were quickly thawed in a 37°C water bath, resuspended in 7 mL growth media and centrifuged at 360xg for 12 minutes. The supernatant was discarded and the cell pellet was resuspended in 10 mL growth media and plated in a T25 cell culture flask (Sigma-Aldrich #CLS430639). Cells were passaged every other day or when cells were ~60% confluent. To differentiate myoblasts, cells were allowed to reach confluency in 96-well plates before media was changed to differentiation media. After 4-5 days on differentiation media when myoblasts were fully differentiated into myotubes, media was changed to low glucose (1 g/L) DMEM with 0.75 mM palmitate-BSA to induce insulin resistance. 12 hours after being put on palmitate media, media was removed and treatment was administered: various concentrations of EA, UA, or both in palmitate-low glucose DMEM, or no-treatment-BSA in low glucose DMEM as a negative control.

*Palmitate Preparation*

The Palmitate-BSA solution was prepared in a 4:1 ratio following a protocol by the Shirihai lab at UCLA. Briefly, BSA was dissolved in 1x PBS at 4 mM. Stock palmitate solution was created at 400 mM in DMSO. 50 mL of 4 mM BSA was constantly stirred and maintained at 40-45°C while five hourly additions of 100i μL 400 mM palmitate were added to produce a solution of 4 mM palmitate conjugated to BSA. One hour after the last 100 μL addition of palmitate, the palmitate-BSA solution was filtered through a 0.22 μm filter, aliquoted, and stored at -80°C. A final concentration of 0.75 mM palmitate-BSA (or 0.5 mM palmitate-BSA for the Seahorse Assay) was created in serum-free low-glucose DMEM (1 g/L glucose) with or without treatments on the day of treating the cells. This concentration has been previously found to induce insulin resistance in C2C12 cells when incubated with cells for 5-24 hours (68-70).

*C2C12 mRNA Isolation*

C2C12 myoblasts were plated into four 6-well plates in growth media until confluent, then switched to differentiation media. On the 6$^{th}$ day of differentiation media, cells were fully differentiated into fused myotubes and administered 0.75 mM palmitate-BSA or 0.75 mM BSA (as control) in low glucose DMEM. After 12 hours, media was removed and cells were administered treatments and left to incubate for another 12 hours. 4 hours before harvesting, 100nM insulin was added to each replicate. To collect RNA, cells were washed with PBS before using RNeasy Plus Mini Kit (Qiagen Cat#74134). As very low readings were obtained when the gDNA column was used, genomic DNA was removed with TURBO™ DNase (Thermo Fisher Cat#2238) after nucleic acids were isolated. cDNA was synthesized using SuperScript™ III First-Strand Synthesis System (Thermo Fisher Cat#1808005) in a 10 μL volume system without

RNaseOUT. cDNA was diluted 2-fold before use. Real-time quantitative PCR was performed with the StepOnePlus™ real-time PCR system and software (Applied Biosystems) using SYBR Green for detection according to the manufacturer's instructions. ß-actin was used as the housekeeping gene.

*Cell Viability*

CellTiter-Glo® Luminescent Cell Viability Assay (Promega #G7570)

Manufacturer's protocol was followed. C2C12 myoblasts were seeded at ~ $5x10^3$ cells/well of a 96 well black plate (Fisher cat # 12-566-07) with growth media. When cells were confluent and beginning to differentiate, media was switched to differentiation media for 4 days before removing differentiation media and changing to 0.75 mM palmitate or 0.75 mM BSA media in low glucose (1 g/L glucose) DMEM for 12 hours. Treatment with or without 1 mM insulin was then added for another 12 hours. CellTiter-Glo Buffer and CellTiter-Glo Substrate were brought to room temperature before reconstituting Substrate with Buffer in amber bottle. Cells were brought to room temperature and 100 µL of the CellTiter-Glo solution was added to each well. Plate was shaken on an orbital shaker for 2 minutes to lyse cells, then incubated at room temperature for 10 minutes to stabilize the luminescent signal. Luminescence was measured using a SpectraMax GeminiEM plate reader (Molecular Devices).

MTT

Thiazolyl Blue Tetrazolium Bromide (MTT) was used to measure cell proliferation. MTT is normally yellow but turns into a dark blue water-insoluble MTT formazan due to mitochondrial dehydrogenases of living cells. The blue crystals are solubilized with DMSO or SDS and the intensity is measured colorimetrically at 570 nm. Background noise is measured at 650 nm and

subtracted from 570 nm readings. 5 mg/mL MTT (Sigma Aldrich #M2128-250MG) was dissolved in PBS and stored, protected from light, at 4°C until use. Cells were treated as in the CellTiter-Glo® Assay, then media from plate was removed. Stock MTT was diluted 1:10 in PBS and 100 µL was administered to each well. After 3 hours of incubation, 100 µL 10% SDS was added to each well and the plate was mixed on an orbital shaker overnight to solubilize the MTT formazan. The absorbance was read at 570 nm and 650 nm in a VersaMax plate reader (Molecular Devices).

ApoTox-Glo Triplex Assay (Promega Cat#G6320)

The ApoTox-Glo Triplex Assay was used to measure cytotoxicity and apoptosis activities of differentiated C2C12 cells. The cell-impermeant peptide bis-alanylalanyl-phenylalanyl-rhodamine 110 measures the activity of dead-cell proteases that are released when cells die. The Caspase-Glo portion of the assay provides a luminogenic caspase 3/7 substrate that measures caspase activity through luciferase activity after cell lysis. Cells were treated as in the CellTiter-Glo Assay, then on the day of the assay, 20 µL of Cytotoxicity Reagent was added to all wells. The plate was placed on an orbital shaker for ~30 seconds, then incubated for 30 minutes at 37°C and fluorescence was measured at 485 $nm_{ex}$/520 $nm_{em}$ for cytotoxicity. 100 µL of Caspase-Glo 3/7 Reagent was then added to each well of the no insulin groups and the cells were placed on an orbital shaker for ~30 seconds before incubation for 30 minutes at room temperature. Luminescence was measured in a SpectraMax GeminiEM plate reader.

Mitchondrial ToxGlo™ Assay (Promega Cat#G8000)

Manufacturer's protocol was followed. Cells were treated as in the CellTiter-Glo® Assay. On the day of the assay, 5x Cytotoxicity Reagent was prepared with pre-warmed bis-AAF-R110 and

Assay Buffer and 2x ATP Detection Reagent was prepared from lyophilized ATP Detection Reagent and ATP Detection Buffer. 20 μL of cytotoxicity reagent was administered to each well of 100 μL media. The plate was mixed and incubated at 37°C for 30 minutes before being read at 485 $nm_{ex}$/520 $nm_{em}$. Next, 100 μL of room-temperature ATP Detection Reagent was added to each well and the plate was placed on an orbital shaker for 5 minutes before luminescence was measured in the SpectraMax GeminiEM plate reader.

*Intramyocellular Lipid Accumulation*

AdipoRed Assay Reagent (Lonza, Walkersville, MD, USA) was used to measure intracellular lipid content on differentiated C2C12 cells according to the manufacturer's protocol. C2C12 cells were grown and treated as in the cell viability assays. On the day of the assay, media were removed, cells were washed with PBS, and each well was filled with 200 μL PBS. 5 μL of AdipoRed Assay Reagent was added to each well with a multichannel pipet and the plate was placed on an orbital shaker for 2 minutes to mix contents. Cells were then incubated at room temperature for 10 minutes before reading in a SpectraMax GeminiEM plate reader (485 $nm_{ex}$/ 572 $nm_{em}$).

*Glucose Uptake Assay*

Glucose Colorimetric Assay Kit (Cayman Chemical Item No. 10009582) was used to determine glucose concentration in the media after incubation with treatment. Cells were treated as in the CellTiter-Glo® Assay then media was transferred to a new 96 well plate and centrifuged at 3148xg for 10 minutes. 2 μL of media from each well was added to a corresponding well of a flat-bottomed clear 96 well plate. Glucose standards were created in 50 mM sodium phosphate ranging from 7.8125 mg/dL to 125 mg/dL. 2 μL of a blank (50 mM sodium phosphate) and each

standard was loaded into the first column of the 96 well plate. The glucose colorimetric enzyme mixture (Cayman Chemicals item #10010100) was reconstituted in 12 mL of 50 mM sodium phosphate. 100 μL of this glucose colorimetric enzyme mixture was added to each well of the 96 well plate containing standards and samples and the plate was mixed on an orbital shaker before being incubated for 10 minutes at 37°C. The absorbance was read at 510 nm (VersaMax, Molecular Devices).

*ROS Measurement*

2 ,7 -dichlorodihydrofluorescein diacetate (DCFDA, Sigma-Aldrich, Cat#D6883), a cell-permeable dye, was used to quantify ROS in differentiated C2C12 myotubes. DCFDA is deacetylated by intracellular esterases to the non-fluorescent compound 2 ,7 -dichlorodihydrofluorescein, which is then oxidized by hydroxyl, peroxyl and other ROSs into the fluorescent 2 ,7 -dichlorofluorescein (DCF). Stock DCFDA was dissolved in DMSO at 20 mM and stored at -80°C until use, where it was diluted in pre-warmed PBS to 20 μM. Cells were treated as in the CellTiter-Glo® Assay. Afterwards, all media was removed and 100 μL of working DCFDA solution was added to each well. The cells were incubated for 30 minutes at 37°C, 5% $CO_2$ before measuring fluorescence at 495 $nm_{ex}$/529 $nm_{em}$ (SpectraMax Gemini EM).

*Oxygen Consumption Rate*

C2C12 myotubes were cultured at ~$5x10^4$ cells/well in a XFe96 Analyzer plate (Seahorse Bioscience). After 3 days on differentiation media, cells were put in either 0.5 mM Palmitate or 0.5 mM BSA in low-glucose (1 g/L) DMEM for 12 hours. Then media was replaced with treatment with or without 1 mM insulin in low glucose DMEM (plain 0.5 mM Palmitate (P), (P) + 1 μM EA, (P) + 20 μM EA, (P) + 1 μM UA, (P) + 20 μM UA, (P) + 1 μM EA&UA, (P) + 20

μM EA&UA, plain 0.5 mM BSA (B), (B) + 1 μM EA, (B) + 20 μM EA, (B) + 1 μM UA, (B) + 20 μM UA, (B) + 1 μM EA&UA, or (B) + 20 μM EA&UA, with at least 3 biological replicates for each condition). Before running the assay, media with treatment was replaced with Seahorse assay medium (8 mM glucose, 2 mM glutamine, 2 mM pyruvate). Seahorse assay medium is non-buffered for measuring proton production. Plates were equilibrated in this medium for 1 hour at 37°C with no $CO_2$. The same media was used as vehicle for injection compounds. The analyzer sequentially injected the following compounds: Port A: oligomycin (2.5 μM final concentration), which blocks ATP synthase and shows the OCR dedicated to ATP production; Port B: carbonyl cyanide 4- (trifluoromethoxy) phenylhydrazone (FCCP: 0.5 μM final concentration), which permeabilizes the inner mitochondrial membrane and shows maximal OCR; Port C: FCCP (0.9 μM final concentration); and Antimycin A and rotenone (4 μM final concentration), which blocks complex I and shows NADH-driven OCR. OCR was measured at four time points during basal respiration, and five after each injection using a Seahorse XFe96 Flux Analyzer (Seahorse Biosciences). OCR measurement were normalized to cell counts.

(Protocol modified from Mclean et al. (71))

*Statistical Analysis*

All data are represented as means ± SD with each group containing at least three biological replicates. SPSS Version 25 (SPSS, Inc. Chicago, Illinois) was used for all statistical analyses. All data except mouse IPITT at 120 minutes were normally distributed and analyzed using one-way ANOVA for multiple comparisons with LSD post-hoc analysis. The Kruskal-Wallis 1-way ANOVA test for not normally distributed data was used for mouse IPITT data at 120 minutes. $p < 0.05$ was considered significant.

## Results

*In Vivo Studies*

*Mouse Characterization*

To assess the efficacy of ellagic acid and urolithin A as treatments for diet-induced insulin resistance, male DBA/2J mice were used as an in vivo model system. Before beginning the study, all mice were verified to be unable to produce UA from EA (non-UA producer metabotype). Then they were grouped into six groups: Low Fat/Low Sucrose Diet (LF/LS), High Fat/High Sucrose Diet (HF/HS), HF/HS + 0.1% Ellagic Acid Diet (EA), HF/HS + 0.1% Urolothin A Diet (UA), HF/HS + 0.1% EA + 0.1% UA Diet (EA&UA), and HF/HS + 0.15% Metformin Diet (Met). A diagram of the experimental design is given in Figure 2. At the end of the study, there were no significant differences in the body weights of HF/HS mice and any of the HF/HS + treatment mice, although all were significantly greater than LF/LS control mice. Food intake was also unaffected by treatment on HF/HS mice (Figure 3).

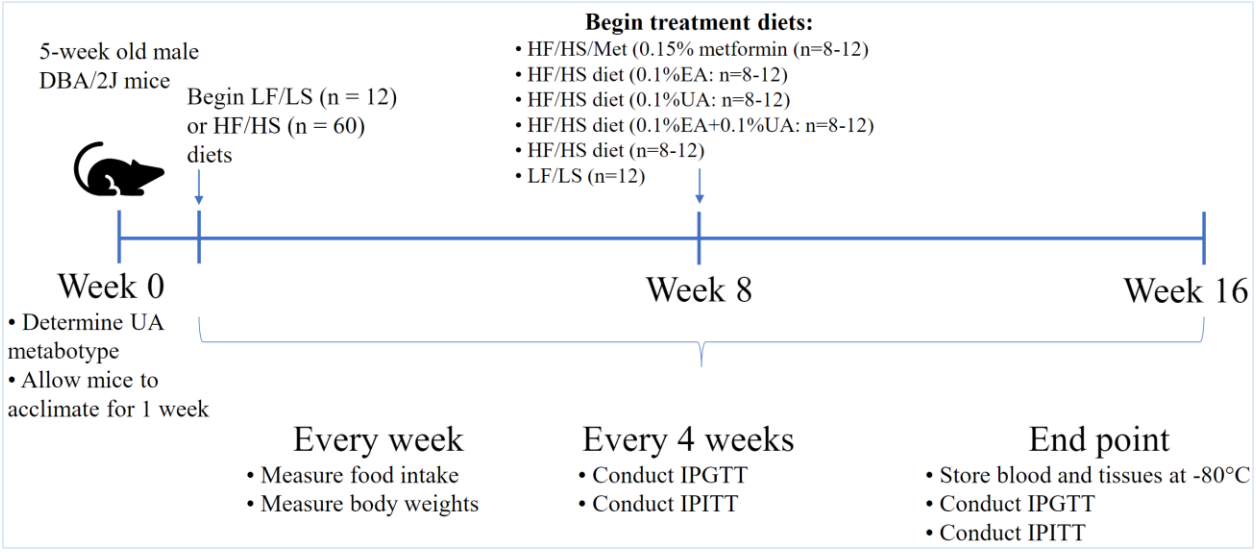


**Figure 2.** Experimental design of in vivo mouse study.

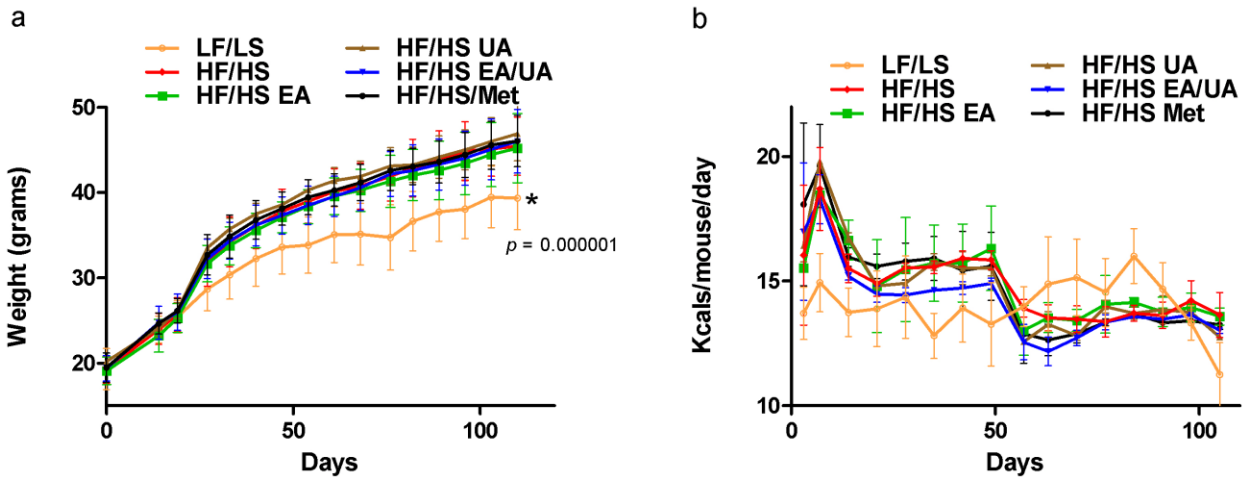


**Figure 3.** (a) Body weights and (b) food intake from baseline to end of 16-week study. Data are represented as mean ± SD. (n = 6-8 for all conditions, p values < 0.05 between group and HF/HS group are displayed and noted with an *)

To verify mice were insulin resistant at the start of treatment administration, intraperitoneal glucose and insulin tolerance tests (IPGTT and IPITT, respectively) were administered at week eight, before the diets were changed to HF/HS + treatment. Before assigning mice to LF/LS and HF/HS groups, glucose and insulin tolerance of all mice were the same (Figure 4). However, blood glucose levels were significantly higher at 15, 30, 60, and 120 minutes after both glucose and insulin injection in HF/HS mice compared to LF/LS mice with 8 weeks of their different diets (Figure 4). Thus, HF/HS mice were significantly more insulin resistant than LF/LS mice before starting treatment.

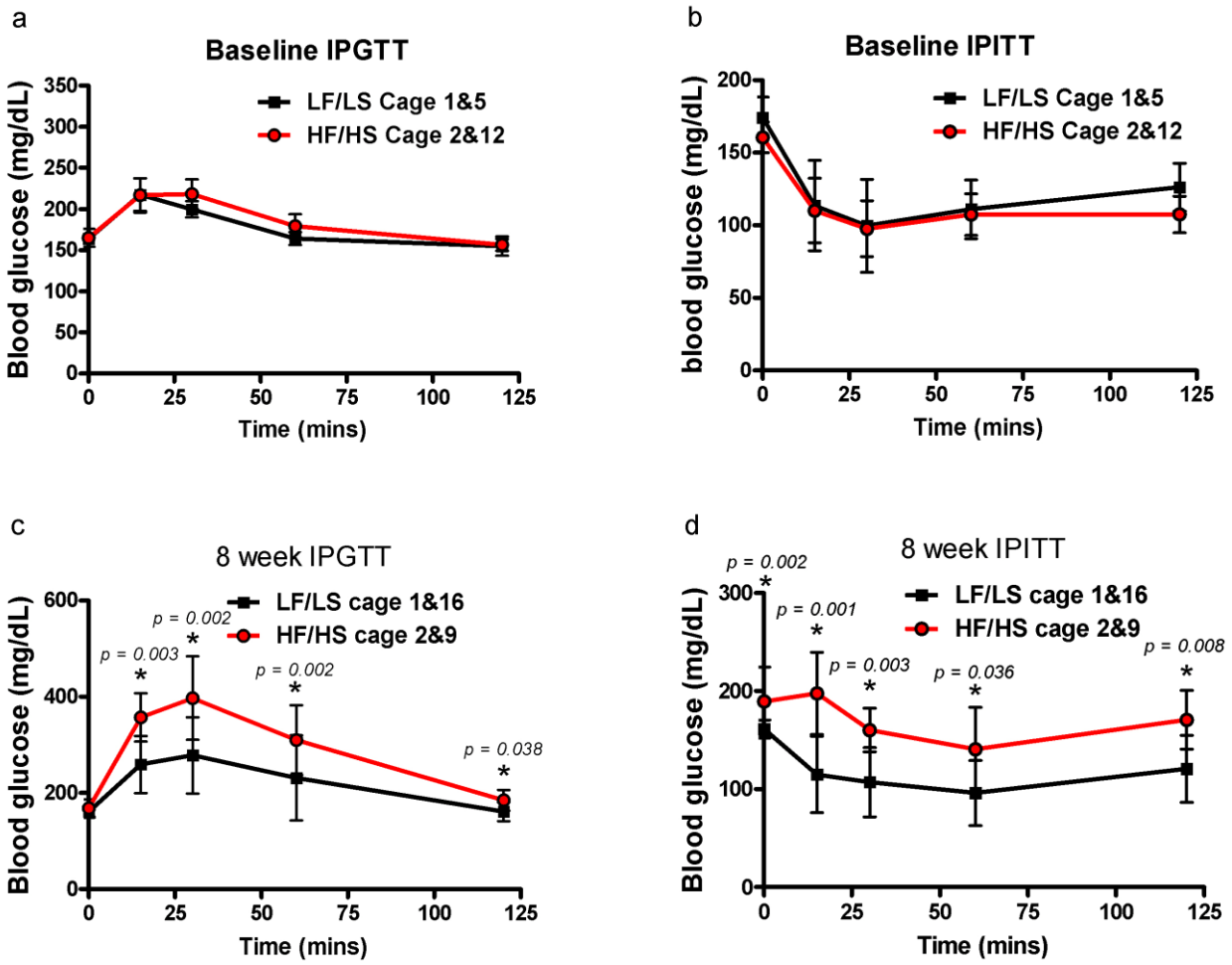


**Figure 4.** Baseline and 8-week IPGTT and IPITTs. Mice were fasted for 6 hours prior to IPGTT and IPITTs. (a) Baseline IPGTTs and (b) IPITTs for 4 cages before administering LF/LS and HF/HS diets. (c) IPGTTs and (d) IPITTs for 2 LF/LS diet cages and 2 HF/HS cages after 8 weeks on different diets. Data are represented as mean ± SD. (n = 8 for each group, p values < 0.05 between LF/LS and HF/HS groups are displayed and noted with *)

*EA&UA combination treatment improves insulin tolerance*

At the end of the 16-week study, the mice were given a final set of IPGTT and IPITTs. Blood glucose levels displayed no significant differences in glucose tolerance tests (data not shown). However, in IPITTS, there were significant decreases in blood glucose relative to initial levels at

the 15 and 120-minute time points for EA&UA combination treatment mice compared to HF/HS controls (Figure 5).

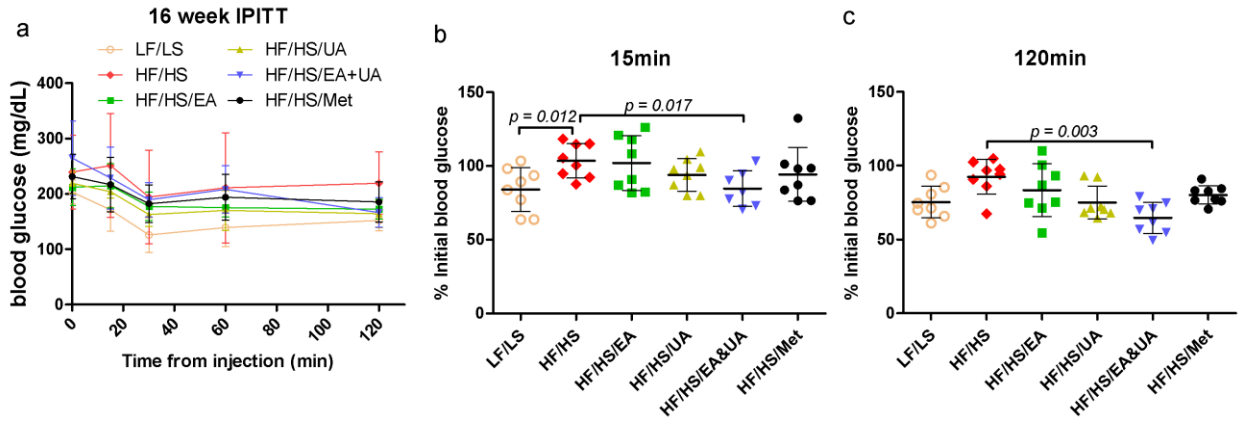


**Figure 5.** IPITTs at end of 16-week study in mice fed LF/LS, HF/HS, and HF/HS + treatment diets. (a) IPITTs with time points taken at 15, 30, 60, and 120 minutes after insulin injection. (b) Glucose levels at 15 minutes after insulin injection as percentages of initial glucose levels. (c) Glucose levels at 120 minutes after insulin injection as percentages of initial glucose levels. Mice were fasted for 6 hours prior to IPITTs. Data are represented as mean ± SD. (n = 8 for all conditions, p values < 0.05 between group and HF/HS group are displayed)

*Treatment Improves Serum Markers of Insulin Resistance*

Although the focus of this project was on skeletal muscle, several blood serum markers are worth noting. Blood was collected upon sacrificing mice at the end of the study. Serum free fatty acid (FFA) and fasting glucose levels were significantly lower in all treatment groups except EA as compared to HF/HS mice while serum adiponectin levels were significantly increased in UA and Met mice at the end of the study (Figure 6).

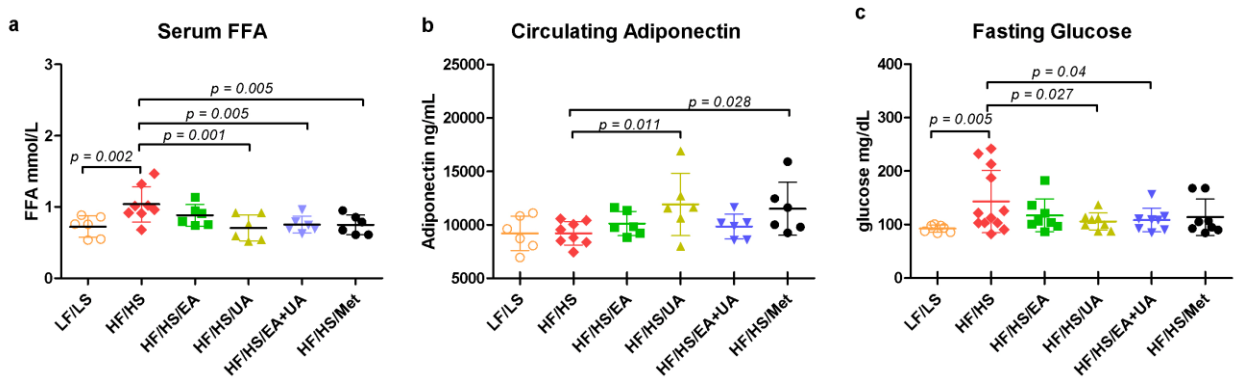


**Figure 6.** Treatment improves serum markers of insulin sensitivity. Serum (a) free fatty acid, (b) adiponectin, and (c) fasting glucose levels at end of study. Blood was collected by cardiac puncture immediately after mice were sacrificed at the end of the 16-week study and prepared prior to freezing at -80°C. Bars represent mean ± SD. (n = 6-8 for all conditions, p values < 0.05 between group and HF/HS are displayed)

*HF/HS Diet had No Effect on Inflammatory Markers in Skeletal Muscle*

Skeletal muscle from the hind legs were stored at -80°C for further analysis. mRNA levels of the inflammatory markers TNF-α and MCP-1 were not significantly different between LF/LS and any of the HF/HS groups in skeletal muscle (Supplementary Figure S1). This contradicts previous findings that a high-fat diet significantly increases TNF-α expression in skeletal muscle (72) and that EA inhibits TNF-α-induced MCP-1 expression (73). However, these results do comply with another study which found no change in TNF-α and MCP-1 levels when raspberry extracts, which are high in EA, were administered to mice on a high fat diet (74).

*HF/HS Diet had No Effect on Intramyocellular Lipids*

None of the analyzed intramyocellular lipids from the frozen muscle exhibited significant differences, which consisted of FFAs, TGs, and cholesterol, even compared to LF/LS mice

(Supplementary Figure S2). This was surprising, as intramyocellular lipid content was found to be positively correlated with insulin resistance (75). However, the lack of difference in this study may have been due to inconsistent muscle sampling, as skeletal muscle is not all homogeneous and some extracellular fat was unable to be removed prior to freezing, perhaps compromising the accuracy of the lipid extraction.

*Treatment Improves Markers of Fatty Acid Regulation*

Since fatty acids play a large role in insulin resistance, measures of fatty acid transport and storage in skeletal muscle were analyzed by qPCR (Figure 7). Fatty acid synthase (FAS) showed no significant differences between groups, cluster of differentiation 36 (CD36, also known as fatty acid translocase, FAT) levels were all higher in treatment groups, but only reached significance in EA&UA and Met mice. Peroxisome proliferator-activated receptor gamma (PPARγ) which induces fatty acid oxidation and white adipose cell differentiation, was reduced in all treatment groups but only reached significance in the EA&UA group.

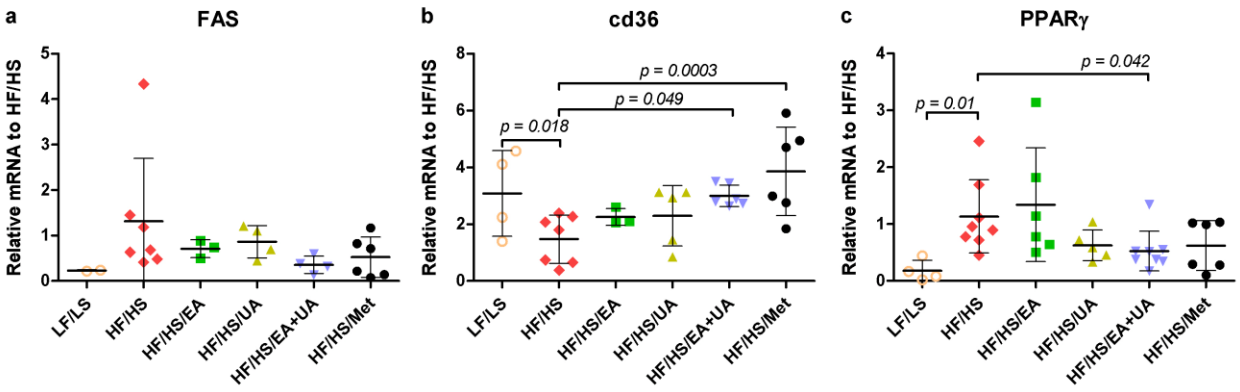


**Figure 7.** qPCR data for (a) Fatty Acid Synthase (FAS), (b) Fatty Acid Translocase (cd36), and (c) Proliferator-Activated Receptor γ (PPARγ) in skeletal muscle. Expression values are given

relative to HF/HS group. Bars represent mean ± SD. (n = 6-8 for all conditions, p values < 0.05 between group and HF/HS are displayed)

*Treatment Increased Markers of Mitochondrial Biogenesis and Mitophagy*

Overall mitochondrial content was determined by comparing mtDNA to nuclear DNA. Mitochondria have their own genetic material which encodes several ETC subunits, rRNAs, and tRNAs that are required to produce mitochondrial proteins. Cyclophilin A is encoded in nuclear DNA on chromosome 7 while cytochrome c oxidase subunit 2 (COX-2) is encoded in mtDNA (76). Mitochondrial content was decreased in HF/HS mice, and UA treatment significantly increased abundance. ATP synthase catalyzes the last step of oxidative phosphorylation by phosphorylating ADP to produce ATP. It consists of 16 subunits, which make up the catalytic $F_1$ domain and the transmembrane $F_0$ domain that shuttles protons into the mitochondrial matrix. ATP6 is one of the mitochondrially encoded polypeptides that comprise the $F_0$ domain required for proper ATP synthase assembly (77). HF/HS feeding significantly decreased ATP6 and all treatments except EA increased these levels to almost LF/LS abundance, being significantly higher than HF/HS mice (Figure 8).

Expression levels of genes associated with mitochondrial biogenesis had an increasing trend in treatment groups compared to the HF/HS control group. PGC1α is an important transcriptional coactivator involved in upregulating mitochondrial biogenesis and metabolism. PGC1α had an increasing trend in treatment groups, but the difference only reached significance in Metformin mice. Estrogen-related receptor α (ERRα) has been found to be involved in mitochondrial metabolism and biogenesis. ERRα was significantly lower in HF/HS mice compared to LF/LS mice and EA&UA and Metformin treatment significantly increased these levels but all

experimental mice were still below LF/LS mice. Although levels of Nrf2, a transcription factor that increases mitochondrial biogenesis and maintains ROS homeostasis (78), were not significantly lower in HF/HS mice compared to LF/LS mice, EA&UA and Metformin significantly increased these levels relative to HF/HS mice, reaching levels higher than LF/LS mice. Mitochondrial Transcription Factor A (TFAM) was drastically lower in HF/HS mice, and all treatments except EA significantly increased these levels. Mitofusin 1 and Mitofusin 2 (Mfn1 and Mfn2) are proteins on the outer mitochondrial membrane required for mitochondrial fusion, a process that is especially important to protect against damage to mitochondrial DNA or other mitochondrial components. UA and UA&EA treatment increased levels of Mfn2 mRNA to that of LF/LS mice or higher. Metformin was the most effective at returning levels to that of LF/LS mice for all genes, although EA&UA treatment appeared as effective for Nrf2 (Figure 8).

PINK and parkin are proteins upregulated in mitophagy. Our results support that mitophagy is downregulated in insulin resistant mice and treatment increases these levels. Yet, only EA&UA combination treatment and Metformin significantly increased levels of both markers (Figure 8).

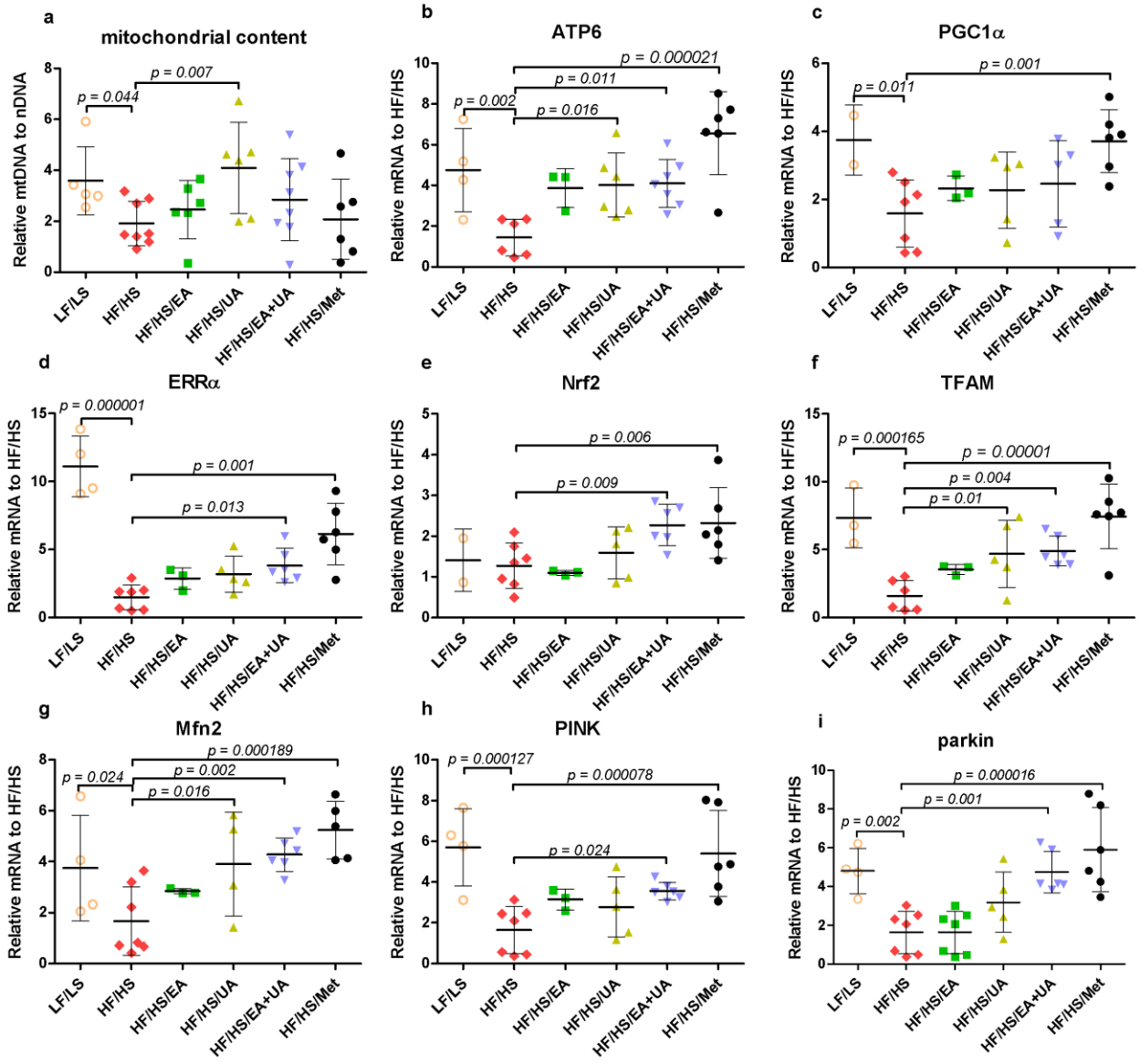


**Figure 8.** Markers of mitochondrial biosynthesis and function in skeletal muscle. (a) Mitochondrial content was calculated by comparing mtDNA to nuDNA abundance, (b) ATP6 is a subunit of ATP Synthase, (c) PGC1α, (d) ERR α, (e) Nrf2, and (f) TFAM are factors necessary for mitochondrial biosynthesis, (g) Mfn2 is involved in mitochondrial fusion, (h) PINK and (i) parkin are involved in mitophagy. Bars represent mean ± SD. (n = 6-8 for all conditions, p values < 0.05 between group and HF/HS are displayed)

*Treatment Increases Expression of ROS Detoxification Enzymes*

In addition to less efficient oxidative phosphorylation, mitochondrial dysfunction can also be characterized by an increased ROS production and/or lowered detoxification activity. Abundance of enzymes that detoxify the cell of ROS can serve as a surrogate for ROS levels. Our data show that PrdxIII was downregulated in HF/HS mice and treatment increased these levels, with significant improvement in the EA&UA and Metformin groups (Figure 9).

Superoxide dismutase (SOD) metalloenzymes carry out redox reactions where the superoxide radical ($O_{2}^{\cdot -}$) is simultaneously reduced and oxidized to $O_2$ and $H_2O_2$. SOD1 is present in the cytoplasm, whereas SOD2 acts in the mitochondrial matrix (79). Catalase or glutathione peroxidase then converts $H_2O_2$ to water, removing the ROS from the cell. There were no significant differences in catalase mRNA levels between the groups, but SOD1 and SOD2 were significantly lower in HF/HS mice compared to LF/LS mice. UA, EA&UA, and Metformin treatment increased both SOD1 and SOD2 levels (Figure 9).

Uncoupling Protein 3 (UCP3), a protein that assists in the transfer of anions across the inner mitochondrial membrane, is downregulated in diabetic and prediabetic individuals. UCP3 is predominantly expressed in skeletal muscle but is also found in brown adipose tissue, cardiac muscle, and parts of the brain. One study found that moderate increases in UCP3 increased fatty acid oxidation without affecting glucose metabolism and decreased ROS production in a non-uncoupling-dependent manner (80). UCP3 was downregulated in HF/HS mice, which is in line with the finding that UCP3 mRNA was reduced by about 50% in T2DM patients (81). Treatment increased these levels, with EA&UA and Metformin treatment reaching significance. Metformin

raised all detoxifying enzyme and UCP3 levels to LF/LS values or higher, being more potent than any of the EA or UA treatments (Figure 9).

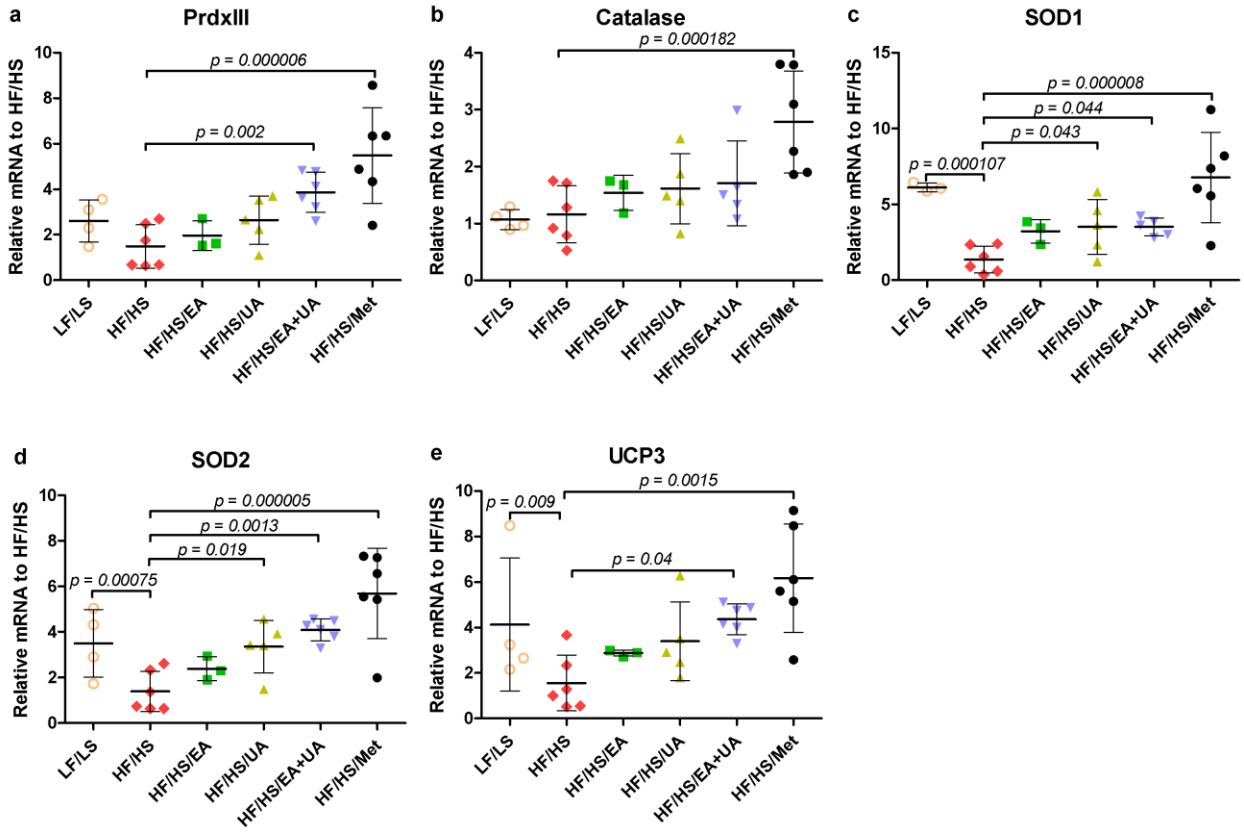


**Figure 9.** Markers of ROS content and detoxification. (a) PrdxIII and (d) SOD2 are ROS detoxifiers in the mitochondria, (b) catalase in the peroxisome, and (c) SOD1 in the cytoplasm. (e) UCP3 dissipates the proton motive force by uncoupling proton movement with ATP production. Data are represented as mean ± SD. (n = 3-8 for all conditions, p values < 0.05 between group and HF/HS are displayed)

Histology was performed on skeletal muscle from hind legs stored in formalin. There were no significant differences between the groups (Supplementary Figure S3).

*In vitro studies*

To further study the effects of EA, UA, and their combination on insulin resistance in skeletal muscle, C2C12 mouse myoblasts (skeletal muscle progenitor cells) were cultured and differentiated. C2C12 myoblasts were grown in growth media until confluent, then switched to differentiation media for 4-5 days until the myoblasts were fully differentiated into myotubes. Cells were treated with either only 0.75 mM palmitate conjugated to BSA in low glucose (1 g/L) DMEM (P), (P) + 1 μM EA, (P) + 20 μM EA, (P) + 1 μM UA, (P) + 20 μM UA, (P) + 1 μM EA & 1 μM UA, (P) + 20 μM EA & 20 μM UA, or plain 0.75 mM BSA (non-insulin resistant control) for all cell assays excluding the Seahorse Assay, where 0.5 mM palmitate-BSA and 0.5 mM BSA were used. The experimental design of in vitro assays is given in Figure 10.

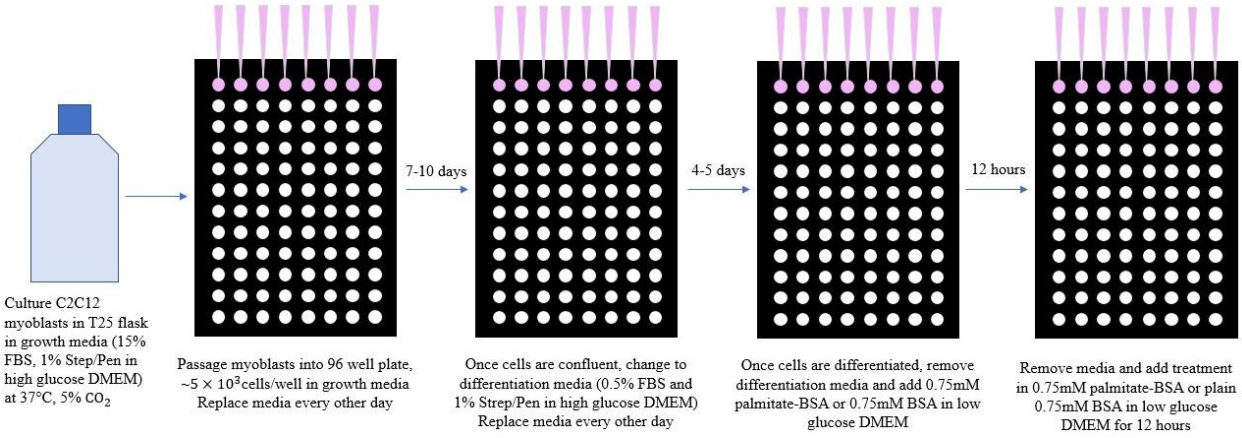

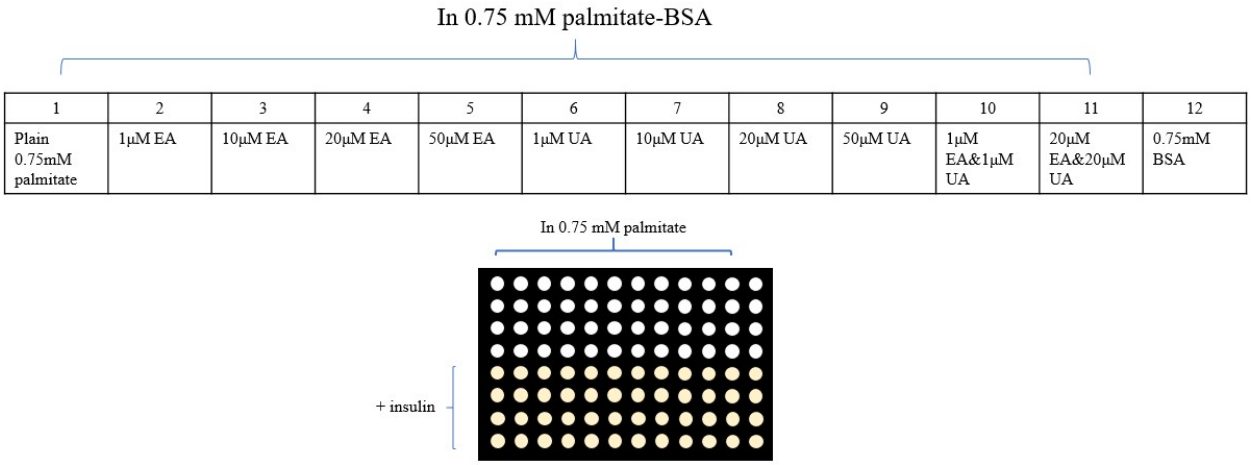


**Figure 10.** Experimental design of C2C12 culture assays.

The in vitro qPCR data had great variability, likely because of small sample sizes (n = 3) and low RNA quality/yield. They were not consistent with the in vivo qPCR data. There was no significant difference between treatment and no treatment (plain palmitate) cells for PGC1α, Mfn2, or parkin. PINK was elevated in palmitate + 1 μM EA & 1 μM UA cells, while TFAM was elevated in palmitate + 20 μM UA cells (Supplementary Figure S4).

All measures of ROS detoxification were not significantly significant except for catalase, where 20 μM UA and 20 μM EA & 20 μM UA had significantly more expression. TNF-α also did not display significant differences in the treatment groups (Supplementary Figure S5).

*Treatment Increases Cellular Health and ATP Production without Affecting Viability*

Several measures of cell health and survival were assessed with Promega kits and MTT. Promega's CellTiter-Glo® Luminescent Cell Viability Assay detects the amount of ATP in a sample of cells which is meant to correlate with the number of live cells. Treatment increased ATP in almost all conditions except 1 μM EA (+ and - insulin), 1 μM UA (- insulin), 10 μM UA (- insulin), and 20 μM UA (- insulin) (Figure 11). The ATP detection portion of Promega's

Mitochondrial ToxGlo™ Assay was mostly consistent with this data, except UA had no significant increase in ATP at any level or condition, and neither did EA&UA at 1 μM (Supplementary Figure S7).

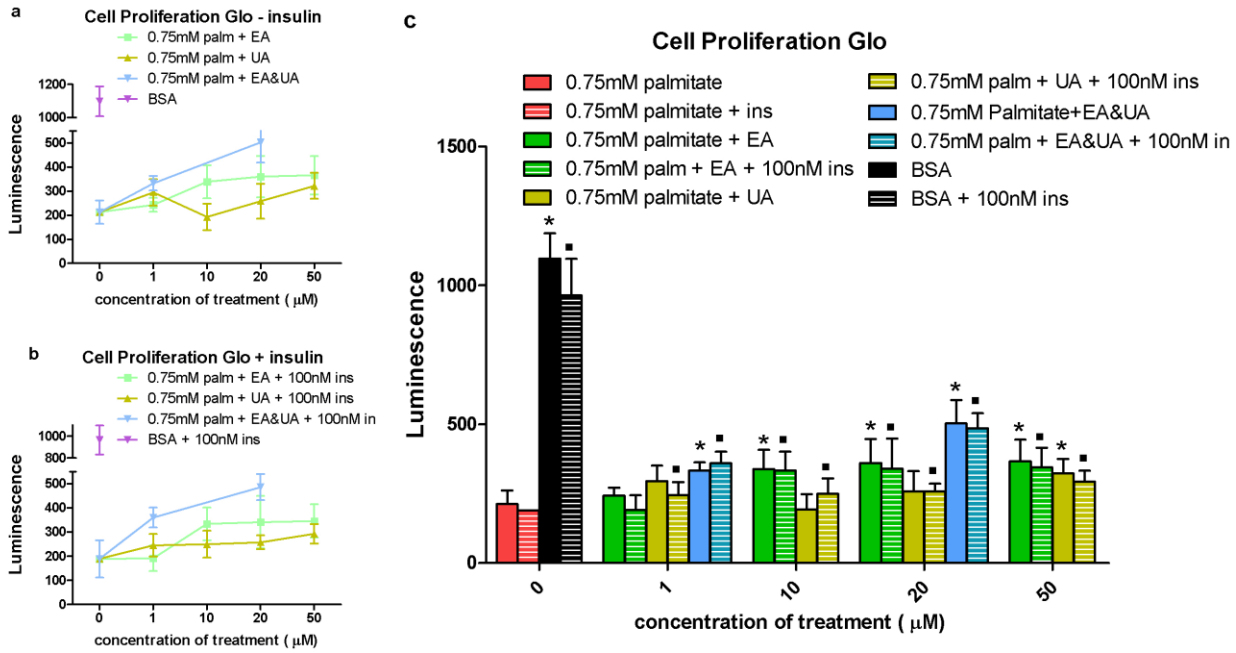


**Figure 11.** CellTiter-Glo® Luminescent Cell Viability Assay by Promega on 4-day differentiated C2C12 myotubes. Luminescence from cells treated (a) without insulin, (b) with 1 mM insulin during treatment, and (c) both with and without insulin. 4-day differentiated C2C12 myotubes were put on 0.75 mM palmitate in 1 g/L glucose DMEM for 12 hours, then on treatment with or without 1 mM insulin for 12 more hours. CellTiter-Glo measures abundance of ATP in samples, indicating amount of live cells. Data are represented as mean ± SD. (n = 3-4 for all conditions, * signifies $p < 0.05$ between (- insulin) groups and (- insulin) 0.75 mM palmitate group, ■ signifies $p < 0.05$ between (+ insulin) groups and (+ insulin) 0.75mM palmitate group)

3- (4,5-dimethylthiazol-2-yl)-2,5-diphenyl-2H-tetrazolium bromide (MTT) is a yellow compound that can be reduced by cellular NADPH-dependent oxidoreductases of live cells to an

insoluble purple formazan product. Cells endocytose MTT, which is then converted into needle-like formazan crystals at the cell surface. The formazan is then solubilized in SDS or DMSO, but DMSO made the media cloudy when it mixed with the palmitate, so 10% SDS was used in this study. The absorbance at 570 nm is proportional to the amount of metabolically active cells (82). Interestingly, treatment did not show the same effects in the MTT assay as the other viability assays from Promega. Only 1 μM UA with and without insulin showed significantly more cellular viability than the no-treatment palmitate group (Figure 12).

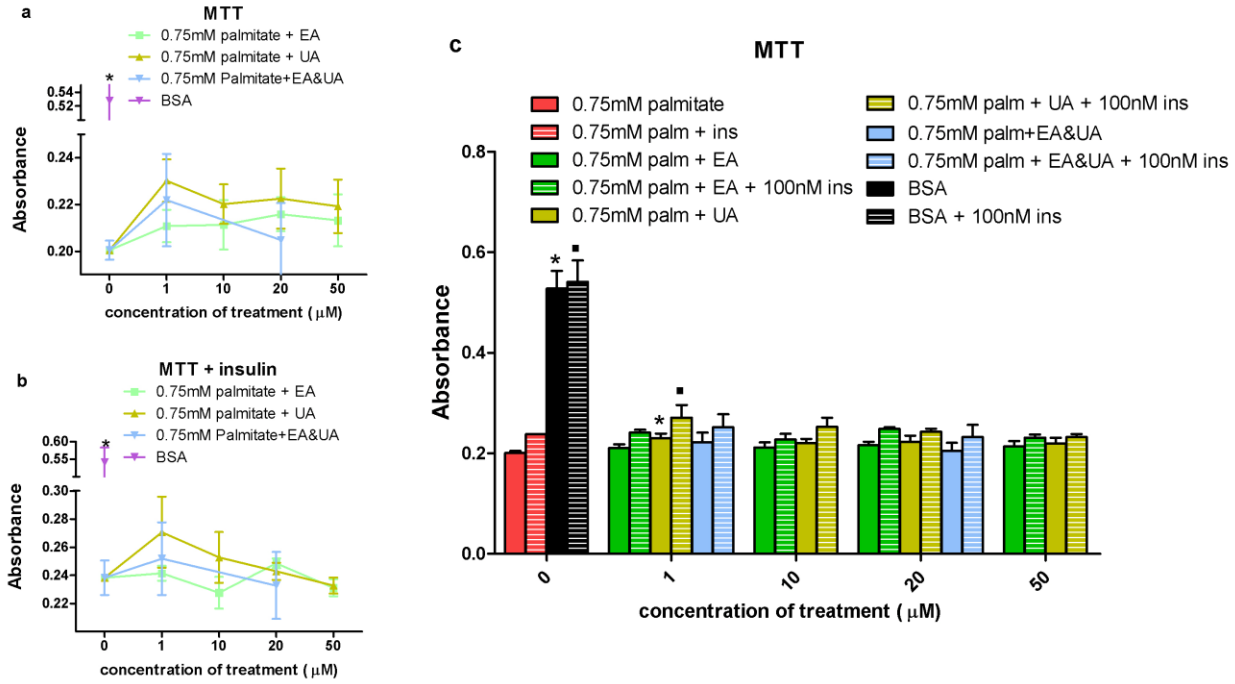


**Figure 12.** MTT viability assay on 4-day differentiated C2C12 myotubes. Absorbance of cells treated (a) without insulin, (b) with 100 nM insulin, and (c) both with and without insulin. MTT measures the amount of live cells by quantifying the activity of succinate dehydrogenase in live cells. Data are represented as mean ± SD. (n = 3-4 for all conditions, * signifies $p < 0.05$ between (- insulin) groups and (- insulin) 0.75 mM palmitate group and ■ signifies $p < 0.05$ between (+ insulin) groups and (+ insulin) 0.75mM palmitate group)

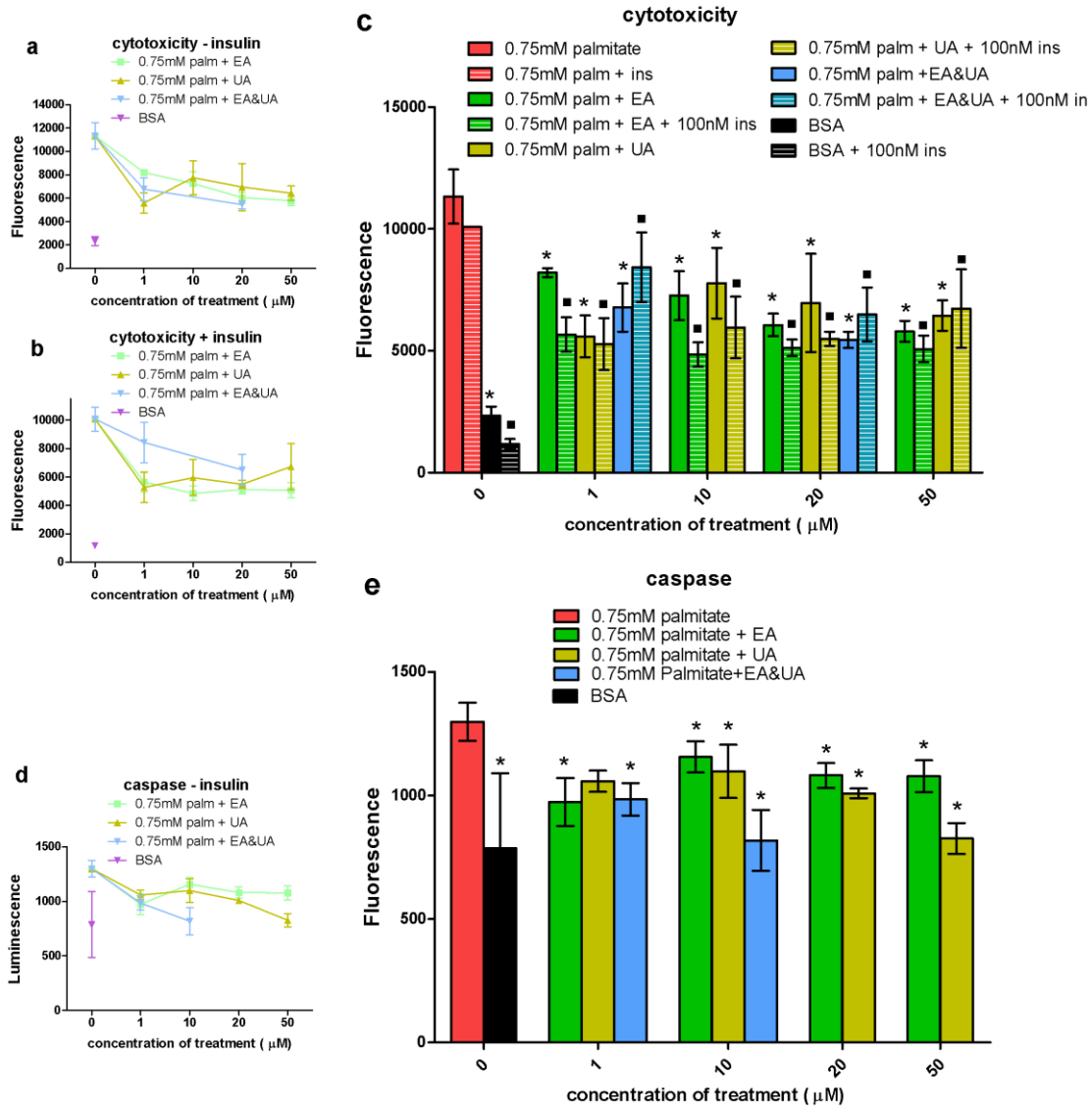


**Figure 13.** Promega Triplex Assay on 4-day differentiated C2C12 myotubes. (a), (b), and (c) Cytotoxicity was assessed with the cell-impermeant substrate bis-alanylalanyl-phenylalanyl-rhodamine 110. Fluorescence was measured at 485 $nm_{ex}$/520 $nm_{em}$ for cytotoxicity. (d) and (e) Caspase activity was measured with the luminogenic caspase 3/7 substrate which luminesces when cleaved by luciferase. Graphs are represented as mean ± SD. (n = 3-4 for all conditions, * signifies $p < 0.05$ between (- insulin) groups and (- insulin) 0.75 mM palmitate group and ■ signifies $p < 0.05$ between (+ insulin) groups and (+ insulin) 0.75mM palmitate group)

The ApoTox-Glo™ Triplex Assay by Promega was used to assess cytotoxicity and apotosis activity. A membrane-impermeable substrate is cleaved by proteases that are released by dead cells such that its fluorescence represents the abundance of dead cells. Apoptosis activity was assessed using a substrate that releases luciferin when cleaved by Caspase-3/7, which luminesces when cleaved by luciferase. Cytotoxicity was significantly decreased in all treatment conditions. Apotosis activity was decreased in all treatment conditions except for 1 μM UA (Figure 13).

*Treatment Decreases Fatty Acid Storage in Vitro*

As for measures of fatty acid storage, 1 μM UA & 1 μM EA treatment significantly increased both 3-hydroxy-3-methyl-glutaryl-CoA (HMG-CoA) reductase and PPARγ, while 20 μM EA significantly increased FAS (Supplementary Figure S6). HMG-CoA reductase is the rate-limiting enzyme in the cholesterol biosynthetic pathway. Its upregulation has been associated with suppression of hyperlipidemia and hyperinsulinemia found in rats on a high fat diet, possibly increasing cholesterol biosynthesis and the excretion of sterol and bile (83).

As an indication of intramyocellular lipid storage, the AdipoRed (Lonza) assay was performed on 4-day differentiated C2C12 myotubes. The AdipoRed reagent fluoresces in a hydrophobic environment and allows quantification of intracellular lipid content. BSA had the least amount of intracellular lipid content, and with the exceptions of combined EA&UA treatment, all other treatments significantly decreased intracellular lipid content in the presence of 0.75 mM palmitate and 1 mM insulin (Figure 14).

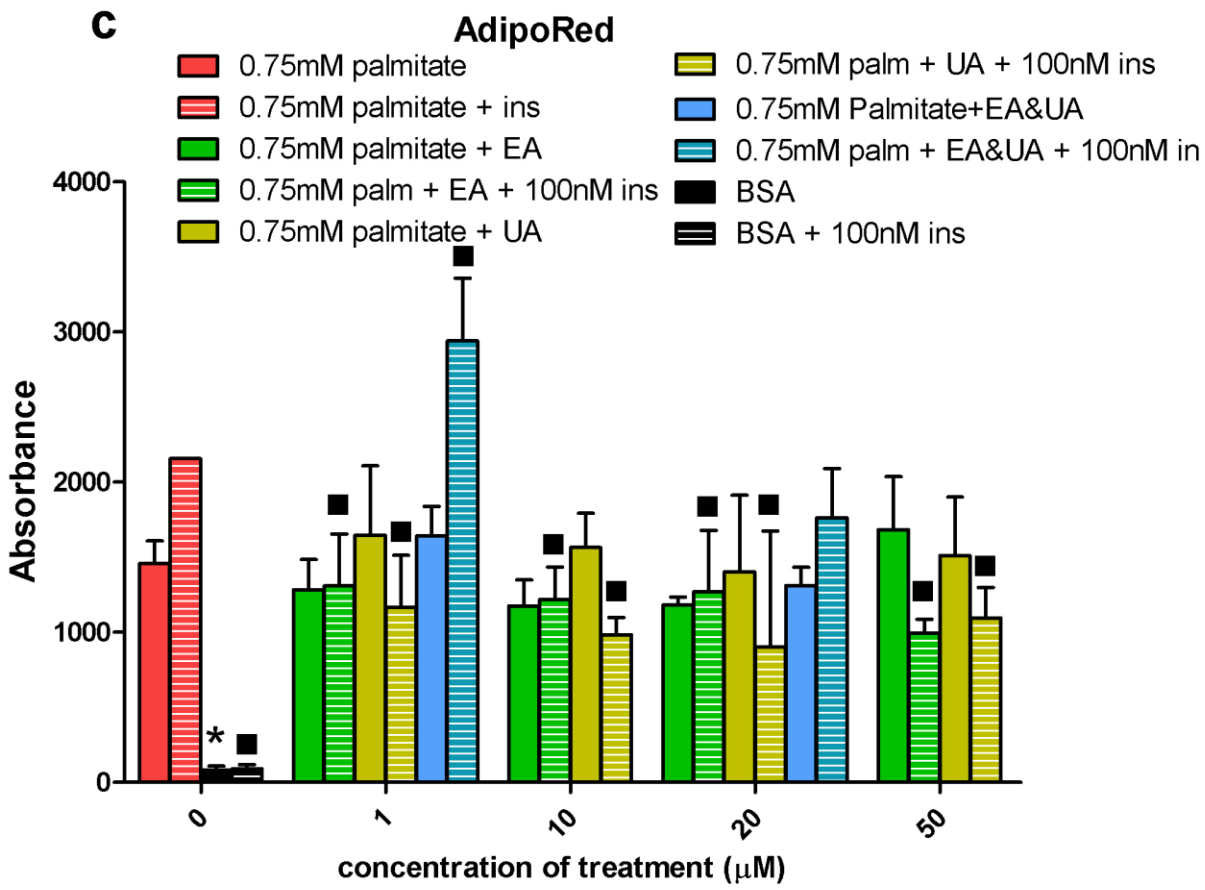


**Figure 14.** Lonza AdipoRed Assay on 4-day differentiated C2C12 myotubes. Intracellular triglyceride content was quantified by AdipoRed staining, which fluoresces in a hydrophobic environment. Data are represented as mean ± SD. (n = 3-4 for all conditions, * signifies $p < 0.05$ between (- insulin) groups and (- insulin) 0.75 mM palmitate group and ■ signifies $p < 0.05$ between (+ insulin) groups and (+ insulin) 0.75mM palmitate group)

*Treatment Differentially Affects Glucose Uptake*

Since EA was previously found to increase glucose uptake in adipose tissue and skeletal muscle (66) and insulin resistance is heavily dependent on glucose uptake in skeletal muscle, insulin-stimulated glucose uptake was assessed with EA, UA, and EA&UA treatment. 1 μM and 20 μM

UA and 1 μM EA&UA significantly decreased glucose uptake, while 10 μM EA, 20 μM EA&UA and 50 μM UA significantly increased glucose uptake (Figure 15).

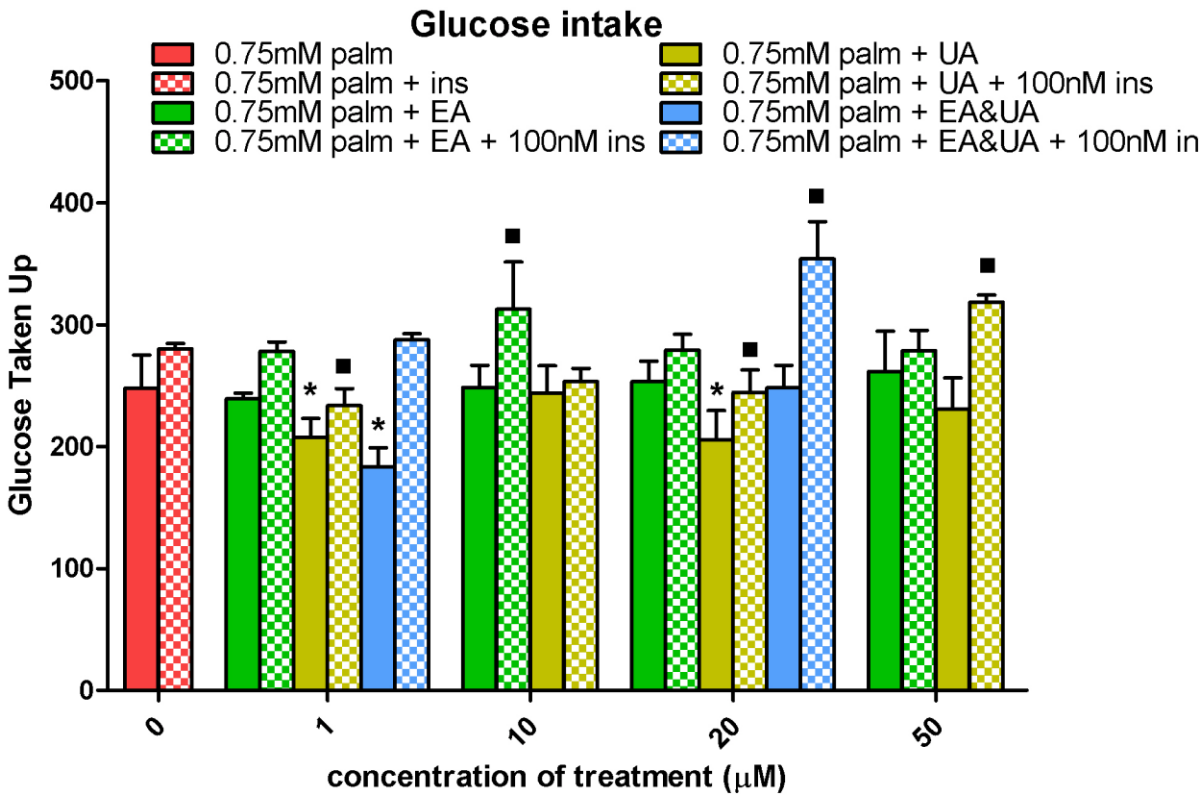


**Figure 15.** Glucose uptake in differentiated C2C12 myotubes. After 4 days of differentiation, media was changed to 0.75 mM palmitate or 0.75 mM BSA in 1 g/L glucose DMEM. After 12 hours, media was changed to treatment in 0.75 mM palmitate or plain 0.75 mM BSA + or - 100 nM insulin. Another 12 hours later, media was transferred into a clean 96 well plate. Glucose concentrations in the media of treated wells were subtracted from the no-cell control media to obtain glucose uptake levels. These values were normalized to cell numbers by dividing by MTT readings. Data are represented as mean ± SD. (n = 3-4 for all conditions, * signifies $p < 0.05$ between (- insulin) groups and (- insulin) 0.75 mM palmitate group and ■ signifies $p < 0.05$ between (+ insulin) groups and (+ insulin) 0.75mM palmitate group)

*Treatment Reduces ROS Levels in Vitro*

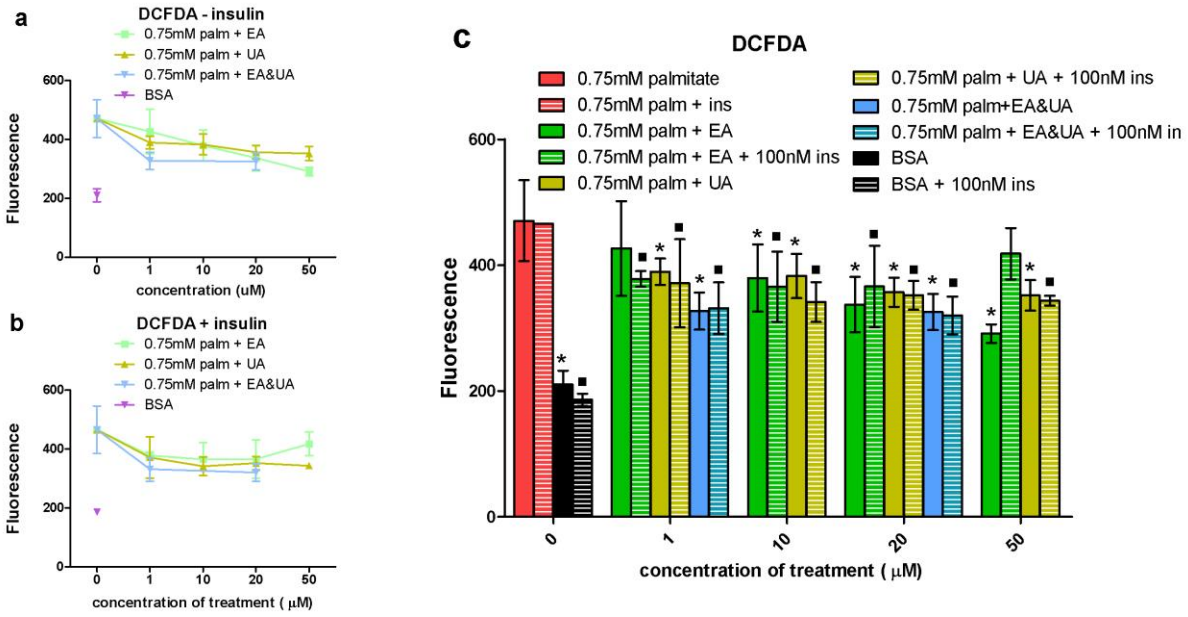


**Figure 16.** ROS levels as measured by the DCFDA Assay. Cells were treated as in glucose uptake assay. Fluorescence of cells treated (a) without insulin, (b) with insulin, and (c) both with and without insulin. Absorbance values were divided by MTT values to normalize. Data are represented as mean ± SD. (n = 3-4 for all conditions, * signifies $p < 0.05$ between (- insulin) groups and (- insulin) 0.75 mM palmitate group and ■ signifies $p < 0.05$ between (+ insulin) groups and (+ insulin) 0.75mM palmitate group)

2′-7′-Dichlorodihydrofluorescein diacetate (DCFH-DA or DCFDA) is a chemiluminescent probe commonly used to measure ROS in live cells. Intracellular esterases cleave DCFDA to release membrane-impermeable $H_2DCF$, which is not fluorescent but yields the highly fluorescent DCF when oxidized. The fluorescence at 485 $nm_{ex}$/530 $nm_{em}$ is proportional to the concentration of hydrogen peroxide in the cell (84). All treatment conditions significantly lowered ROS levels,

besides 1 μM EA without insulin and 50 μM EA with insulin (Figure 16). This is in line with the finding that EA and UA have antioxidant activities (85).

*Metabolic Function is Affected Differently in Palmitate vs BSA-Treated Cells by Treatment*

As a final determination of mitochondrial function, Seahorse XFe96 analysis was performed on differentiated C2C12 cells with various EA, UA, and EA&UA treatments in either 0.5 mM palmitate or 0.5 mM BSA with or without 1 mM insulin. Seahorse XF Analyzers measure oxygen consumption rates (OCRs) and extracellular acidification rates (ECARs) which can bring insight into cellular metabolism. However, ECAR measurements were unable to be optimized for the differentiated myotubes in this study, so only OCR data is presented.

Basal OCR is the amount of oxygen consumed under normal circumstances and is composed of ATP-synthesis derived oxygen consumption and proton leakage. After oligomycin is added, ATP synthase is inhibited and the resulting oxygen consumption (oligo-resistant OCR) reflects that used in proton leakage. From this, ATP-linked OCR can be calculated. Oxygen is consumed even when ATP Synthase is inhibited because of proton leakage, a small amount of which is due to diffusion across the lipid-bilayer while the majority is from translocating through ATP-synthase without coupling to ATP synthesis. Other proteins like uncoupling proteins (UCPs) regulate leakage in relation to heat formation and ROS production. Maximum OCR indicates the cell's ability to respond to an increased energy demand, which is not reflected in basal OCR. This maximal rate is measured by adding FCCP which dissipates the pmf by shuttling protons into the matrix, forcing an increased respiration to maintain the pmf. The spare capacity is the difference between maximal and basal OCR and reflects the ability of the cell to respond to stress that requires more ATP. Bioenergetic efficiency, also called coupling efficiency, is the

fraction of ATP-linked OCR over basal OCR and reflects how well the cell pairs oxygen consumption to ATP production (86).

Palmitate treatment affected cellular function, seen by comparing groups treated with BSA and palmitate alone (without EA and/or UA). Palmitate treatment significantly decreased spare capacity (Figure 17a). In the presence of 1 mM insulin, palmitate-treated cells had significantly lower max OCR and spare capacity. ATP-linked OCR was borderline significantly decreased with palmitate treatment ($p = 0.0497$) (Figure 17b).

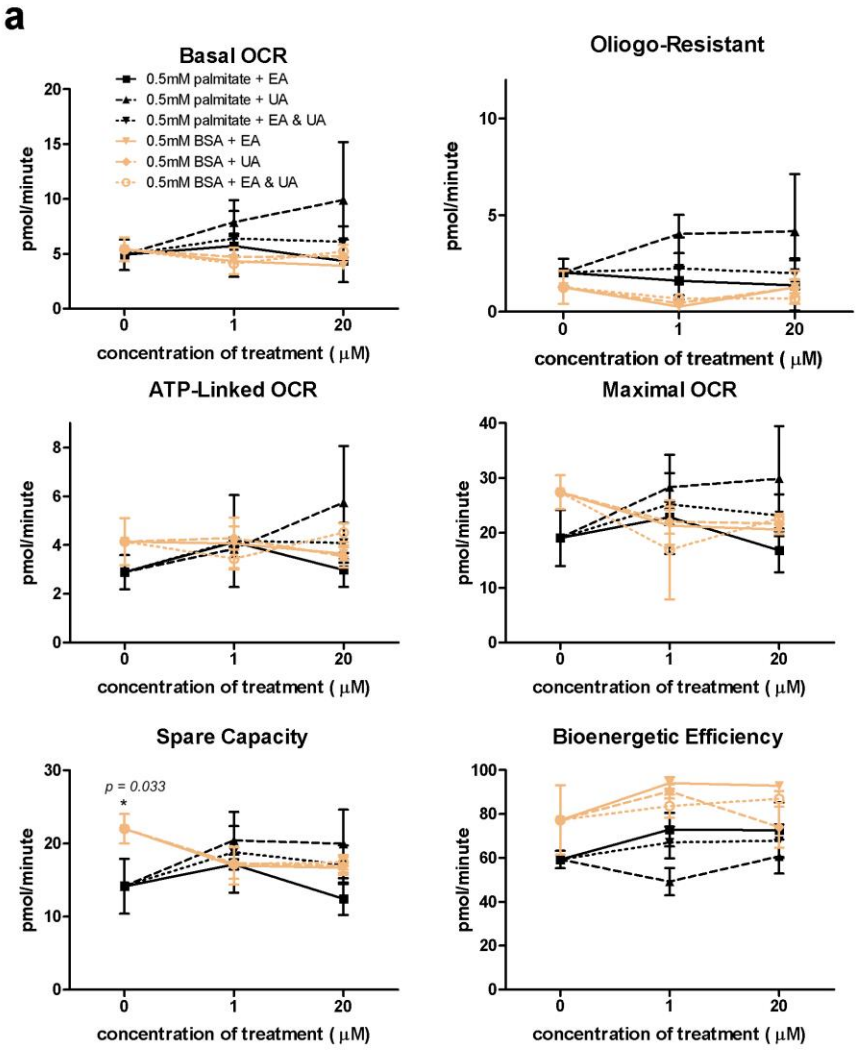

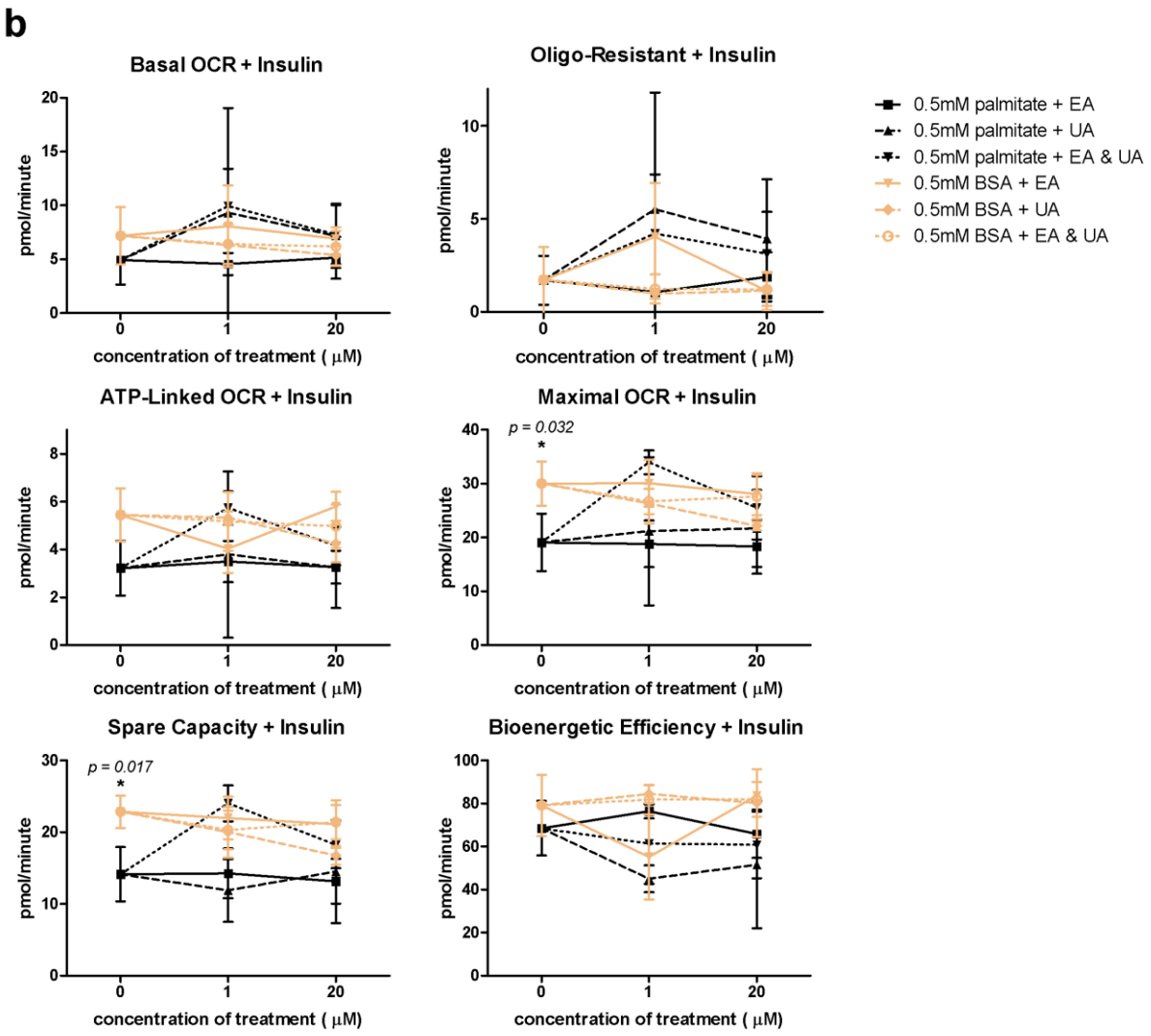


**Figure 17.** Cellular respiration data for 4-day differentiated C2C12 myotubes (a) without insulin and (b) with 1 mM insulin. Myoblasts were seeded at ~ $5x10^4$ cells/well in an XF96 plate and grown in growth media until confluent. Media was changed to differentiation media for 4 days until cells fused into myotubes, then media was changed to either 0.5 mM palmitate-BSA or 0.5 mM BSA in 1 g/L glucose DMEM. After 12 hours, treatment was administered in 0.5 mM palmitate-BSA or 0.5 mM BSA with or without 1 mM insulin for another 12 hours before conducting Seahorse Assays. Data are represented as mean ± SD. (n = 3-4 for all conditions, p values < 0.05 between plain BSA and plain palmitate groups are displayed)

In 0.5 mM BSA without insulin, treatment with 1 μM EA & 1 μM UA significantly decreased maximal OCR and spare capacity, while 1 μM EA, 20 μM EA, and 1 μM UA significantly increased bioenergetic efficiency. Maximal OCR and spare capacity seemed to decrease in all treatment groups compared to plain 0.5 mM BSA. Although not significant, treatments aside from 20 μM UA decreased oligo-resistant OCR, indicating reduced uncoupling (Figure 18).

With the addition of 1 mM insulin, 1 μM EA significantly decreased bioenergetic efficiency while 20 μM UA significantly decreased spare capacity. Oligo-resistant OCR was insignificantly increased by 1 μM EA, but seemingly lowered by other treatments (Figure 19).

Cells incubated with 0.5 mM palmitate had different responses to treatment. 20 μM UA significantly increased basal OCR and ATP-linked OCR, while 1 μM EA and 20 μM EA significantly increased bioenergetic efficiency. 1 μM UA and 20 μM UA significantly increased oligo-resistant OCR and maximal OCR, and 1 μM UA significantly increased spare capacity (Figure 20).

In the presence of 1 mM insulin, 1 μM UA significantly increase oligo-resistant OCR and significantly decreased bioenergetic efficiency, 1 μM EA & 1 μM UA treatment significantly increased ATP-linked OCR, maximal OCR, and spare capacity (Figure 21).

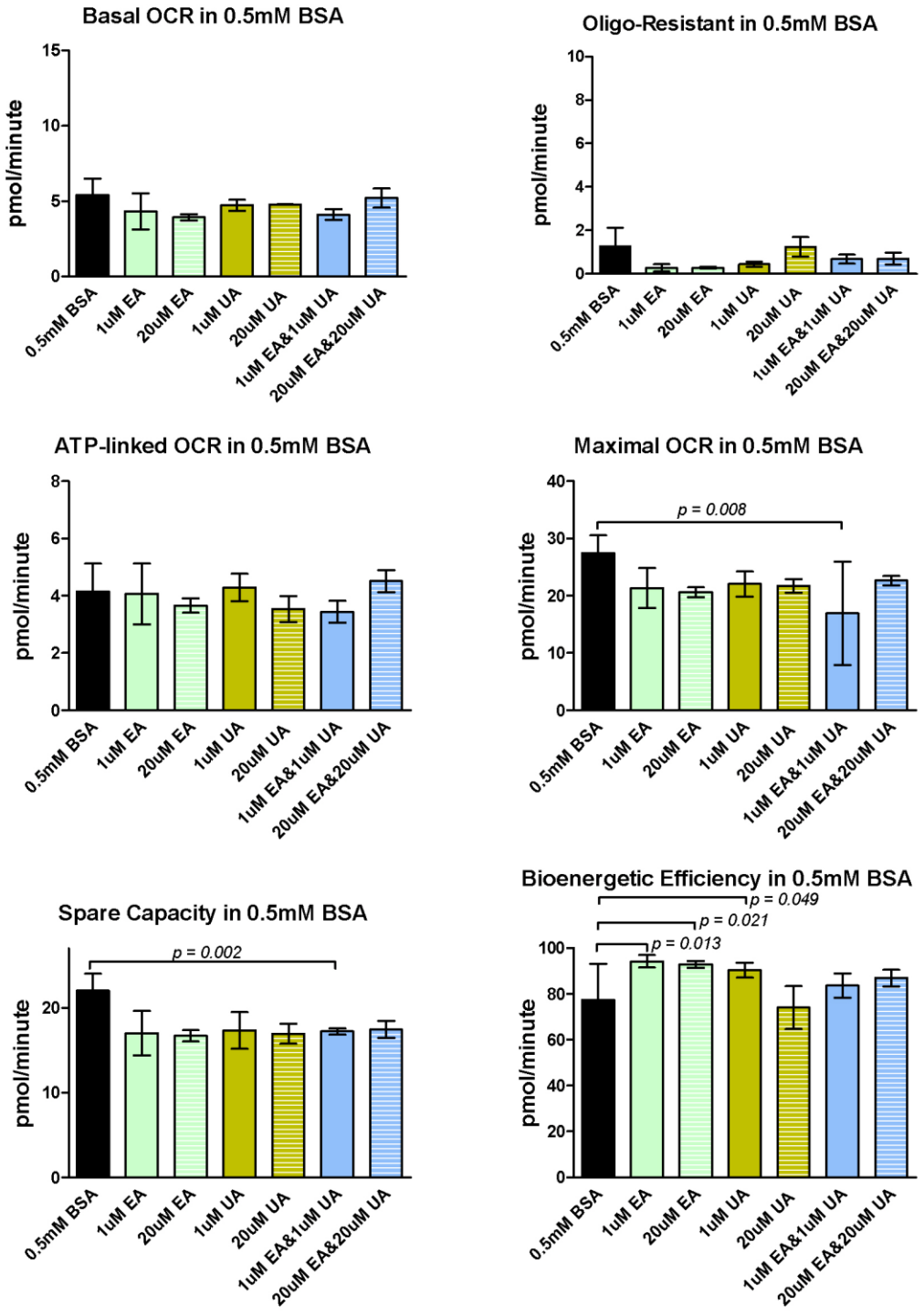


**Figure 18.** Seahorse Data for cells in 0.5 mM BSA without insulin. Data are represented as mean ± SD. (n = 3-4 for all conditions, p values < 0.05 with (- ins) 0.5 mM BSA group are displayed)

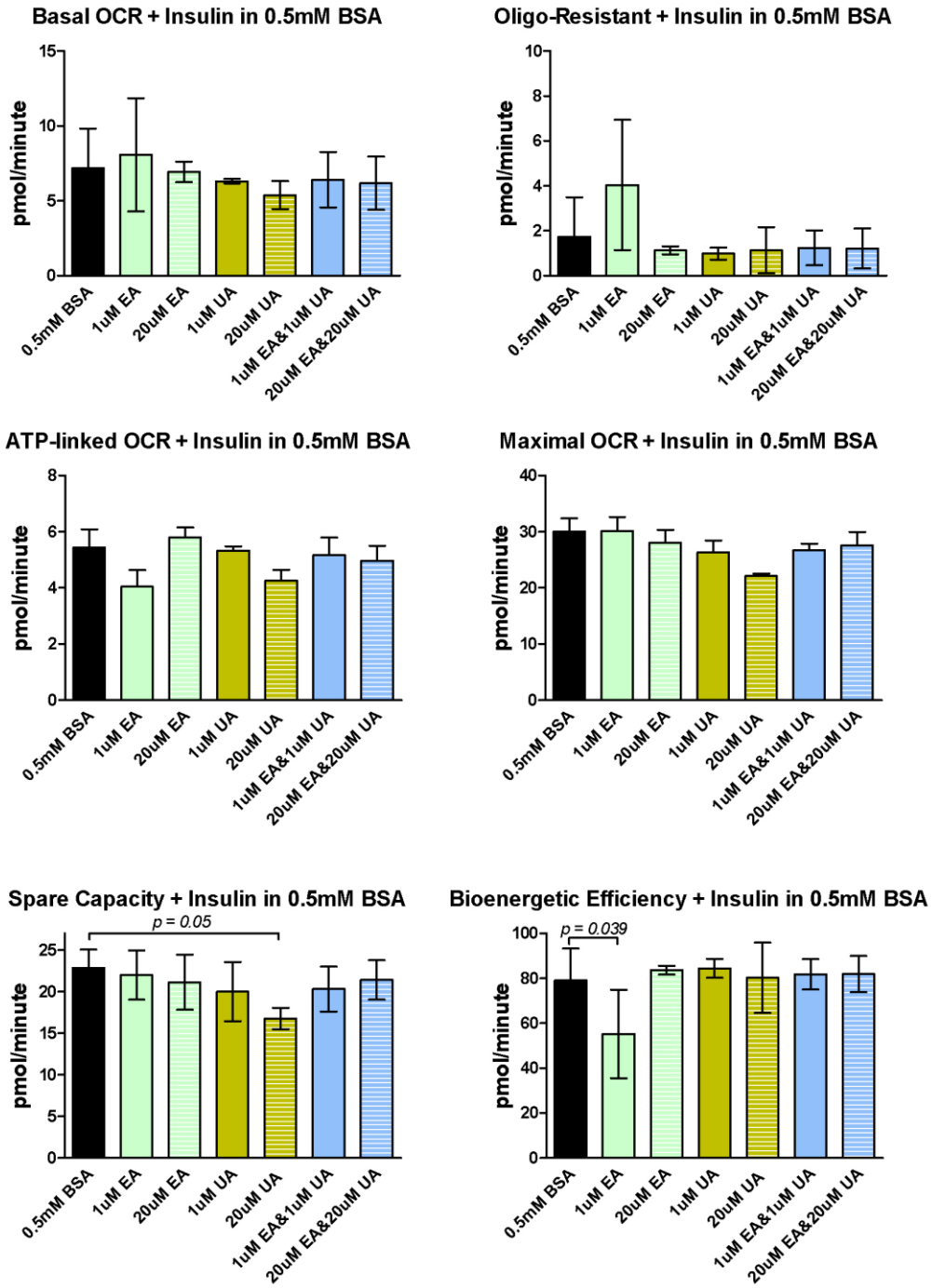


**Figure 19.** Seahorse Data for cells in 0.5 mM BSA with 1 mM insulin. Data are represented as mean ± SD. (n = 3-4 for all conditions, p values < 0.05 with (+ ins) 0.5 mM BSA group are displayed)

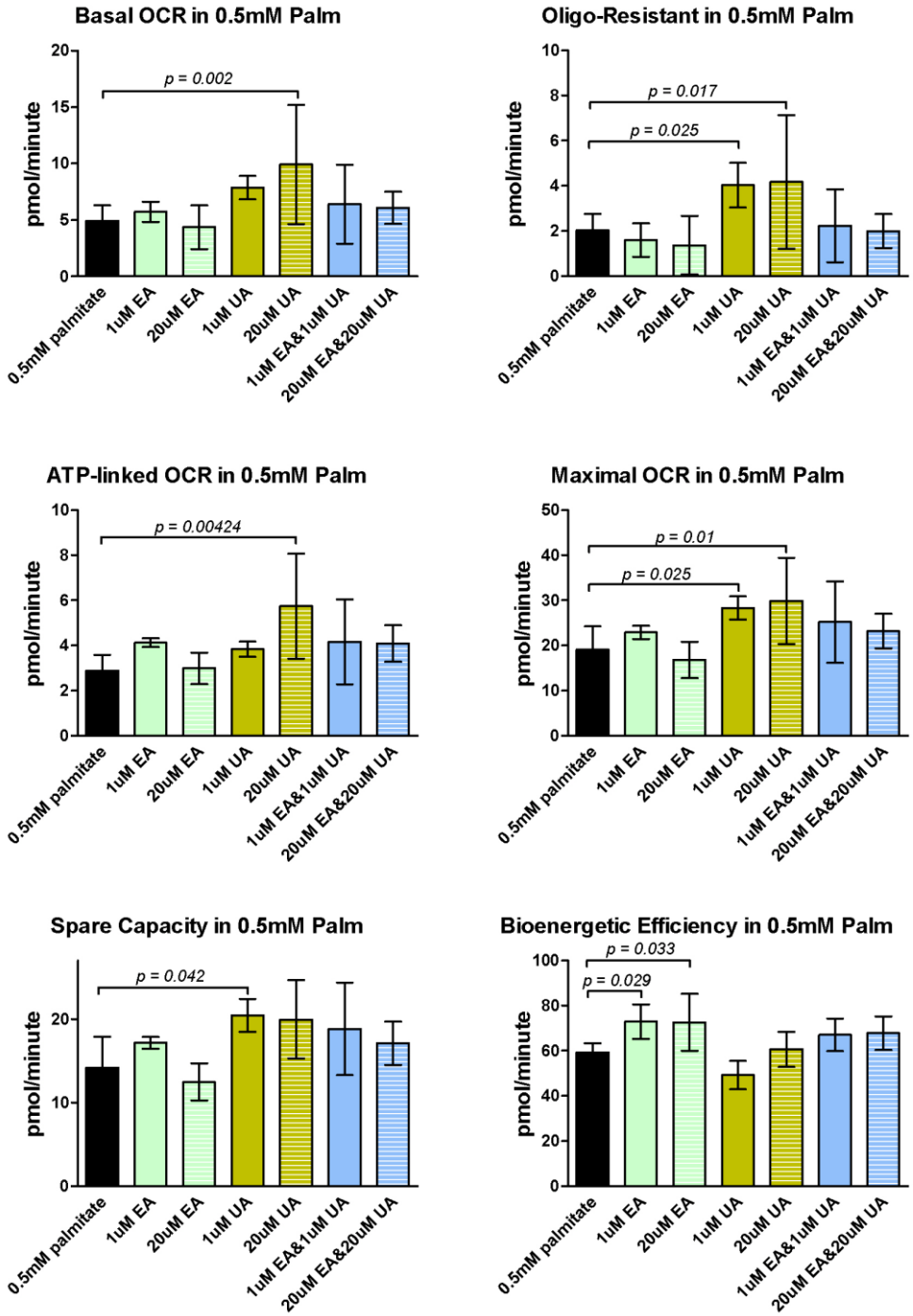


**Figure 20.** Seahorse Data for cells in 0.5 mM palmitate without insulin. Data are represented as mean ± SD. (n = 3-4 for all conditions, p values < 0.05 with (- ins) 0.5 mM palmitate group are displayed)

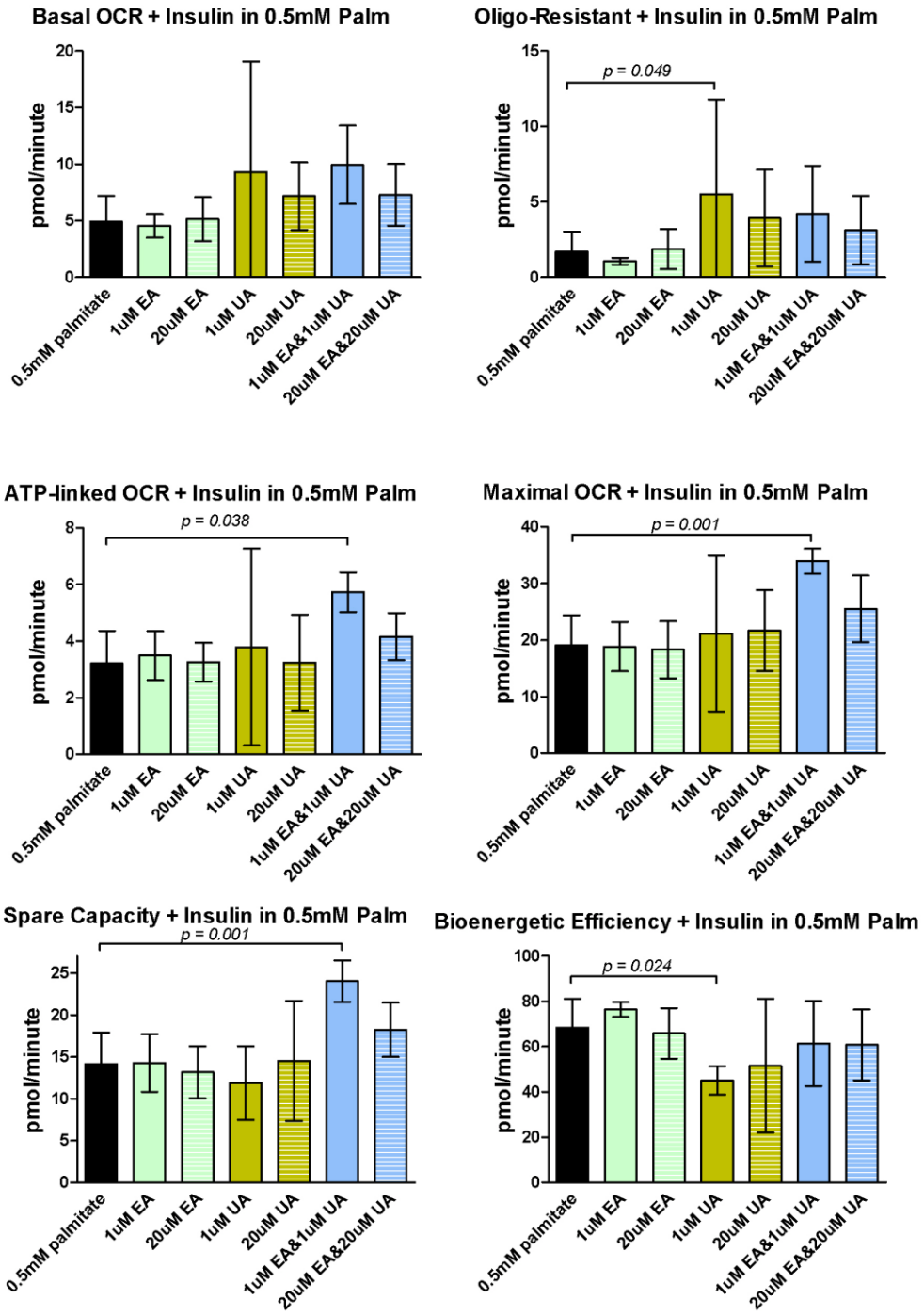


**Figure 21.** Seahorse Data for cells in 0.5 mM palmitate with 1 mM insulin. Data are represented as mean ± SD. (n = 3-4 for all conditions, p values < 0.05 with (+ ins) 0.5 mM palmitate group are displayed)

## Discussion

The growing issue of T2D and insulin resistance in general is spurring a need for more affordable and accessible treatments. Plant-derived compounds, especially ellagic acid and its metabolite urolithin A have received much attention for their anti-cancer and antioxidant capabilities (87-90). In this study, EA, UA, and their combination were assessed as potential treatments for insulin resistance in skeletal muscles of diet-induced insulin resistant mice and in insulin resistant C2C12 skeletal muscle cell cultures. Since skeletal muscles play a major role in glucose uptake, their insulin sensitivity is very important in keeping the whole body healthy. Additionally, mitochondrial dysfunction has been implicated in many metabolic diseases, including insulin resistance and the metabolic syndrome (91). As major regulators of cellular metabolism, proper mitochondrial function is vital for normal cellular activity. Thus, the goal of this thesis was to study how EA and UA treatment affected skeletal muscle and mitochondrial performance in skeletal muscle within the context of insulin resistance.

One study has been instrumental in uncovering the potential of UA as treatment for symptoms of aging. Ryu et al. found UA induced autophagy and mitophagy and improved several bodily functions in *C. elegans* and mammalian cells (92). In worms, UA also directly extended life span which was dependent of the expression of several autophagy genes. Older worms exhibited increased mitochondrial content when treated with UA, while young worms had lower mitochondrial content. In C2C12 mouse skeletal myoblasts, autophagy and mitophagy biomarkers were elevated upon treatment with UA. Additionally, mitochondrial membrane potential ($\Delta\psi_M$), a trigger for mitophagy, was decreased with UA treatment which resulted in an upregulation of PINK1 expression. Importantly, they found that Complex II-driven ATP production was increased with UA treatment, meaning that fatty acid oxidation was favored over

aerobic glycolysis. In mice fed a high fat diet (HFD) supplemented with UA, body weight and fat mass were not altered compared to HFD mice, but treatment mice had significantly stronger grip strength and increased running endurance. Autophagic and mitophagic markers were also upregulated in mice muscle tissue, but the mtDNA:nuDNA ratio was not altered (92). From these findings, UA seemed a promising treatment for metabolic diseases involving mitochondrial dysfunction.

Although treatment had no significant effect on bodyweight or food intake in the end of the present study, which is consistent with previous studies (91-93), all treatment groups except EA had significantly lower fasting glucose and EA&UA treatment decreased blood glucose at 15 and 120 minutes during the final IPITT. These results indicate that EA and UA in combination have potential to induce insulin-stimulated glucose uptake in insulin resistant mice.

To elucidate how these compounds might improve insulin sensitivity, several serum markers were assessed. Serum free fatty acid levels were significantly decreased in all treatment mice groups except EA compared to no-treatment HF/HS diet mice. This is an important finding because serum free fatty acids are inversely correlated with insulin sensitivity (94,95). It was therefore possible that treatment increased insulin sensitivity by decreasing serum FFAs, as doing so has been found to increase insulin-stimulated glucose uptake in diabetic patients (96). However, during intraperitoneal insulin tolerance tests, only EA mice showed a significant decrease in blood glucose at 15 and 120 minutes. All other groups had insignificant decreases in blood glucose at all time points. Unfortunately, lean body mass measurements were not obtainable, so the amount of insulin administered was based on total body weight. This may have caused the variation seen in the IPITT data.

Additionally, adiponectin levels were increased with all treatments, but only significantly in UA mice. Adiponectin is a protein hormone secreted by adipotissue that regulates β-oxidation in skeletal muscle and reduces gluconeogenesis in the liver. Levels are lowered in obese and T2D patients, and injection of recombinant adiponectin into healthy and insulin resistant mice significantly decreased plasma glucose. Adiponectin knockout mice fed a HF/HS diet developed severe insulin resistance and exhibited increased serum FFA levels, but when they were subjected to adenoviruses that caused an overproduction of adiponectin, the mice displayed improved insulin sensitivity and reduced serum FFAs. This and other data indicate overnutrition-based hypoadiponectin may be a factor in causing insulin resistance (97). In combination, the lowered serum FFAs and fasting glucose levels and increased adiponectin in this study are signs that EA, and more promisingly UA, improved insulin sensitivity.

Although other studies have found increased intramyocellular levels of FFAs, TGs, and other lipids in obese and insulin resistant animals and humans (98,99) there were no significant differences found in FFAs, TGs, or cholesterol in the skeletal muscle of the mice in this study. However, this may be due to improper sample preparation; not all extracellular fat was able to be removed prior to freezing and different areas of the frozen tissue were likely sampled for lipid content, possibly affecting the quality of intramyocellular lipid extraction. This may explain the large variation in lipid levels within the groups. However, since intramyocellular lipids have been strongly correlated with insulin resistance (75,100-102) and lipid preparations were not fully optimized, there is reason to believe the readings from this study are not reliable. The finding that higher serum FFA levels resulted in increased intramyocellular lipids (103), suggests further that these measurements should be reevaluated. It would have been ideal if noninvasive magnetic resonance spectroscopy (MRS) was used to measure intramyocellular TG content.

However, since it has more recently been hypothesized that the lipid intermediates DAGs and ceramides are the main initiators of insulin resistance as opposed to intramyocellular TGs (11,13,14,100,104), it would be best to monitor changes in DAG and ceramide levels in skeletal muscle. Trained endurance athletes have elevated intramyocellular TGs, yet their oxidative capacity still functions well, explaining the lack of lipid-intermediate buildup. This finding supports the idea that lipid intermediates as opposed to TGs are better markers of insulin resistance (100,104).

Markers of lipid storage and synthesis in muscle tissue reflected improvements in insulin sensitivity with EA and UA treatment. FAS, cd36, and PPARγ all trended towards LF/LS levels with treatment, with EA&UA mice reaching significance for cd36 and PPARγ. In obese nondiabetic and type II diabetic patients, PPARγ mRNA is elevated in both muscle tissue and cultures with insulin increasing its expression (105,106). This, along with the finding that muscle PPARγ-knockout mice exhibited insulin resistance and excess adiposity (107), suggest a role for muscle PPARγ in insulin resistance. Paradoxically, both PPARγ activation and reduction improve insulin sensitivity. Activation alleviates insulin resistance by directing more TGs to adipotissue instead of ectopic tissues, while deficiency decreases TG content in both adipotissue and ectopic lipids by increasing fatty acid oxidation (108). Thus, the decrease in PPARγ mRNA here may indicate an improvement in insulin sensitivity by the latter mechanism. This would agree with other studies that have found a reduction in PPARγ in adipose tissue with EA treatment (109,110). The results of this study indicate that EA and UA have a synergistic effect on improving lipid regulation in insulin resistant mice. When administered together, they exhibit more improvement in muscle fatty acid translocase and PPARγ levels compared to either alone.

These improvements in fatty acid utilization and storage may relate to the effects of EA and UA on mitochondrial biogenesis and function. Markers of mitochondrial biogenesis tended to increase with treatment, although significance was only reached in ERRα, Nrf2, and TFAM with combined EA&UA treatment. ERRα is required for PGC1α-mediated mitochondrial biogenesis and may be capable of inducing biogenesis in the absence of PGC1α by regulating the expression of nuclear genes required for proper mitochondrial function (111,112). Although not significant, treatment increased PGC1α levels. In addition to upregulating mitochondrial biogenesis, PGC1α increases uncoupled respiration and ROS detoxification. In partnership with PPARγ, PGC1α induces brown adipocyte differentiation, which is important for thermogenesis. Overexpression of PGC1α was found to increase resting respiration when mice were given palmitoyl CoA-cartnitine but not carbohydrate. These mice had more citrate synthase and ß-hydroxyacyl CoA dehydrogenase activity, in addition to higher levels of ETC subunits. This may explain the increase in oligo-resistant respiration in palmitate-treated cells with UA administration while no effect was seen in BSA-treated cells from this study. PGC1α induces the expression of Nrf1 and Nrf2 which stimulate expression of ETC subunits and TFAM (111). TFAM in turn increases mtDNA replication, a necessary step in mitochondrial biogenesis (113). Between EA and UA, UA tended to have a stronger effect increasing biogenesis markers. This is in line with previous reports of UA alleviating the hypertension-induced decrease in mitochondrial biogenesis (114). UA has also been elucidated as an inducer of mitophagy (92) which may explain why it increases mitochondrial biogenesis, as more mitochondrial production would be required to maintain an adequate supply of ATP. PINK and parkin, markers of mitophagy, were significantly elevated with EA&UA combination treatment, which supports UA's mitophagic stimulatory role.

Mitochondrial fusion is important for energy homeostasis and signaling, as Mfn2 overexpression increases membrane potential and glucose oxidation (115,116). When nutrients are in excess, fission is increased which is linked to increased uncoupled respiration (117). Additionally, Type 2 diabetic patients exhibit a lowered Mfn2 expression in skeletal muscle which may be tied to mitochondrial dysfunction and the development of insulin resistance (118). In the current study, Mfn2 levels were decreased in HF/HS mice compared to LF/LS mice, but UA and EA&UA treatment significantly increased its abundance. Strangely, a study on treating hypertensive rats with pomegranate extract, high in UA, found a decrease in Mfn2 with treatment which they interpreted as improving mitochondrial dynamics (114). Mfn2 may have different roles in different diseases, as Bach et al. found Mfn2 to be lowered in obese and type II diabetic subjects but intense weight loss and improved insulin sensitivity significantly increased Mfn2 levels (119). Thus, the increases in genes related to mitochondrial biogenesis, mitophagy, and fusion observed in this study may indicate an improved mitochondrial function and quality control.

Overall mitochondrial content exhibited great variation, but UA treatment significantly increased levels compared to HF/HS mice. Perhaps in this case, biogenesis rates were higher than mitophagic ones, resulting in a net increase of mitochondria. All treatments except EA significantly increased ATP6 mRNA levels compared to no treatment-HF/HS mice, indicating an upregulation of mitochondrial gene synthesis, as ATP6 is encoded in mtDNA, and supporting the potential for increased mitochondrial biogenesis.

Oxidative stress has been implicated in the development of insulin resistance and a study by Anderson et al. found that a high fat diet increased $H_2O_2$ production by Complex I in the skeletal muscle mitochondria of rats (120). Furthermore, administration of an antioxidant that localized to the inner membrane of mitochondria fully reversed the increase in ROS brought about by the

high-fat diet. More importantly, the mitochondrially-targeted antioxidant completely prevented insulin resistance in rats fed a high-fat diet which control high-fat diet mice developed, as confirmed by glucose tolerance tests and Akt phosphorylation after glucose administration (120). Agreeing with another study (33), catalase targeted to skeletal mitochondria of high-fat diet mice preserved whole body insulin sensitivity, again supporting the role of mitochondria-derived $H_2O_2$ in the development of insulin resistance. Indirect measures in the current study indicate EA and UA decrease ROS in HF/HS mice. Detoxifying enzymes in the mitochondria, PrdxIII and SOD2, were significantly increased by EA&UA treatment, with UA also significantly increasing SOD2. These findings agree with a previous study on hypoxia/reoxidation damage to cardiomyocytes where UA decreased ROS and increased SOD levels (121). This suggests that UA and EA&UA administration may decrease mitochondrial $H_2O_2$ emission.

Overnutrition leads to mitochondrial fission and this in turn is associated with increasing ROS production which negatively affects the insulin transduction pathway (122-124). High levels of ROS activate stress pathways like NF-κB, JNK/SAPK, and p38 MAPK, in addition to serine/threonine kinases PKC, PKB, mTOR, and GSK3 which then phosphorylate IR and IRSs to inhibit insulin signaling (125). Our findings that UA and EA&UA treatment significantly increased Mfn2 and mitochondrial detoxification enzymes suggest an improvement in mitochondrial dynamics with more fusion and less ROS emission. These results are supported by ROS detection in differentiated C2C12 myotubes. Four-day differentiated C2C12 myoblasts were incubated in 0.75 mM palmitate-BSA for 12 hours to induce insulin resistance, then treated with various concentrations of EA, UA, or EA&UA, with or without 1 mM insulin in 0.75 mM palmitate-BSA and incubated for another 12 hours. Detecting with DCFDA, a great jump in ROS was found in cells treated with palmitate-BSA compared to BSA control cells and almost all

forms of treatment significantly lowered these levels, excluding 1 μM EA without insulin and 50 μM EA with insulin. Although the DCFDA assay did not distinguish the origin of ROS, it still indicated that treatment beneficially stimulated their removal. These results are consistent with other studies that have found antioxidant capabilities of EA and UA (126,127). Considering the positive correlation of ROS and insulin resistance found in other studies and reviews (125,128,129), these detoxifying capabilities are promising findings.

Cellular health appeared to improve with treatment, according to the results of cell culture assays. Cytotoxicity, as measured by a cell-impermeant substrate whose fluorescence is proportional to the amount of dead-cell protease in solution, indicated that all concentrations of EA, UA, and EA&UA administered significantly decreased the cytotoxicity that 0.75 mM palmitate-BSA induced. In addition, all conditions except 1 μM UA diminished levels of apoptosis. ATP as a measurement of cell viability was significantly increased by most concentrations of treatment, except 1 μM EA with and without insulin and 1 μM and 10 μM UA without insulin. The increased ATP in treatment cells may indicate either an increase in cell viability or an increase in mitochondrial function. Since results from the MTT assay indicate no significant difference in cell viability besides 1 μM UA (with and without insulin), it is likely that treatment improved mitochondrial function. Interestingly, EA&UA together appeared to increase ATP production more than either alone. Indeed, according to Seahorse data, 1 μM EA & 1 μM UA combined treatment resulted in significantly higher ATP-linked OCR in 0.5 mM palmitate-BSA (with insulin). As mitochondrial biogenesis markers are upregulated in EA&UA treated mice, this may indicate that combined treatment stimulates increased rates of ATP synthesis through improved mitochondrial turnover.

The lack of effect on glucose uptake by EA was somewhat surprising, given the finding that EA was found to stimulate glucose uptake in differentiated adipose and muscle cells (66,130). Poulose et al. used EA concentrations 1 nM to 500 nM, and glucose uptake had started to decrease at higher concentrations, potentially explaining why the concentrations of 1 μM to 50 μM EA in this study did not increase glucose uptake (66). However, Mehta et al. found a significant increase in glucose uptake with 10 μM EA in neuronal cells (131). This matches the results in the current study, as 10 μM EA with insulin also increased glucose uptake in differentiated C2C12 myoblasts. Urolithin A, on the other hand, exhibited decreased glucose uptake at 1 μM and 20 μM, and insignificant changes at 10 μM. This decrease may have been a response to the nutrient-overloaded cell condition in attempts to reduce ROS production by reducing fuel intake and oxidation.

As the concentration of EA in human plasma after ingestion of pomegranate juice was found to be at a maximum of 100 nM (132), the concentrations used in the *in vitro* sections of this study may not be particularly biologically relevant. Future studies should focus on administering lower concentrations of EA to cells, as lower concentrations may increase glucose uptake. However, UA has been found to be ~25-80x more abundant than EA in blood, suggesting that the concentrations in this study were appropriate (133).

In insulin sensitive C2C12 myotubes (treated with 0.5 mM BSA) EA and UA had little effect on cellular respiration. However, 1 μM and 20 μM EA and 1 μM UA significantly increased bioenergetic efficiency in cells without insulin treatment, indicating improved mitochondrial regulation even in healthy cells. Oligo-resistant OCR was increased when cells in treatment were incubated with 1 mM insulin for 12 hours, suggesting that long term treatment of insulin increased uncoupling, which may explain the slight increase in basal OCR with insulin.

Bioenergetic efficiency was significantly lower in cells treated with 1 μM EA + insulin compared to 0.5 mM BSA + insulin. Possibly explaining this result, 1 μM EA had higher, although not significantly so, oligo-resistant OCR. EA mice did not have significantly more UCP3, however, so another method of uncoupling may have been responsible.

When 0.5 mM palmitate-BSA was administered to differentiated C2C12 cells, spare capacity was significantly decreased compared to 0.5 mM BSA-only treated cells. This appears to be due to a decrease in maximal OCR with palmitate, as oligo-resistant OCR was unchanged between the two conditions. With the addition of 1 mM insulin, ATP-linked OCR was borderline significantly decreased in palmitate cells compared to BSA cells ($p = 0.05$), while maximal OCR and spare capacity were significantly decreased in palmitate cells. The decrease in ATP-linked OCR and maximal OCR amounted to a decrease in spare capacity, as oligo-resistant OCR remained unchanged. Thus, insulin resistance in C2C12 myotubes treated with insulin appears to decrease maximal OCR in greater proportions to its decrease in ATP-linked OCR. Yet, uncoupled OCR was unchanged in the presence of palmitate, suggesting respiration was affected in a non-uncoupled related manner. Perhaps mitochondria became dysfunctional and produced less ATP when inundated with palmitate, causing a decreased OCR potential.

In insulin resistant C2C12 myotubes without insulin, UA increased all OCR measures except bioenergetics efficiency. UA was the only treatment that increased oligo-resistant OCR, suggesting an increase in uncoupled respiration. qPCR data support these findings, in that UCP3 is upregulated in UA treated mice, and significantly so in EA&UA treated mice. Yet, in the DCFDA assay, UA decreased ROS production compared to palmitate-alone treatment. This suggests a greater ability for UA to remove or prevent ROS than EA, as it increased respiration while still decreasing ROS levels. 20 μM UA was the most potent at increasing basal, ATP-

linked, oligo-resistant, and maximal OCR. Yet it did not significantly alter bioenergetics efficiency or spare capacity. The increase in ATP-linked OCR was proportional to the increase in oligo-resistant OCR such that the overall bioenergetics efficiency was unchanged. This may indicate a positive role for UA in the treatment of obesity and T2D in that it stimulates more respiration while still decreasing ROS in muscle cells. Although UA decreased glucose uptake, it increased OCR, indicating a higher reliance on fatty acids as fuel. In support of this, all EA and UA administrations in palmitate-treated cell cultures with insulin reduced intramyocellular lipid content compared to palmitate control cells, indicated by the AdipoRed assay. A potential future study would be to observe fatty acid usage in response to EA and UA. If lipids were more heavily utilized, ectopic lipid storage may decrease, resulting in increased insulin sensitivity, similar to the result of downregulating PPARγ. Both concentrations of EA in palmitate treated cells exhibited no significant differences in OCR measurements, except for bioenergetics efficiency, which was increased with EA treatment. Here, ATP-linked OCR was slightly increased, while oligo-resistant OCR was slightly decreased, resulting in the increase in bioenergetics efficiency. While this indicates an improvement in mitochondrial function, it does not seem to promote the utilization of more energy fuels when this may be ideal in obese subjects. Thus, UA may be a better treatment for obesity. However, EA still shows potential for improving the issues resulting from obesity.

In the presence of 1 mM insulin in 0.5 mM palmitate, UA still increased oligo-resistant OCR and decreased bioenergetics efficiency, but other changes were not significant. EA had no significant effect on any parameters, but 1 μM EA & 1 μM UA treatment significantly increased ATP-linked OCR, maximal OCR, and spare capacity. Thus, uncoupled respiration was unaffected while ATP production was enhanced, but this did not lead to increased bioenergetics efficiency.

The increased capacity of the mitochondria to produce ATP, along with the decreased glucose uptake with 1 μM EA & 1 μM UA treatment suggest a heavier utilization of fatty acids or other fuels as substrates. Again, this may be beneficial in the case of obesity and T2D. Although it was suggested earlier that using more fatty acids as fuel may cause an unfavorable buildup of lipid metabolites that have the potential to reduce insulin signaling, this buildup may be prevented if the mitochondria are able to accommodate the increase in energy metabolites. Seeing as UA treatment in palmitate generally increased basal respiration and decreased bioenergetics efficiency, this may be a sign of increased ETC activity, potentially avoiding a buildup of energy intermediates.

Overall, the results from this study indicate EA, UA and their combined administration have potential to improve subjects with insulin resistance and/or T2D. Although weight and food intake were not altered in mice fed a HF/HS diet, several markers of insulin sensitivity were improved: fasting glucose and serum FFAs were lowered, serum adiponectin was increased, blood glucose was lowered in the final IPITT, fatty acid transport was increased while adipogenesis genes were decreased, mitochondrial turnover genes were increased, ROS detoxification genes were increased, ROS production was decreased, cytotoxicity and apoptosis were decreased, ATP levels were increased without a significant change in cell viability, some conditions increased glucose uptake, and UA increased cellular respiration without the detrimental increase of ROS.

Future studies should administrate doses of EA that are more comparable to levels in human circulation after ingestion of ellagitannin-rich foods, as well as levels of insulin that are present in insulin resistance and T2D. Since intramyocellular lipids seem to play an important role in the development and intensity of insulin resistance, more accurate measurements should be taken in

skeletal muscle of diabetic subjects in response to EA and UA treatment. This would elucidate whether these phytochemicals act through decreasing ectopic lipid accumulation or some independent method. At the molecular level, phosphorylation of PKCθ, IRS, Akt, and other members of the pathway should be measured to determine if treatment improves sensitivity. To better understand effects on glucose uptake, monitoring GLUT4 mobilization to the cell membrane would be beneficial. Mitochondrial turnover appears to be upregulated with EA and UA treatment, and to monitor this phenomenon more closely, MitoTimer may be a valuable method. MitoTimer is a red fluorescent protein targeted to the mitochondria that changes from green to red as the protein it is targeted to matures, thus providing a measurable indication of protein turnover. In addition to mitophagy, MitoTimer can also be used to assess mitochondrial biogenesis, providing more insight on how mitochondrial dynamics are altered by EA and UA (134). Given the strong potential for these compounds to positively impact cellular health in multiple disease states, they deserve more attention as safe and cost-effective treatments for insulin resistance and the metabolic syndrome.

**Supplementary Data**

**Supplementary Table S1:** Macronutrient Compositions of LF/HS and HF/HS diets.

| **LF/LS Diet: TD.08485 (**Kcal/g: 3.6) | | |
|---|---|---|
| Macronutrient | % by weight | % kcal from |
| Protein | 17.3 | 19.1 |
| Carbohydrate | 61.3 | 67.9 |
| Fat | 5.2 | 13.0 |

| **HF/HS Diet: TD.88137 (**Kcal/g: 4.5) | | |
|---|---|---|
| Macronutrient | % by weight | % kcal from |
| Protein | 17.3 | 15.2 |
| Carbohydrate | 48.5 | 42.7 |
| Fat | 21.2 | 42.0 |

**Supplementary Table S2:** Primers used for qPCR. F indicates forward primer and R indicates reverse primer. Primers are written 5' to 3' and were purchased from Sigma Life Science.

| **For mtDNA Quantification** | |
|---|---|
| COX1-F | ACTATACTACTACTAACAGACCG |
| COX1-R | GGTTCTTTTTTTCCGGAGTA |
| cyclophilin A-F | ACACGCCATAATGGCACTGG |
| cyclophilin A-R | CAGTCTTGGCAGTGCAGAT |
| **MtBiosynthesis and replication** | |
| PGC1α-F | TCC TCT GAC CCC AGA GTC AC |
| PGC1α-R | CTT GGT TGG CTT TAT GAG GAG G |
| NRF2-F | CCA AGT CCT GCA TTG GGT GG |
| NRF2-R | GCA AAA ACT GCC ATA GTT GG |
| ERRα-F | GGT GTG GCA TCC TGT GAG GC |
| ERRα-R | AGG CAC TTG GTG AAG CGG CA |
| Mfn2-F | AAG CAC TTT GTC ACT GCC AAG |
| Mfn2-R | TTG TCC CAG AGC ATG GCA TTG |
| TFAM-F | GAAGGGAATGGGAAAGGTAGAG |
| TFAM-R | ACAGGACATGGAAAGCAGATTA |
| ATP6-F | AATTACAGGCTTCCGACACAAAC |
| ATP6-R | TGGAATTAGTGAAATTGGAGTTCCT |
| **Mitophagy genes** | |
| PINK-F | ACCAGCATGTTGGCCTGCGGCT |
| PINK-R | ATGGGCTGTGGACACCTCAGGGGC |
| Parkin-F | TGGGAGGTGTGCTGTGCCCCCG |

| | |
|---|---|
| Parkin-R | AAAACAAACCCGCAGCCCAGGCCGT |
| **Uncoupling and ROS detoxification genes** | |
| UCP3-F | TGCTGAGATGGTGACCTACG |
| UCP3-R | GCGTTCATGTATCGGGTCTT |
| SOD1-F | CAGCATGGGTTCCACGTCCA |
| SOD1-R | CACATTGGCCACACCGTCCT |
| SOD2-F | CATTAACGCGCAGATCATGC |
| SOD2-R | CCCAAAGTCACGCTTGATAGC |
| Prdx III-F | GTTGCAGTTTCAGTGGATTCCC |
| Prdx III-R | CTTTGGAAGCTGTTGGACTTGG |
| Catalase-F | CCAGCGACCAGATGAAGCAG |
| Catalase-R | CCACTCTCTCAGGAATCCGC |

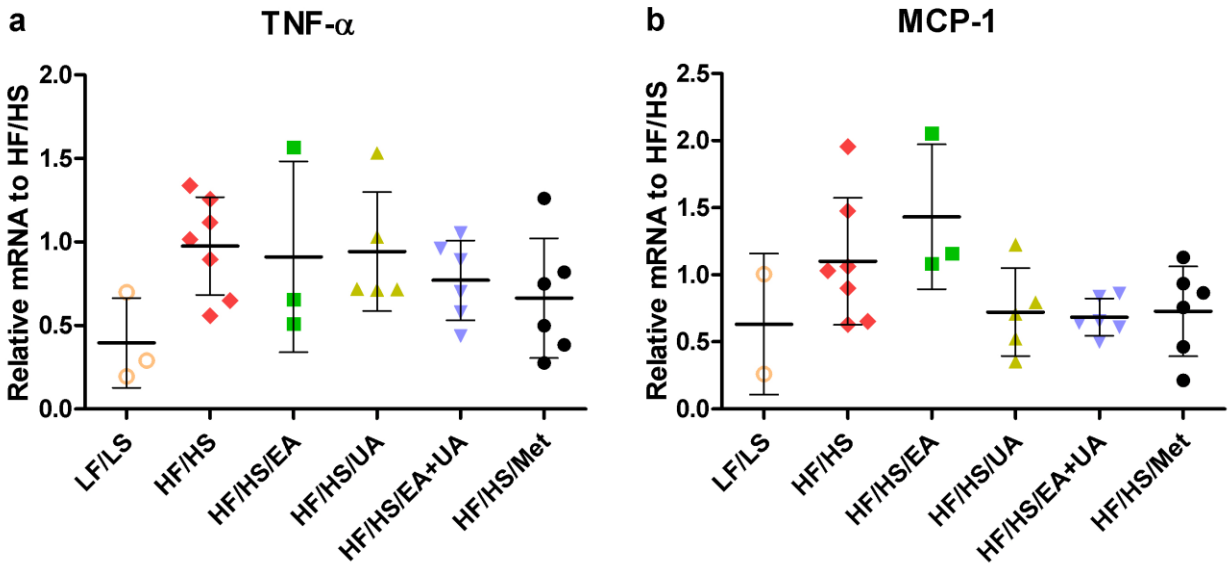


**Supplementary Figure S1.** Inflammatory markers in mouse skeletal muscle. (a) TNF-α and (b) MCP-1 mRNA levels were not significantly different from HF/HS mice in any treatment group. (n = 6-8 for all groups except LF/LS group. p values < 0.05 between group and HF/HS mice are displayed)

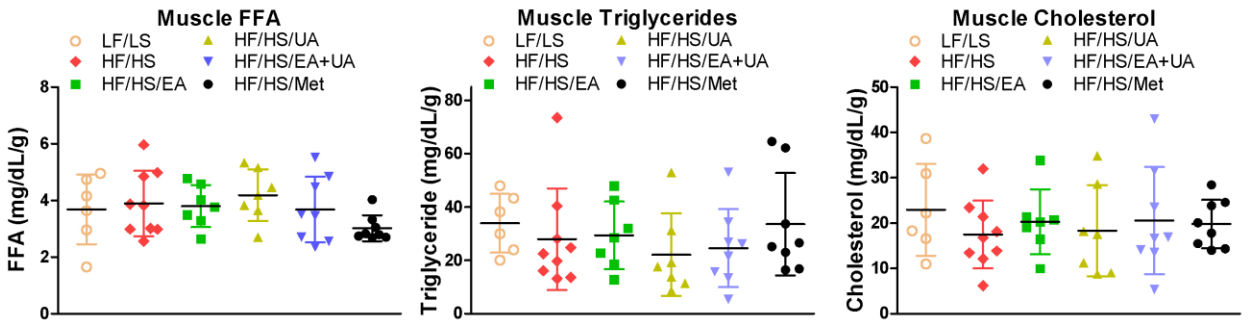


**Supplementary Figure S2.** Intramyocellular levels of free fatty acids, triglycerides, and cholesterol from hind leg skeletal muscle. (n = 6-8 for all groups. p values < 0.05 between experimental groups and HF/HS mice are displayed)

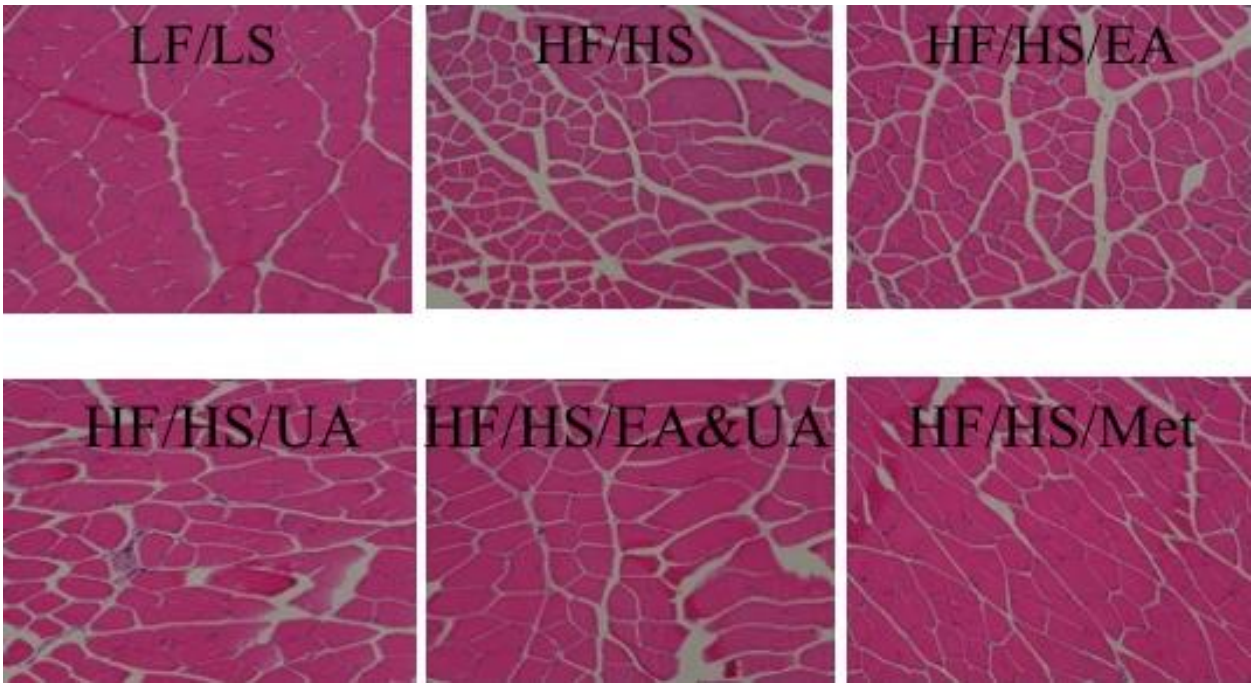


**Supplementary Figure S3.** Histology of mice skeletal muscle at the end of the 16-week study. Hind leg skeletal muscles were stored in formalin at 4°C until use.

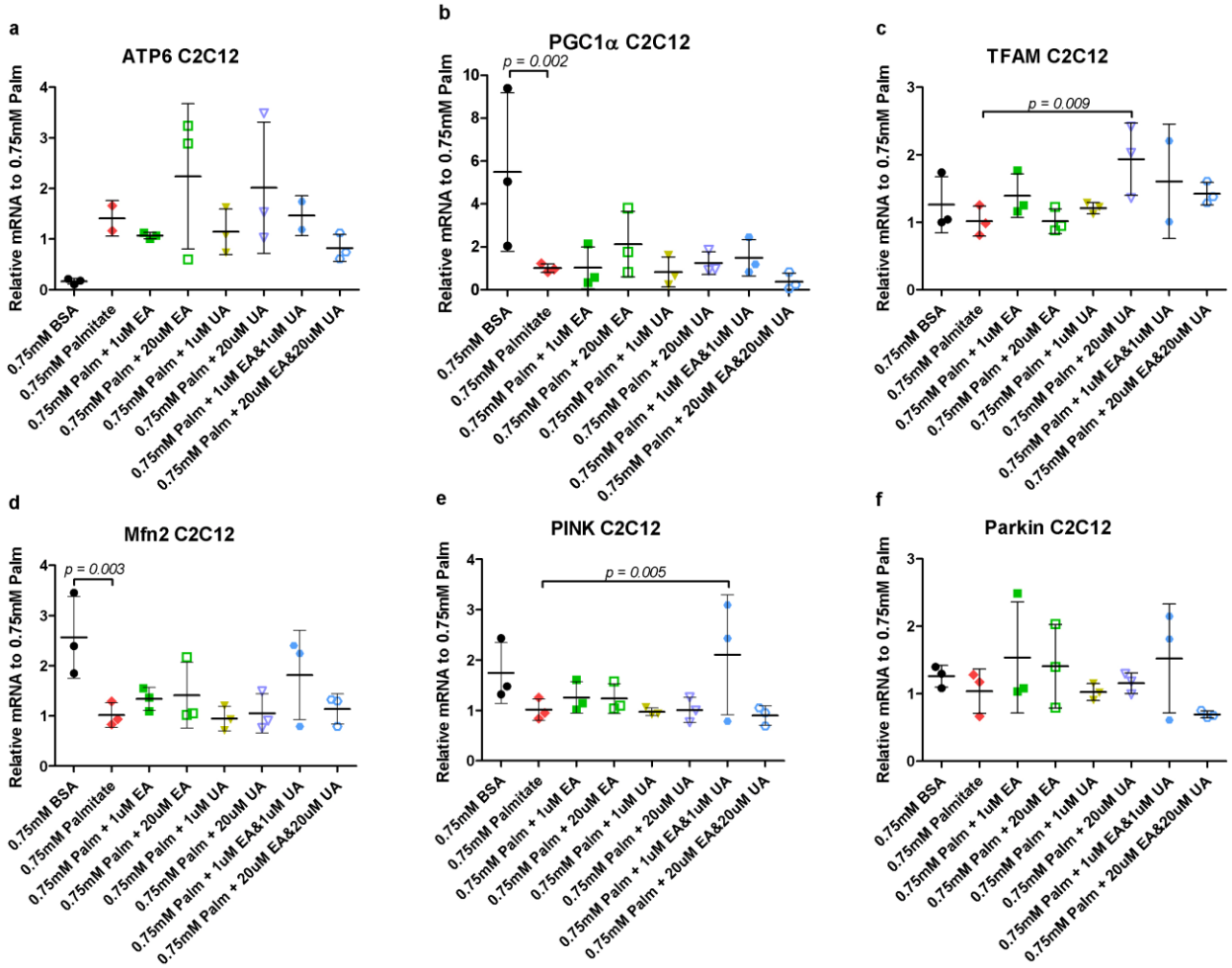


**Supplementary Figure S4.** Mitochondrial biogenesis and function markers in 6-day differentiated C2C12 myotubes. (a) ATP6 as a marker of ATP Synthase abundance, (b) PGC1α and (c) TFAM as markers of mitochondrial biogenesis, (d) Mfn2 as a marker of mitochondrial fusion, (e) PINK and (f) parkin as markers of mitophagy. C2C12 myoblasts were grown in growth media until confluent, then switched to differentiation media. On day 6 of differentiation media, cells were put in 0.75 mM palmitate in 1 g/L glucose DMEM or 0.75 mM BSA in 1 g/L glucose DMEM for 12 hours. Then media was switched to treatment in 0.75 mM palmitate or plain 0.75 mM BSA. 4 hours before harvesting RNA, 100 nM insulin was added to cells. (n = 3-4 for all conditions, p values < 0.05 between group and 0.75 mM palmitate group are displayed)

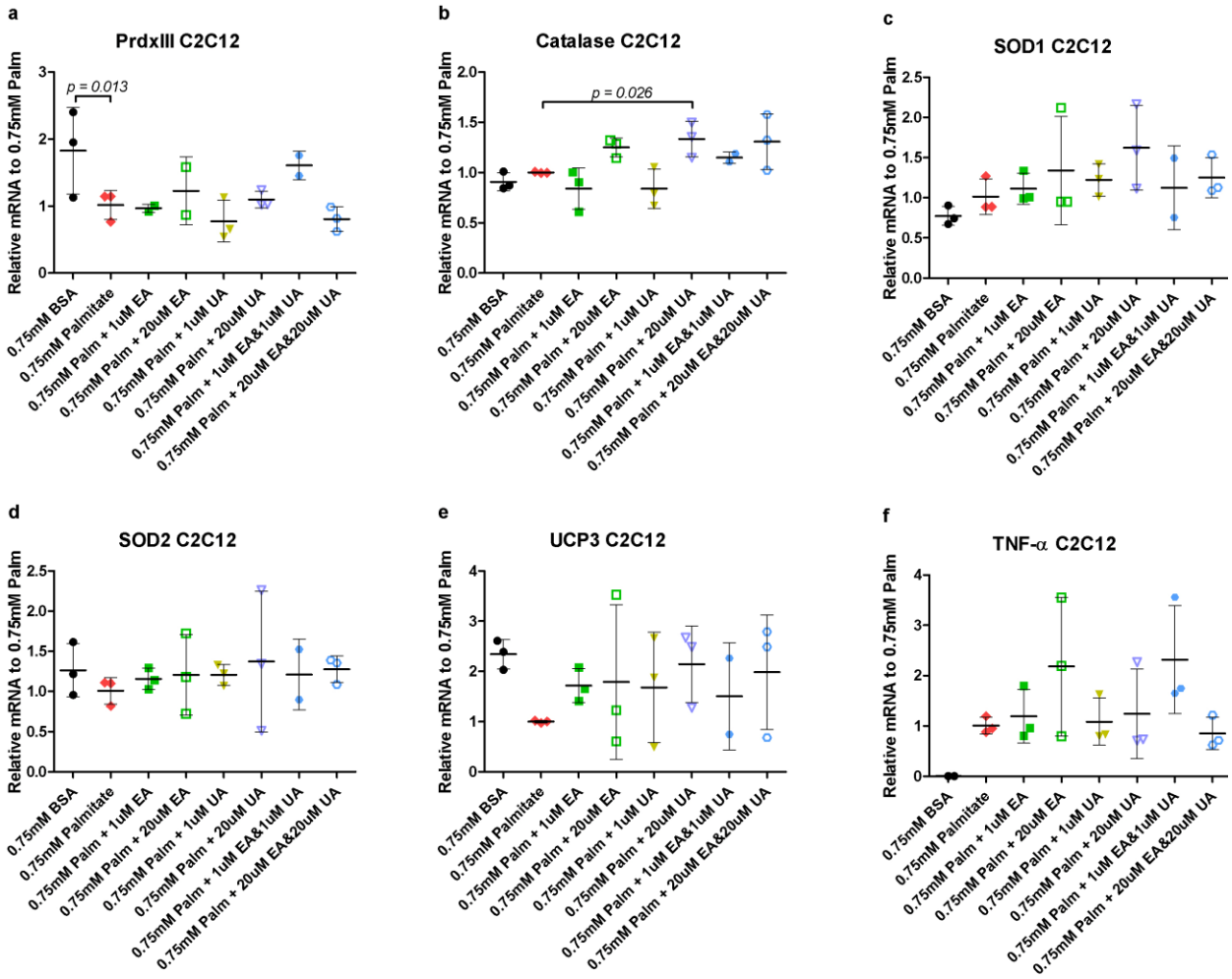


**Supplementary Figure S5.** ROS detoxification and inflammatory markers of 6-day differentiated C2C12 myotubes. (a) PrdxIII and (b) SOD2 detoxify ROS in mitochondria, (b) Catalase acts in the peroxisome, (c) SOD1 acts in the cytoplasm, and (f) TNFα is an inflammatory marker. (n = 3-4 for all conditions, p values < 0.05 between group and 0.75 mM palmitate group are displayed)

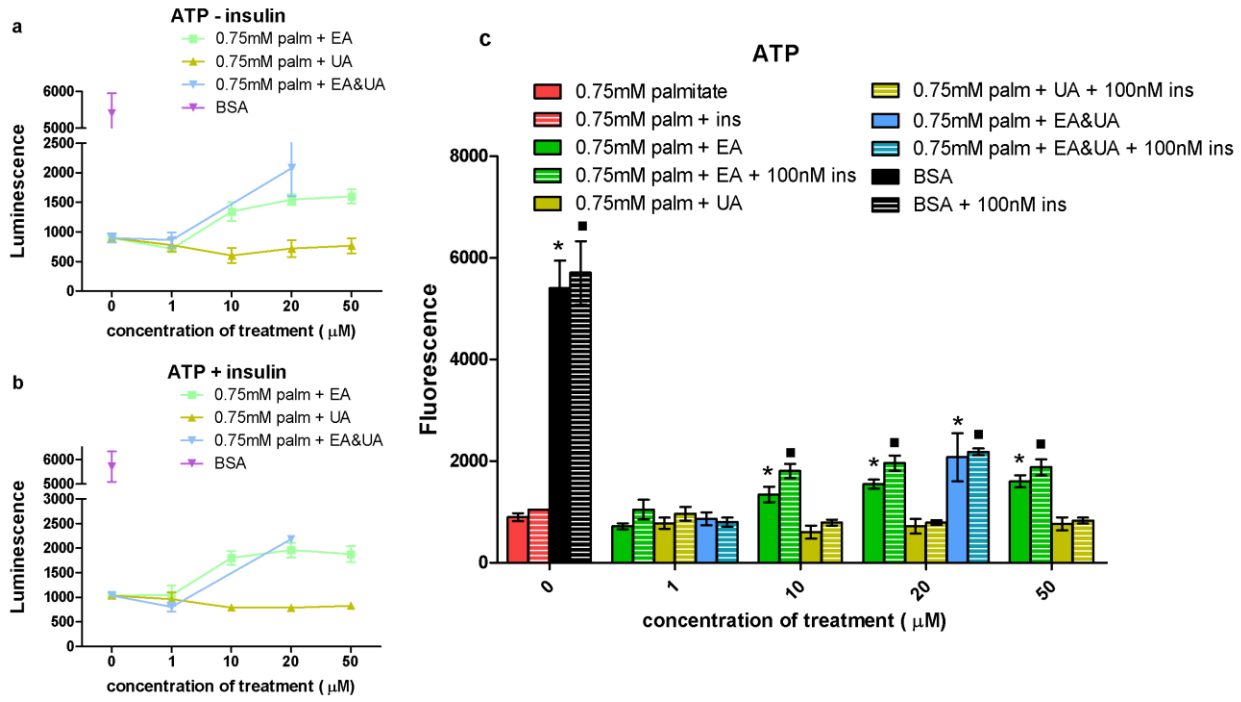


**Supplementary Figure S6.** ATP content measured by Mitochondrial ToxGlo™ (Promega) on 4-day differentiated C2C12 myotubes. ATP levels in cells (a) without insulin, (b) with 1 mM insulin for duration of treatment, and (c) both with and without insulin. Cells were treated as in the DCFDA Assay. (n = 3-4 for all conditions, * signifies $p < 0.05$ in no insulin groups compared to no insulin 0.75 mM palmitate group and ■ signifies $p < 0.05$ in with insulin groups compared to 0.75 mM palmitate with 1mM insulin group)

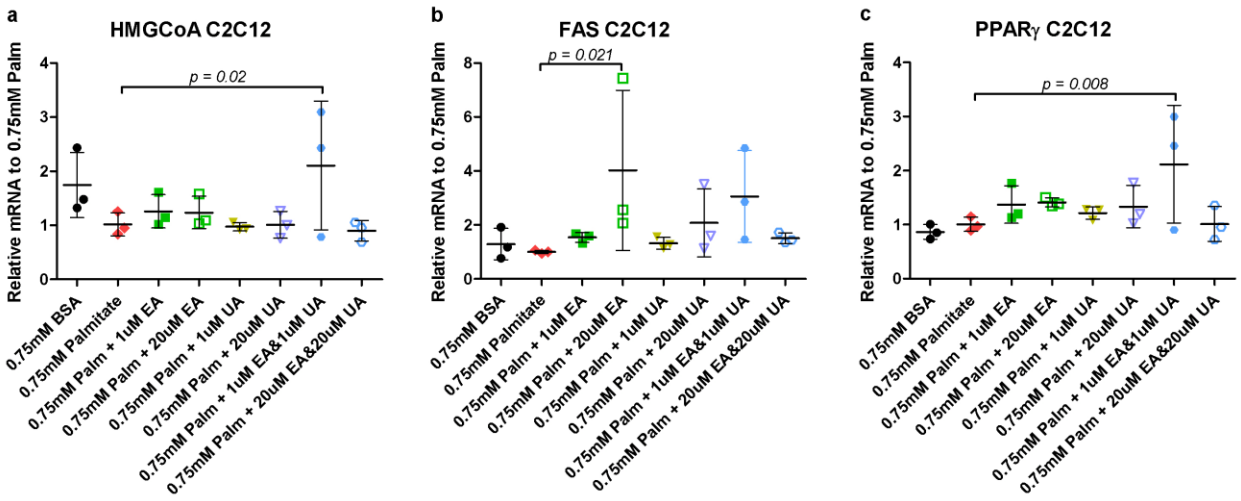


**Supplementary Figure S7.** Fatty acid storage and synthesis markers in 6-day differentiated C2C12 myotubes. (a) HMGCoA is involved in cholesterol synthesis, while (b) FAS and (c) PPARγ regulate fatty acid oxidation and storage. (n = 3-4 for all conditions, p values < 0.05 between group and 0.75 mM palmitate group are displayed)

## References


1. Zimmet, P. Z., Magliano, D. J., Herman, W. H., and Shaw, J. E. (2014) Diabetes: a 21st century challenge. *Lancet Diabetes Endocrinol* **2**, 56-64

2. Kadowaki, T., Ueki, K., Yamauchi, T., and Kubota, N. (2012) SnapShot: Insulin signaling pathways. *Cell* **148**, 624, 624 e621

3. Rowley, W. R., Bezold, C., Arikan, Y., Byrne, E., and Krohe, S. (2017) Diabetes 2030: Insights from Yesterday, Today, and Future Trends. *Popul Health Manag* **20**, 6-12

4. Shaw, J. E., Sicree, R. A., and Zimmet, P. Z. (2010) Global estimates of the prevalence of diabetes for 2010 and 2030. *Diabetes Res Clin Pract* **87**, 4-14

5. Magliano, D. J., Soderberg, S., Zimmet, P. Z., Chen, L., Joonas, N., Kowlessur, S., Larhubarbe, J., Gaoneadry, D., Pauvaday, V., Tuomilehto, J., Alberti, K. G., and Shaw, J. E. (2012) Explaining the increase of diabetes prevalence and plasma glucose in Mauritius. *Diabetes Care* **35**, 87-91

6. Kharroubi, A. T., and Darwish, H. M. (2015) Diabetes mellitus: The epidemic of the century. *World J Diabetes* **6**, 850-867

7. Martin, B. C., Warram, J. H., Krolewski, A. S., Bergman, R. N., Soeldner, J. S., and Kahn, C. R. (1992) Role of glucose and insulin resistance in development of type 2 diabetes mellitus: results of a 25-year follow-up study. *Lancet* **340**, 925-929

8. Samuel, V. T., and Shulman, G. I. (2012) Integrating Mechanisms for Insulin Resistance: Common Threads and Missing Links. *Cell* **148**, 852-871

9. Zhang, J., and Liu, F. (2014) Tissue-specific insulin signaling in the regulation of metabolism and aging. *IUBMB Life* **66**, 485-495

10. Randle, P. J., Garland, P. B., Hales, C. N., and Newsholme, E. A. (1963) The glucose fatty-acid cycle. Its role in insulin sensitivity and the metabolic disturbances of diabetes mellitus. *Lancet* **1**, 785-789

11. Dresner, A., Laurent, D., Marcucci, M., Griffin, M. E., Dufour, S., Cline, G. W., Slezak, L. A., Andersen, D. K., Hundal, R. S., Rothman, D. L., Petersen, K. F., and Shulman, G. I. (1999) Effects of free fatty acids on glucose transport and IRS-1–associated phosphatidylinositol 3-kinase activity. *Journal of Clinical Investigation* **103**, 253-259

12. Roden, M., Price, T. B., Perseghin, G., Petersen, K. F., Rothman, D. L., Cline, G. W., and Shulman, G. I. (1996) Mechanism of free fatty acid-induced insulin resistance in humans. *Journal of Clinical Investigation* **97**, 2859-2865

13. Yu, C., Chen, Y., Cline, G. W., Zhang, D., Zong, H., Wang, Y., Bergeron, R., Kim, J. K., Cushman, S. W., Cooney, G. J., Atcheson, B., White, M. F., Kraegen, E. W., and Shulman, G. I. (2002) Mechanism by Which Fatty Acids Inhibit Insulin Activation of

Insulin Receptor Substrate-1 (IRS-1)-associated Phosphatidylinositol 3-Kinase Activity in Muscle. *Journal of Biological Chemistry* **277**, 50230-50236

14. Haus, J. M., Kashyap, S. R., Kasumov, T., Zhang, R., Kelly, K. R., Defronzo, R. A., and Kirwan, J. P. (2009) Plasma ceramides are elevated in obese subjects with type 2 diabetes and correlate with the severity of insulin resistance. *Diabetes* **58**, 337-343

15. Aguirre, V., Uchida, T., Yenush, L., Davis, R., and White, M. F. (2000) The c-Jun NH (2)-terminal kinase promotes insulin resistance during association with insulin receptor substrate-1 and phosphorylation of Ser (307). *J Biol Chem* **275**, 9047-9054

16. Gao, Z., Hwang, D., Bataille, F., Lefevre, M., York, D., Quon, M. J., and Ye, J. (2002) Serine Phosphorylation of Insulin Receptor Substrate 1 by Inhibitor κB Kinase Complex. *Journal of Biological Chemistry* **277**, 48115-48121

17. Hotamisligil, G. S. (1999) Mechanisms of TNF-alpha-induced insulin resistance. *Exp Clin Endocrinol Diabetes* **107**, 119-125

18. Finck, B. N., Bernal-Mizrachi, C., Han, D. H., Coleman, T., Sambandam, N., LaRiviere, L. L., Holloszy, J. O., Semenkovich, C. F., and Kelly, D. P. (2005) A potential link between muscle peroxisome proliferator- activated receptor-α signaling and obesity-related diabetes. *Cell Metabolism* **1**, 133-144

19. Rindler, P. M., Crewe, C. L., Fernandes, J., Kinter, M., and Szweda, L. I. (2013) Redox regulation of insulin sensitivity due to enhanced fatty acid utilization in the mitochondria. *American Journal of Physiology-Heart and Circulatory Physiology* **305**, H634-H643

20. Gavrilova, O., Marcus-Samuels, B., Graham, D., Kim, J. K., Shulman, G. I., Castle, A. L., Vinson, C., Eckhaus, M., and Reitman, M. L. (2000) Surgical implantation of adipose tissue reverses diabetes in lipoatrophic mice. *J Clin Invest* **105**, 271-278

21. Kim, J. K., Gavrilova, O., Chen, Y., Reitman, M. L., and Shulman, G. I. (2000) Mechanism of insulin resistance in A-ZIP/F-1 fatless mice. *J Biol Chem* **275**, 8456-8460

22. Keung, W., Ussher, J. R., Jaswal, J. S., Raubenheimer, M., Lam, V. H., Wagg, C. S., and Lopaschuk, G. D. (2013) Inhibition of carnitine palmitoyltransferase-1 activity alleviates insulin resistance in diet-induced obese mice. *Diabetes* **62**, 711-720

23. DeFronzo, R. A., Jacot, E., Jequier, E., Maeder, E., Wahren, J., and Felber, J. P. (1981) The effect of insulin on the disposal of intravenous glucose. Results from indirect calorimetry and hepatic and femoral venous catheterization. *Diabetes* **30**, 1000-1007

24. Petersen, K. F., Dufour, S., Savage, D. B., Bilz, S., Solomon, G., Yonemitsu, S., Cline, G. W., Befroy, D., Zemany, L., Kahn, B. B., Papademetris, X., Rothman, D. L., and Shulman, G. I. (2007) The role of skeletal muscle insulin resistance in the pathogenesis of the metabolic syndrome. *Proc Natl Acad Sci U S A* **104**, 12587-12594

25. Nicolson, G. L. (2014) Mitochondrial Dysfunction and Chronic Disease: Treatment With Natural Supplements. *Integr Med (Encinitas)* **13**, 35-43

26. Bonnard, C., Durand, A., Peyrol, S., Chanseaume, E., Chauvin, M.-A., Morio, B., Vidal, H., and Rieusset, J. (2008) Mitochondrial dysfunction results from oxidative stress in the skeletal muscle of diet-induced insulin-resistant mice. *The Journal of Clinical Investigation* **118**, 789-800

27. Newsholme, P., Haber, E. P., Hirabara, S. M., Rebelato, E. L., Procopio, J., Morgan, D., Oliveira-Emilio, H. C., Carpinelli, A. R., and Curi, R. (2007) Diabetes associated cell stress and dysfunction: role of mitochondrial and non-mitochondrial ROS production and activity. *J Physiol* **583**, 9-24

28. Korshunov, S. S., Skulachev, V. P., and Starkov, A. A. (1997) High protonic potential actuates a mechanism of production of reactive oxygen species in mitochondria. *FEBS Lett* **416**, 15-18

29. Hoehn, K. L., Salmon, A. B., Hohnen-Behrens, C., Turner, N., Hoy, A. J., Maghzal, G. J., Stocker, R., Van Remmen, H., Kraegen, E. W., Cooney, G. J., Richardson, A. R., and James, D. E. (2009) Insulin resistance is a cellular antioxidant defense mechanism. *Proceedings of the National Academy of Sciences of the United States of America* **106**, 17787-17792

30. Fisher-Wellman, K. H., and Neufer, P. D. (2012) Linking mitochondrial bioenergetics to insulin resistance via redox biology. *Trends Endocrinol Metab* **23**, 142-153

31. Houstis, N., Rosen, E. D., and Lander, E. S. (2006) Reactive oxygen species have a causal role in multiple forms of insulin resistance. *Nature* **440**, 944

32. Olson, D. H., Burrill, J. S., Kuzmicic, J., Hahn, W. S., Park, J.-M., Kim, D.-H., and Bernlohr, D. A. (2017) Down regulation of Peroxiredoxin-3 in 3T3-L1 adipocytes leads to oxidation of Rictor in the mammalian-target of rapamycin complex 2 (mTORC2). *Biochemical and Biophysical Research Communications* **493**, 1311-1317

33. Lee, H. Y., Choi, C. S., Birkenfeld, A. L., Alves, T. C., Jornayvaz, F. R., Jurczak, M. J., Zhang, D., Woo, D. K., Shadel, G. S., Ladiges, W., Rabinovitch, P. S., Santos, J. H., Petersen, K. F., Samuel, V. T., and Shulman, G. I. (2010) Targeted expression of catalase to mitochondria prevents age-associated reductions in mitochondrial function and insulin resistance. *Cell Metab* **12**, 668-674

34. Anderson, E. J., Lustig, M. E., Boyle, K. E., Woodlief, T. L., Kane, D. A., Lin, C.-T., Price, J. W., Kang, L., Rabinovitch, P. S., Szeto, H. H., Houmard, J. A., Cortright, R. N., Wasserman, D. H., and Neufer, P. D. (2009) Mitochondrial H (2)O (2) emission and cellular redox state link excess fat intake to insulin resistance in both rodents and humans. *The Journal of Clinical Investigation* **119**, 573-581

35. Kubli, D. A., Zhang, X., Lee, Y., Hanna, R. A., Quinsay, M. N., Nguyen, C. K., Jimenez, R., Petrosyan, S., Murphy, A. N., and Gustafsson, A. B. (2013) Parkin protein deficiency exacerbates cardiac injury and reduces survival following myocardial infarction. *J Biol Chem* **288**, 915-926

36. Arkinson, C., and Walden, H. (2018) Parkin function in Parkinson's disease. *Science* **360**, 267-268

37. Pickrell, A. M., and Youle, R. J. (2015) The roles of PINK1, parkin, and mitochondrial fidelity in Parkinson's disease. *Neuron* **85**, 257-273

38. Tarpey, M. D., Davy, K. P., McMillan, R. P., Bowser, S. M., Halliday, T. M., Boutagy, N. E., Davy, B. M., Frisard, M. I., and Hulver, M. W. (2017) Skeletal muscle autophagy and mitophagy in endurance-trained runners before and after a high-fat meal. *Molecular Metabolism* **6**, 1597-1609

39. Jayaprakasam, B., Olson, L. K., Schutzki, R. E., Tai, M. H., and Nair, M. G. (2006) Amelioration of obesity and glucose intolerance in high-fat-fed C57BL/6 mice by anthocyanins and ursolic acid in Cornelian cherry (Cornus mas). *J Agric Food Chem* **54**, 243-248

40. Oz, H. S. (2017) Chronic Inflammatory Diseases and Green Tea Polyphenols. *Nutrients* **9**

41. Yin, J., Xing, H., and Ye, J. (2008) Efficacy of Berberine in Patients with Type 2 Diabetes. *Metabolism: clinical and experimental* **57**, 712-717

42. Festa, A., D'Agostino, R., Jr., Tracy, R. P., Haffner, S. M., and Insulin Resistance Atherosclerosis, S. (2002) Elevated levels of acute-phase proteins and plasminogen activator inhibitor-1 predict the development of type 2 diabetes: the insulin resistance atherosclerosis study. *Diabetes* **51**, 1131-1137

43. Cefalu, W. T. (2009) Inflammation, insulin resistance, and type 2 diabetes: back to the future? *Diabetes* **58**, 307-308

44. Plomgaard, P., Bouzakri, K., Krogh-Madsen, R., Mittendorfer, B., Zierath, J. R., and Pedersen, B. K. (2005) Tumor necrosis factor-alpha induces skeletal muscle insulin resistance in healthy human subjects via inhibition of Akt substrate 160 phosphorylation. *Diabetes* **54**, 2939-2945

45. Saghizadeh, M., Ong, J. M., Garvey, W. T., Henry, R. R., and Kern, P. A. (1996) The expression of TNF alpha by human muscle. Relationship to insulin resistance. *J Clin Invest* **97**, 1111-1116

46. Arkan, M. C., Hevener, A. L., Greten, F. R., Maeda, S., Li, Z. W., Long, J. M., Wynshaw-Boris, A., Poli, G., Olefsky, J., and Karin, M. (2005) IKK-beta links inflammation to obesity-induced insulin resistance. *Nat Med* **11**, 191-198

47. Li, Z., Geng, Y. N., Jiang, J. D., and Kong, W. J. (2014) Antioxidant and anti-inflammatory activities of berberine in the treatment of diabetes mellitus. *Evid Based Complement Alternat Med* **2014**, 289264

48. Stohs, S. J., Miller, H., and Kaats, G. R. (2012) A Review of the Efficacy and Safety of Banaba (Lagerstroemia speciosa L.) and Corosolic Acid. *Phytotherapy Research* **26**, 317-324

49. Mooney, M. H., Fogarty, S., Stevenson, C., Gallagher, A. M., Palit, P., Hawley, S. A., Hardie, D. G., Coxon, G. D., Waigh, R. D., Tate, R. J., Harvey, A. L., and Furman, B. L. (2008) Mechanisms underlying the metabolic actions of galegine that contribute to weight loss in mice. *British Journal of Pharmacology* **153**, 1669-1677

50. Liu, W., Liu, P., Tao, S., Deng, Y., Li, X., Lan, T., Zhang, X., Guo, F., Huang, W., Chen, F., Huang, H., and Zhou, S. F. (2008) Berberine inhibits aldose reductase and oxidative stress in rat mesangial cells cultured under high glucose. *Arch Biochem Biophys* **475**, 128-134

51. Yamaguchi, Y., Yamada, K., Yoshikawa, N., Nakamura, K., Haginaka, J., and Kunitomo, M. (2006) Corosolic acid prevents oxidative stress, inflammation and hypertension in SHR/NDmcr-cp rats, a model of metabolic syndrome. *Life Sciences* **79**, 2474-2479

52. Adams, L. S., Seeram, N. P., Aggarwal, B. B., Takada, Y., Sand, D., and Heber, D. (2006) Pomegranate juice, total pomegranate ellagitannins, and punicalagin suppress inflammatory cell signaling in colon cancer cells. *J Agric Food Chem* **54**, 980-985

53. Hayashi, T., Maruyama, H., Kasai, R., Hattori, K., Takasuga, S., Hazeki, O., Yamasaki, K., and Tanaka, T. (2002) Ellagitannins from Lagerstroemia speciosa as Activators of Glucose Transport in Fat Cells. *Planta Med* **68**, 173-175

54. Mullen, W., Stewart, A. J., Lean, M. E., Gardner, P., Duthie, G. G., and Crozier, A. (2002) Effect of freezing and storage on the phenolics, ellagitannins, flavonoids, and antioxidant capacity of red raspberries. *J Agric Food Chem* **50**, 5197-5201

55. Landete, J. M. (2011) Ellagitannins, ellagic acid and their derived metabolites: A review about source, metabolism, functions and health. *Food Research International* **44**, 1150-1160

56. Espin, J. C., Larrosa, M., Garcia-Conesa, M. T., and Tomas-Barberan, F. (2013) Biological Significance of Urolithins, the Gut Microbial Ellagic Acid-Derived Metabolites: The Evidence So Far. *Evidence-Based Complementary and Alternative Medicine* **2013**, 15

57. Feldman, K. S., Sahasrabudhe, K., Lawlor, M. D., Wilson, S. L., Lang, C. H., and Scheuchenzuber, W. J. (2001) In vitro and In vivo inhibition of LPS-stimulated tumor necrosis factor-alpha secretion by the gallotannin beta-D-pentagalloylglucose. *Bioorg Med Chem Lett* **11**, 1813-1815

58. Tsukamoto, H., Takeuchi, S., Kubota, K., Kobayashi, Y., Kozakai, S., Ukai, I., Shichiku, A., Okubo, M., Numasaki, M., Kanemitsu, Y., Matsumoto, Y., Nochi, T., Watanabe, K., Aso, H., and Tomioka, Y. (2018) Lipopolysaccharide (LPS)-binding protein stimulates CD14-dependent Toll-like receptor 4 internalization and LPS-induced TBK1-IKKϵ-IRF3 axis activation. *Journal of Biological Chemistry*

59. Okuda, T., Kimura, Y., Yoshida, T., Hatano, T., Okuda, H., and Arichi, S. (1983) Studies on the activities of tannins and related compounds from medicinal plants and drugs. I. Inhibitory effects on lipid peroxidation in mitochondria and microsomes of liver. *Chem Pharm Bull (Tokyo)* **31**, 1625-1631

60. Seeram, N. P., Adams, L. S., Henning, S. M., Niu, Y., Zhang, Y., Nair, M. G., and Heber, D. (2005) In vitro antiproliferative, apoptotic and antioxidant activities of punicalagin, ellagic acid and a total pomegranate tannin extract are enhanced in combination with other polyphenols as found in pomegranate juice. *The Journal of Nutritional Biochemistry* **16**, 360-367

61. Losso, J. N., Bansode, R. R., Trappey, A., Bawadi, H. A., and Truax, R. (2004) In vitro anti-proliferative activities of ellagic acid. *The Journal of Nutritional Biochemistry* **15**, 672-678

62. Umesalma, S., and Sudhandiran, G. (2011) Ellagic acid prevents rat colon carcinogenesis induced by 1, 2 dimethyl hydrazine through inhibition of AKT-phosphoinositide-3 kinase pathway. *European Journal of Pharmacology* **660**, 249-258

63. Suzuki, N., Masamune, A., Kikuta, K., Watanabe, T., Satoh, K., and Shimosegawa, T. (2009) Ellagic acid inhibits pancreatic fibrosis in male Wistar Bonn/Kobori rats. *Dig Dis Sci* **54**, 802-810

64. Okla, M., Kang, I., Kim, D. M., Gourineni, V., Shay, N., Gu, L., and Chung, S. (2015) Ellagic acid modulates lipid accumulation in primary human adipocytes and human hepatoma Huh7 cells via discrete mechanisms. *J Nutr Biochem* **26**, 82-90

65. Kang, I., Buckner, T., Shay, N. F., Gu, L., and Chung, S. (2016) Improvements in Metabolic Health with Consumption of Ellagic Acid and Subsequent Conversion into Urolithins: Evidence and Mechanisms. *Adv Nutr* **7**, 961-972

66. Poulose, N., Prasad, C. V., Haridas, P. N., and Anilkumar, G. (2011) Ellagic Acid Stimulates Glucose Transport in Adipocytes and Muscles through AMPK Mediated Pathway. *J Diabetes Metab* **2**, 2155-6156

67. Viollet, B., Guigas, B., Sanz Garcia, N., Leclerc, J., Foretz, M., and Andreelli, F. (2012) Cellular and molecular mechanisms of metformin: an overview. *Clin Sci (Lond)* **122**, 253-270

68. Haghani, K., Pashaei, S., Vakili, S., Taheripak, G., and Bakhtiyari, S. (2015) TNF-α knockdown alleviates palmitate-induced insulin resistance in C2C12 skeletal muscle cells. *Biochemical and Biophysical Research Communications* **460**, 977-982

69. Jove, M., Planavila, A., Sanchez, R. M., Merlos, M., Laguna, J. C., and Vazquez-Carrera, M. (2006) Palmitate induces tumor necrosis factor-alpha expression in C2C12 skeletal muscle cells by a mechanism involving protein kinase C and nuclear factor-kappaB activation. *Endocrinology* **147**, 552-561

70. Meshkani, R., Sadeghi, A., Taheripak, G., Zarghooni, M., Gerayesh-Nejad, S., and Bakhtiyari, S. (2014) Rosiglitazone, a PPARgamma agonist, ameliorates palmitate-induced insulin resistance and apoptosis in skeletal muscle cells. *Cell biochemistry and function* **32**, 683-691

71. McLean, J. B., Moylan, J. S., and Andrade, F. H. (2014) Mitochondria dysfunction in lung cancer-induced muscle wasting in C2C12 myotubes. *Frontiers in Physiology* **5**, 503

72. Borst, S. E., and Conover, C. F. (2005) High-fat diet induces increased tissue expression of TNF-alpha. *Life Sci* **77**, 2156-2165

73. Masamune, A., Satoh, M., Kikuta, K., Suzuki, N., Satoh, K., and Shimosegawa, T. (2005) Ellagic acid blocks activation of pancreatic stellate cells. *Biochem Pharmacol* **70**, 869-878

74. Luo, T., Miranda-Garcia, O., Adamson, A., Sasaki, G., and Shay, N. F. (2016) Development of obesity is reduced in high-fat fed mice fed whole raspberries, raspberry juice concentrate, and a combination of the raspberry phytochemicals ellagic acid and raspberry ketone. *Journal of Berry Research* **6**, 213-223

75. Krssak, M., Falk Petersen, K., Dresner, A., DiPietro, L., Vogel, S. M., Rothman, D. L., Roden, M., and Shulman, G. I. (1999) Intramyocellular lipid concentrations are correlated with insulin sensitivity in humans: a 1H NMR spectroscopy study. *Diabetologia* **42**, 113-116

76. Ascunce, M. S., Hasson, E., and Mudry, M. D. (2002) Description of the cytochrome c oxidase subunit II gene in some genera of New World monkeys (primates, Platyrrhini). *Genetica* **114**, 253-267

77. Nijtmans, L. G., Klement, P., Houstek, J., and van den Bogert, C. (1995) Assembly of mitochondrial ATP synthase in cultured human cells: implications for mitochondrial diseases. *Biochim Biophys Acta* **1272**, 190-198

78. Dinkova-Kostova, A. T., and Abramov, A. Y. (2015) The emerging role of Nrf2 in mitochondrial function. *Free Radical Biology and Medicine* **88**, 179-188

79. Nojima, Y., Ito, K., Ono, H., Nakazato, T., Bono, H., Yokoyama, T., Sato, R., Suetsugu, Y., Nakamura, Y., Yamamoto, K., Satoh, J., Tabunoki, H., and Fugo, H. (2015)

Superoxide dismutases, SOD1 and SOD2, play a distinct role in the fat body during pupation in silkworm Bombyx mori. *PLoS One* **10**, e0116007

80. MacLellan, J. D., Gerrits, M. F., Gowing, A., Smith, P. J., Wheeler, M. B., and Harper, M. E. (2005) Physiological increases in uncoupling protein 3 augment fatty acid oxidation and decrease reactive oxygen species production without uncoupling respiration in muscle cells. *Diabetes* **54**, 2343-2350

81. Schrauwen, P., Hesselink, M. K., Blaak, E. E., Borghouts, L. B., Schaart, G., Saris, W. H., and Keizer, H. A. (2001) Uncoupling protein 3 content is decreased in skeletal muscle of patients with type 2 diabetes. *Diabetes* **50**, 2870-2873

82. Kuete, V., Karaosmanoğlu, O., and Sivas, H. (2017) Chapter 10 - Anticancer Activities of African Medicinal Spices and Vegetables. in *Medicinal Spices and Vegetables from Africa (*Kuete, V. ed.), Academic Press. pp 271-297

83. Chen, C. W., and Cheng, H. H. (2006) A rice bran oil diet increases LDL-receptor and HMG-CoA reductase mRNA expressions and insulin sensitivity in rats with streptozotocin/nicotinamide-induced type 2 diabetes. *The Journal of nutrition* **136**, 1472-1476

84. Eruslanov, E., and Kusmartsev, S. (2010) Identification of ROS using oxidized DCFDA and flow-cytometry. *Methods in molecular biology (Clifton, N.J.)* **594**, 57-72

85. Wang, Y., Qiu, Z., Zhou, B., Liu, C., Ruan, J., Yan, Q., Liao, J., and Zhu, F. (2015) In vitro antiproliferative and antioxidant effects of urolithin A, the colonic metabolite of ellagic acid, on hepatocellular carcinomas HepG2 cells. *Toxicol In Vitro* **29**, 1107-1115

86. Divakaruni, A. S., Paradyse, A., Ferrick, D. A., Murphy, A. N., and Jastroch, M. (2014) Analysis and interpretation of microplate-based oxygen consumption and pH data. *Methods Enzymol* **547**, 309-354

87. Gonzalez-Sarrias, A., Espin, J. C., Tomas-Barberan, F. A., and Garcia-Conesa, M. T. (2009) Gene expression, cell cycle arrest and MAPK signalling regulation in Caco-2 cells exposed to ellagic acid and its metabolites, urolithins. *Mol Nutr Food Res* **53**, 686-698

88. Ishimoto, H., Tai, A., Yoshimura, M., Amakura, Y., Yoshida, T., Hatano, T., and Ito, H. (2012) Antioxidative Properties of Functional Polyphenols and Their Metabolites Assessed by an ORAC Assay. *Bioscience, Biotechnology, and Biochemistry* **76**, 395-399

89. Larrosa, M., Gonzalez-Sarrias, A., Yanez-Gascon, M. J., Selma, M. V., Azorin-Ortuno, M., Toti, S., Tomas-Barberan, F., Dolara, P., and Espin, J. C. (2010) Anti-inflammatory properties of a pomegranate extract and its metabolite urolithin-A in a colitis rat model and the effect of colon inflammation on phenolic metabolism. *J Nutr Biochem* **21**, 717-725

90. Seeram, N. P., Aronson, W. J., Zhang, Y., Henning, S. M., Moro, A., Lee, R. P., Sartippour, M., Harris, D. M., Rettig, M., Suchard, M. A., Pantuck, A. J., Belldegrun, A., and Heber, D. (2007) Pomegranate ellagitannin-derived metabolites inhibit prostate cancer growth and localize to the mouse prostate gland. *J Agric Food Chem* **55**, 7732-7737

91. Khanduja, K. L., Gandhi, R. K., Pathania, V., and Syal, N. (1999) Prevention of N-nitrosodiethylamine-induced lung tumorigenesis by ellagic acid and quercetin in mice. *Food Chem Toxicol* **37**, 313-318

92. Ryu, D., Mouchiroud, L., Andreux, P. A., Katsyuba, E., Moullan, N., Nicolet-Dit-Felix, A. A., Williams, E. G., Jha, P., Lo Sasso, G., Huzard, D., Aebischer, P., Sandi, C., Rinsch, C., and Auwerx, J. (2016) Urolithin A induces mitophagy and prolongs lifespan in C. elegans and increases muscle function in rodents. *Nat Med* **22**, 879-888

93. Savi, M., Bocchi, L., Mena, P., Dall'Asta, M., Crozier, A., Brighenti, F., Stilli, D., and Del Rio, D. (2017) In vivo administration of urolithin A and B prevents the occurrence of cardiac dysfunction in streptozotocin-induced diabetic rats. *Cardiovasc Diabetol* **16**, 80

94. Arner, P., and Ryden, M. (2015) Fatty Acids, Obesity and Insulin Resistance. *Obes Facts* **8**, 147-155

95. Miller, M. R., Pereira, R. I., Langefeld, C. D., Lorenzo, C., Rotter, J. I., Chen, Y. D., Bergman, R. N., Wagenknecht, L. E., Norris, J. M., and Fingerlin, T. E. (2012) Levels of free fatty acids (FFA) are associated with insulin resistance but do not explain the relationship between adiposity and insulin resistance in Hispanic Americans: the IRAS Family Study. *The Journal of clinical endocrinology and metabolism* **97**, 3285-3291

96. Santomauro, A. T., Boden, G., Silva, M. E., Rocha, D. M., Santos, R. F., Ursich, M. J., Strassmann, P. G., and Wajchenberg, B. L. (1999) Overnight lowering of free fatty acids with Acipimox improves insulin resistance and glucose tolerance in obese diabetic and nondiabetic subjects. *Diabetes* **48**, 1836-1841

97. Lihn, A. S., Pedersen, S. B., and Richelsen, B. (2005) Adiponectin: action, regulation and association to insulin sensitivity. *Obes Rev* **6**, 13-21

98. Kuhlmann, J., Neumann-Haefelin, C., Belz, U., Kalisch, J., Juretschke, H. P., Stein, M., Kleinschmidt, E., Kramer, W., and Herling, A. W. (2003) Intramyocellular lipid and insulin resistance: a longitudinal in vivo 1H-spectroscopic study in Zucker diabetic fatty rats. *Diabetes* **52**, 138-144

99. Li, Y., Xu, S., Zhang, X., Yi, Z., and Cichello, S. (2015) Skeletal intramyocellular lipid metabolism and insulin resistance. *Biophys Rep* **1**, 90-98

100. Gemmink, A., and Hesselink, M. (2015) Intramyocellular lipid storage and insulin resistance. *Diapedia*

101. He, J., Watkins, S., and Kelley, D. E. (2001) Skeletal muscle lipid content and oxidative enzyme activity in relation to muscle fiber type in type 2 diabetes and obesity. *Diabetes* **50**, 817-823

102. Kuhlmann, J., Neumann-Haefelin, C., Belz, U., Kramer, W., Juretschke, H. P., and Herling, A. W. (2005) Correlation between insulin resistance and intramyocellular lipid levels in rats. *Magn Reson Med* **53**, 1275-1282

103. Boden, G., Lebed, B., Schatz, M., Homko, C., and Lemieux, S. (2001) Effects of acute changes of plasma free fatty acids on intramyocellular fat content and insulin resistance in healthy subjects. *Diabetes* **50**, 1612-1617

104. Montgomery, M. K., and Turner, N. (2015) Mitochondrial dysfunction and insulin resistance: an update. *Endocr Connect* **4**, R1-R15

105. Kruszynska, Y. T., Mukherjee, R., Jow, L., Dana, S., Paterniti, J. R., and Olefsky, J. M. (1998) Skeletal muscle peroxisome proliferator- activated receptor-gamma expression in obesity and non- insulin-dependent diabetes mellitus. *J Clin Invest* **101**, 543-548

106. Park, K. S., Ciaraldi, T. P., Abrams-Carter, L., Mudaliar, S., Nikoulina, S. E., and Henry, R. R. (1997) PPAR-gamma gene expression is elevated in skeletal muscle of obese and type II diabetic subjects. *Diabetes* **46**, 1230-1234

107. Verma, N. K., Singh, J., and Dey, C. S. (2004) PPAR-gamma expression modulates insulin sensitivity in C2C12 skeletal muscle cells. *Br J Pharmacol* **143**, 1006-1013

108. Yamauchi, T., Kamon, J., Waki, H., Murakami, K., Motojima, K., Komeda, K., Ide, T., Kubota, N., Terauchi, Y., Tobe, K., Miki, H., Tsuchida, A., Akanuma, Y., Nagai, R., Kimura, S., and Kadowaki, T. (2001) The Mechanisms by Which Both Heterozygous Peroxisome Proliferator-activated Receptor γ (PPARγ) Deficiency and PPARγ Agonist Improve Insulin Resistance. *Journal of Biological Chemistry* **276**, 41245-41254

109. Woo, M. S., Choi, H. S., Seo, M. J., Jeon, H. J., and Lee, B. Y. (2015) Ellagic acid suppresses lipid accumulation by suppressing early adipogenic events and cell cycle arrest. *Phytother Res* **29**, 398-406

110. Yoshimura, Y., Nishii, S., Zaima, N., Moriyama, T., and Kawamura, Y. (2013) Ellagic acid improves hepatic steatosis and serum lipid composition through reduction of serum resistin levels and transcriptional activation of hepatic ppara in obese, diabetic KK-A (y) mice. *Biochem Biophys Res Commun* **434**, 486-491

111. Austin, S., and St-Pierre, J. (2012) PGC1α and mitochondrial metabolism – emerging concepts and relevance in ageing and neurodegenerative disorders. *Journal of Cell Science* **125**, 4963-4971

112. Schreiber, S. N., Emter, R., Hock, M. B., Knutti, D., Cardenas, J., Podvinec, M., Oakeley, E. J., and Kralli, A. (2004) The estrogen-related receptor alpha (ERRalpha)

functions in PPARgamma coactivator 1alpha (PGC-1alpha)-induced mitochondrial biogenesis. *Proc Natl Acad Sci U S A* **101**, 6472-6477

113. Jornayvaz, F. R., and Shulman, G. I. (2010) Regulation of mitochondrial biogenesis. *Essays in biochemistry* **47**, 69-84

114. Sun, W., Yan, C., Frost, B., Wang, X., Hou, C., Zeng, M., Gao, H., Kang, Y., and Liu, J. (2016) Pomegranate extract decreases oxidative stress and alleviates mitochondrial impairment by activating AMPK-Nrf2 in hypothalamic paraventricular nucleus of spontaneously hypertensive rats. *Sci Rep* **6**, 34246

115. Eisner, V., Lenaers, G., and Hajnóczky, G. (2014) Mitochondrial fusion is frequent in skeletal muscle and supports excitation–contraction coupling. *The Journal of Cell Biology* **205**, 179-195

116. Pich, S., Bach, D., Briones, P., Liesa, M., Camps, M., Testar, X., Palacin, M., and Zorzano, A. (2005) The Charcot-Marie-Tooth type 2A gene product, Mfn2, up-regulates fuel oxidation through expression of OXPHOS system. *Human molecular genetics* **14**, 1405-1415

117. Liesa, M., and Shirihai, O. S. (2013) Mitochondrial dynamics in the regulation of nutrient utilization and energy expenditure. *Cell Metab* **17**, 491-506

118. Zorzano, A., Liesa, M., and Palacin, M. (2009) Mitochondrial dynamics as a bridge between mitochondrial dysfunction and insulin resistance. *Archives of physiology and biochemistry* **115**, 1-12

119. Bach, D., Naon, D., Pich, S., Soriano, F. X., Vega, N., Rieusset, J., Laville, M., Guillet, C., Boirie, Y., Wallberg-Henriksson, H., Manco, M., Calvani, M., Castagneto, M., Palacin, M., Mingrone, G., Zierath, J. R., Vidal, H., and Zorzano, A. (2005) Expression of Mfn2, the Charcot-Marie-Tooth neuropathy type 2A gene, in human skeletal muscle: effects of type 2 diabetes, obesity, weight loss, and the regulatory role of tumor necrosis factor alpha and interleukin-6. *Diabetes* **54**, 2685-2693

120. Anderson, E. J., Lustig, M. E., Boyle, K. E., Woodlief, T. L., Kane, D. A., Lin, C. T., Price, J. W., 3rd, Kang, L., Rabinovitch, P. S., Szeto, H. H., Houmard, J. A., Cortright, R. N., Wasserman, D. H., and Neufer, P. D. (2009) Mitochondrial H2O2 emission and cellular redox state link excess fat intake to insulin resistance in both rodents and humans. *J Clin Invest* **119**, 573-581

121. Tang, L., Mo, Y., Li, Y., Zhong, Y., He, S., Zhang, Y., Tang, Y., Fu, S., Wang, X., and Chen, A. (2017) Urolithin A alleviates myocardial ischemia/reperfusion injury via PI3K/Akt pathway. *Biochem Biophys Res Commun* **486**, 774-780

122. Boucher, J., Kleinridders, A., and Kahn, C. R. (2014) Insulin receptor signaling in normal and insulin-resistant states. *Cold Spring Harbor perspectives in biology* **6**

123. Pletjushkina, O. Y., Lyamzaev, K. G., Popova, E. N., Nepryakhina, O. K., Ivanova, O. Y., Domnina, L. V., Chernyak, B. V., and Skulachev, V. P. (2006) Effect of oxidative stress on dynamics of mitochondrial reticulum. *Biochim Biophys Acta* **1757**, 518-524

124. Yu, T., Robotham, J. L., and Yoon, Y. (2006) Increased production of reactive oxygen species in hyperglycemic conditions requires dynamic change of mitochondrial morphology. *Proc Natl Acad Sci U S A* **103**, 2653-2658

125. Rains, J. L., and Jain, S. K. (2011) OXIDATIVE STRESS, INSULIN SIGNALING AND DIABETES. *Free radical biology & medicine* **50**, 567-575

126. Kallio, T., Kallio, J., Jaakkola, M., Maki, M., Kilpelainen, P., and Virtanen, V. (2013) Urolithins display both antioxidant and pro-oxidant activities depending on assay system and conditions. *J Agric Food Chem* **61**, 10720-10729

127. Qiu, Z., Zhou, B., Jin, L., Yu, H., Liu, L., Liu, Y., Qin, C., Xie, S., and Zhu, F. (2013) In vitro antioxidant and antiproliferative effects of ellagic acid and its colonic metabolite, urolithins, on human bladder cancer T24 cells. *Food Chem Toxicol* **59**, 428-437

128. Diniz Vilela, D., Gomes Peixoto, L., Teixeira, R. R., Belele Baptista, N., Carvalho Caixeta, D., Vieira de Souza, A., Machado, H., #xe9, Lara, l., Pereira, M. N., Sabino-Silva, R., and Espindola, F. S. (2016) The Role of Metformin in Controlling Oxidative Stress in Muscle of Diabetic Rats. *Oxidative Medicine and Cellular Longevity* **2016**, 9

129. Gorogawa, S.-i., Kajimoto, Y., Umayahara, Y., Kaneto, H., Watada, H., Kuroda, A., Kawamori, D., Yasuda, T., Matsuhisa, M., Yamasaki, Y., and Hori, M. (2002) Probucol preserves pancreatic β-cell function through reduction of oxidative stress in type 2 diabetes. *Diabetes Research and Clinical Practice* **57**, 1-10

130. McNabney, S. M., and Henagan, T. M. (2017) Short Chain Fatty Acids in the Colon and Peripheral Tissues: A Focus on Butyrate, Colon Cancer, Obesity and Insulin Resistance. *Nutrients* **9**

131. Mehta, V., Verma, P., Sharma, N., Sharma, A., Thakur, A., and Malairaman, U. (2017) Quercetin, ascorbic acid, caffeine and ellagic acid are more efficient than rosiglitazone, metformin and glimepiride in interfering with pathways leading to the development of neurological complications associated with diabetes: A comparative in-vitro study. *Bulletin of Faculty of Pharmacy, Cairo University* **55**, 115-121

132. Seeram, N. P., Lee, R., and Heber, D. (2004) Bioavailability of ellagic acid in human plasma after consumption of ellagitannins from pomegranate (Punica granatum L.) juice. *Clin Chim Acta* **348**, 63-68

133. Seeram, N. P., Zhang, Y., McKeever, R., Henning, S. M., Lee, R. P., Suchard, M. A., Li, Z., Chen, S., Thames, G., Zerlin, A., Nguyen, M., Wang, D., Dreher, M., and Heber, D. (2008) Pomegranate juice and extracts provide similar levels of plasma and urinary ellagitannin metabolites in human subjects. *J Med Food* **11**, 390-394

134. Hernandez, G., Thornton, C., Stotland, A., Lui, D., Sin, J., Ramil, J., Magee, N., Andres, A., Quarato, G., Carreira, R. S., Sayen, M. R., Wolkowicz, R., and Gottlieb, R. A. (2013) MitoTimer: a novel tool for monitoring mitochondrial turnover. *Autophagy* **9**, 1852-1861